

การสังเคราะห์คอนจูเกตพอลิเมอร์ที่มีรูพรุนขนาดเล็กจากอนุพันธ์ไทโอพีนชนิดใหม่



บทคัดย่อและแฟ้มข้อมูลฉบับเต็มของวิทยานิพนธ์ตั้งแต่ปีการศึกษา 2554 ที่ให้บริการในคลังปัญญาจุฬาฯ (CUIR)  
เป็นแฟ้มข้อมูลของนิสิตเจ้าของวิทยานิพนธ์ ที่ส่งผ่านทางบัณฑิตวิทยาลัย

The abstract and full text of theses from the academic year 2011 in Chulalongkorn University Intellectual Repository (CUIR)  
are the thesis authors' files submitted through the University Graduate School.

วิทยานิพนธ์นี้เป็นส่วนหนึ่งของการศึกษาตามหลักสูตรปริญญาวิทยาศาสตรดุษฎีบัณฑิต

สาขาวิชาเคมี ภาควิชาเคมี

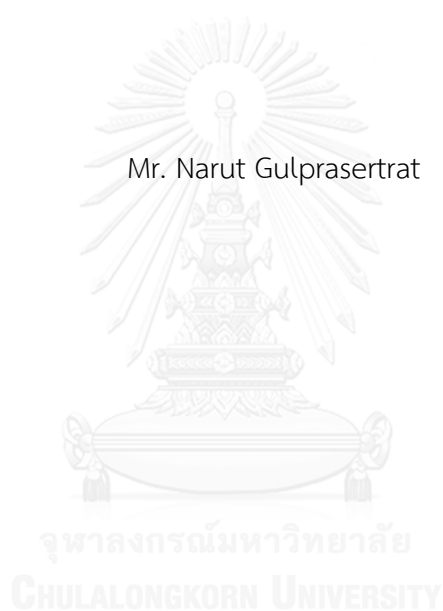
คณะวิทยาศาสตร์ จุฬาลงกรณ์มหาวิทยาลัย

ปีการศึกษา 2557

ลิขสิทธิ์ของจุฬาลงกรณ์มหาวิทยาลัย

SYNTHESIS OF CONJUGATED MICROPOROUS POLYMER FROM NEW THIOPHENE  
DERIVATIVES

Mr. Narut Gulprasertat



A Dissertation Submitted in Partial Fulfillment of the Requirements  
for the Degree of Doctor of Philosophy Program in Chemistry

Department of Chemistry

Faculty of Science

Chulalongkorn University

Academic Year 2014

Copyright of Chulalongkorn University

Thesis Title	SYNTHESIS OF CONJUGATED MICROPOROUS POLYMER FROM NEW THIOPHENE DERIVATIVES
By	Mr. Narut Gulprasertrat
Field of Study	Chemistry
Thesis Advisor	Assistant Professor Yongsak Sritana-anant, Ph.D.

---

Accepted by the Faculty of Science, Chulalongkorn University in Partial  
Fulfillment of the Requirements for the Doctoral Degree

.....Dean of the Faculty of Science  
(Professor Supot Hannongbua, Dr.rer.nat.)

THESIS COMMITTEE

.....Chairman  
(Assistant Professor Warinthorn Chavasiri, Ph.D.)

.....Thesis Advisor  
(Assistant Professor Yongsak Sritana-anant, Ph.D.)

.....Examiner  
(Sakulsuk Unarunotai, Ph.D.)

.....Examiner  
(Associate Professor Voravee Hoven, Ph.D.)

.....External Examiner  
(Associate Professor Vuthichai Ervithayasuporn, Ph.D.)

นฤตม์ กุลประเสริฐรัตน์ : การสังเคราะห์คอนจูเกตพอลิเมอร์ที่มีรูพรุนขนาดเล็กจากอนุพันธ์ไทโอฟีนชนิดใหม่ (SYNTHESIS OF CONJUGATED MICROPOROUS POLYMER FROM NEW THIOPHENE DERIVATIVES) อ.ที่ปรึกษาวิทยานิพนธ์หลัก: ผศ. ดร. ยงศักดิ์ ศรีธนาอนันต์, 129 หน้า.

อนุพันธ์ของไทโอฟีน 4 ชนิด ได้แก่ (5,7-ไดโบรโม-2,3-ไดไฮโดรไทโอฟีน[3,4-ปี[1,4]ไดออกซิน-2-อิล)เมทานอล (สารหมายเลข 29), (5,7-ไดโบรโม-2,3-ไดไฮโดรไทโอฟีน [3,4-ปี[1,4]ไดออกซิน-2-อิล)เมทิล 4-เมทิลเบนซีนซัลโฟเนต (สารหมายเลข 30), (5,7-ไดโบรโม-2,3-ไดไฮโดรไทโอฟีน[3,4-ปี[1,4]ไดออกซิน-2-อิล)เมทิล 2-คลอโรอะซิเตต (สารหมายเลข 32) และ (±)-1,3-ไดโบรโม-4a,5,6,7,8,8a-เฮกซะไฮโดรเบนโซ[อี]ไทโอฟีน [3,4-ปี[1,4]ไดออกซิน (สารหมายเลข 37) ถือเป็นโมโนเมอร์กลุ่มหนึ่งที่สามารถเกิดเป็นพอลิเมอร์ในวัฏภาคของแข็งได้ โดยปฏิกิริยาของพอลิเมอร์ในกลุ่มนี้สามารถเกิดได้เร็วกว่า 2,5-ไดโบรโม-3,4-เอทิลีนไดออกซีไทโอฟีน แม้ว่าสารหมายเลข 37 จะต้องการอุณหภูมิที่สูงกว่าในการเกิดปฏิกิริยา ซึ่งพอลิเมอร์ของสารหมายเลข 29, 30 และ 37 แสดงค่าการนำไฟฟ้าที่สูงกว่าพอลิ 3,4-เอทิลีนไดออกซีไทโอฟีน

ส่วนอนุพันธ์ของไทโอฟีน 2 หน่วยหรือมากกว่าที่ถูกเชื่อมเข้าด้วยกันได้แก่ บิส((2,3-ไดไฮโดรไทโอฟีน[3,4-ปี]ไดออกซิน-2-อิล)เมทิล) [1',4']เบนซีน ไดคาร์บอกซีเลต, บิส((2,3-ไดไฮโดรไทโอฟีน[3,4-ปี[1,4]ไดออกซิน-2-อิล)เมทิล)มาโลเนต และ ทริส((2,3-ไดไฮโดรไทโอฟีน[3,4-ปี[1,4]ไดออกซิน-2-อิล)เมทิล) เบนซีน-1,3,5-ไตรคาร์บอกซีเลต ซึ่งถูกเตรียมขึ้น สามารถถูกเปลี่ยนเป็นพอลิเมอร์ได้โดยกระบวนการทางเคมี จากค่าการนำไฟฟ้า สารในกลุ่มนี้เป็นตัวนำไฟฟ้าที่ไม่ดีนัก อย่างไรก็ตามการผสม พอลิบิส((2,3-ไดไฮโดรไทโอฟีน[3,4-ปี]ไดออกซิน-2-อิล)เมทิล) [1',4']เบนซีน ไดคาร์บอกซีเลต 5% เข้ากับ พอลิ 3,4-เอทิลีนไดออกซีไทโอฟีนไม่ได้ทำให้สมบัติในการนำไฟฟ้าหรือลักษณะโครงสร้างของพอลิเมอร์ดังกล่าวเกิดการเปลี่ยนแปลง แต่สามารถเพิ่มพื้นที่ผิวของพอลิเมอร์ได้อย่างเห็นได้ชัดและทำให้พอลิเมอร์ผสมดังกล่าวเป็นวัสดุมีรูพรุนได้

ภาควิชา เคมี

ลายมือชื่อนิสิต .....

สาขาวิชา เคมี

ลายมือชื่อ อ.ที่ปรึกษาหลัก .....

ปีการศึกษา 2557

# # 5172331023 : MAJOR CHEMISTRY

KEYWORDS: CONDUCTING POLYMERS / THIOPHENE / PEDOT / SOLID STATE  
POLYMERIZATION

NARUT GULPRASERTRAT: SYNTHESIS OF CONJUGATED MICROPOROUS  
POLYMER FROM NEW THIOPHENE DERIVATIVES. ADVISOR: ASST. PROF.  
YONGSAK SRITANA-ANANT, Ph.D., 129 pp.

Four brominated thiophene derivatives: (5,7-dibromo-2,3-dihydrothieno[3,4-b][1,4]dioxin-2-yl)methanol (compound 29), (5,7-Dibromo-2,3-dihydrothieno[3,4-b][1,4]dioxin-2-yl)methyl 4-methylbenzenesulfonate (compound 30), (5,7-dibromo-2,3-dihydrothieno[3,4-b][1,4]dioxin-2-yl)methyl 2-chloroacetate (compound 32) and ( $\pm$ )-1,3-Dibromo-4a,5,6,7,8,8a-hexahydrobenzo[e]thieno[3,4-b][1,4]dioxine (compound 37) were a group of monomers that could undergo solid state polymerization. The reactions of compound 29 and 30 were more facile than DBEDOT, although the SSP of compound 37 required higher temperature. Polymers of compound 29, 30 and 37 show higher conductivity than PEDOT.

Three derivatives of linked multithiophenes: Bis((2,3-dihydrothieno[3,4-b]dioxin-2-yl)methyl) [1',4']benzene dicarboxylate, Bis((2,3-dihydrothieno[3,4-b][1,4]dioxin-2-yl)methyl)malonate and Tris((2,3-dihydrothieno[3,4-b][1,4]dioxin-2-yl)methyl) benzene-1,3,5-tricarboxylate were prepared. They could be turned into the corresponding polymers by chemical polymerizations. The conductivity data indicated that they were relatively poor conductors. However, incorporating 5% of Poly (bis((2,3-dihydrothieno[3,4-b]dioxin-2-yl)methyl) [1',4']benzene dicarboxylate) into PEDOT did not alter electrical conductivity and morphology of PEDOT, but significantly increased the surface area and turned the polymer mixture into a porous conductive material.

Department: Chemistry

Student's Signature .....

Field of Study: Chemistry

Advisor's Signature .....

Academic Year: 2014

## ACKNOWLEDGEMENTS

My utmost gratitude goes to my thesis advisor, Assist. Prof. Yongsak Sritana-anant, for his expertise, kindness, support, and most of all, for his patience during the course of research including completing this thesis. I am sincerely grateful to the members of the thesis committee, Assist. Prof. Warinthorn Chavasiri, Assoc. Prof. Voravee P. Hoven, Dr. Sakulsuk Unarunotai and Assoc. Prof. Dr. Vuthichai Ervithayasuporn for their valuable comments and suggestions. I gratefully acknowledge the members of the research groups on the fourteenth floor room 1408, Mahamakut building for their companionship and friendship. Finally, I would like to take this opportunity to express my sincere appreciation and thanks to my parents and Chulalongkorn University.



## CONTENTS

	Page
THAI ABSTRACT .....	iv
ACKNOWLEDGEMENTS .....	vi
CONTENTS .....	vii
LIST OF FIGURES .....	xii
LIST OF TABLES .....	xiii
LIST OF SCHEMES .....	xiv
LIST OF ABBREVIATIONS .....	xv
CHAPTER I INTRODUCTION.....	1
1.1 Conjugated polymers .....	1
1.2 Applications of organic conducting polymers .....	2
1.3 Conjugated polymers and their conductive properties .....	3
1.4 Doping process .....	6
1.5 Conductive Processes.....	7
1.6 Effective conjugation length (ECL).....	8
1.7 Polythiophene .....	9
1.8 Synthesis of polythiophene .....	9
1.9 Solid state polymerization .....	11
1.10 Porous materials.....	15
1.11 Conjugated microporous polymer.....	16
1.12 Application of CMP .....	17
1.13 Multitopic thiophene precursors .....	19
1.14 Literature review .....	22

	Page
1.15 Statement of the problem and objectives.....	25
CHAPTER II EXPERIMENTS.....	27
2.1 Chemicals.....	27
2.2 Instruments and equipment .....	28
2.3 Monomer Synthesis .....	28
2.3.1 Ethyl chloroacetate (12).....	28
2.3.2 Diethyl thiodiglycolate (13).....	29
2.3.3 Diethyl 3,4-dihydroxythiophene-2,5-dicarboxylate (14).....	29
2.3.4 Diethyl 2-(hydroxymethyl)-2,3-dihydrothieno[3,4- <i>b</i> ]-1,4-dioxine-5,7- dicarboxylate (15).....	30
2.3.5 2,3-Dihydrothieno[3,4- <i>b</i> ]-1,4-dioxin-2-yl methanol (16).....	31
2.3.6 (2,3-Dihydrothieno[3,4- <i>b</i> ][1,4]dioxin-2-yl)methyl-4'-methylbenzene sulfonate (17) .....	31
2.3.7 (2,3-Dihydrothieno[3,4- <i>b</i> ][1,4]dioxin-2-yl)methyl methanesulfonate(18)..	32
2.3.8 2-(Azidomethyl)-2,3-dihydrothieno[3,4- <i>b</i> ][1,4]dioxine (19).....	33
2.3.9 Ethyl 2-((2,3-dihydrothieno[3,4- <i>b</i> ][1,4]dioxin-2-yl)methoxy)acetate (20)...	33
2.3.10 2-((2,3-Dihydrothieno[3,4- <i>b</i> ][1,4]dioxin-2-yl)methoxy)acetic acid (21) .....	34
2.3.11 (2,3-Dihydrothieno[3,4- <i>b</i> ][1,4]dioxin-2-yl)methyl 2'-chloroacetate (22)..	35
2.3.12 Bis((2,3-dihydrothieno[3,4- <i>b</i> ]dioxin-2-yl)methyl) [1',4']benzene dicarboxylate (23).....	35
2.3.13 Bis((2,3-dihydrothieno[3,4- <i>b</i> ][1,4]dioxin-2-yl)methyl) malonate (24).....	36
2.3.14 Tris((2,3-dihydrothieno[3,4- <i>b</i> ][1,4]dioxin-2-yl)methyl) benzene- 1',3',5'-tricarboxylate (25).....	37
2.3.15 2-(Chloromethyl)-2,3-dihydrothieno[3,4- <i>b</i> ][1,4]dioxine (26) .....	38



2.3.16 ( $\pm$ )-4a,5,6,7,8,8a-Hexahydrobenzo[e]thieno[3,4-b][1,4]dioxine (27).....	38
2.4 Brominations of thiophene derivatives.....	39
2.4.1 2,5-Dibromo-3,4-ethylenedioxythiophene (28) .....	39
2.4.2 (5,7-dibromo-2,3-dihydrothieno[3,4-b][1,4]dioxin-2-yl)methanol (29) .....	40
2.4.3 (5,7-Dibromo-2,3-dihydrothieno[3,4-b][1,4]dioxin-2-yl)methyl 4'- methylbenzenesulfonate (30) .....	40
2.4.4 2-(Azidomethyl)-5,7-dibromo-2,3-dihydrothieno[3,4-b][1,4]dioxine (31) ...	41
2.4.5 (5,7-Dibromo-2,3-dihydrothieno[3,4-b][1,4]dioxin-2-yl)methyl 2'- chloroacetate (32) .....	41
2.4.6 Bis((5,7-dibromo-2,3-dihydrothieno[3,4-b][1,4]dioxin-2-yl)methyl) terephthalate (33) .....	42
2.4.7 Bis((5,7-dibromo-2,3-dihydrothieno[3,4-b][1,4]dioxin-2-yl)methyl) malonate (34).....	43
2.4.8 Tris((5,7-dibromo-2,3-dihydrothieno[3,4-b][1,4]dioxin-2-yl)methyl) benzene-1',3',5'-tricarboxylate (35).....	43
2.4.9 5,7-Dibromo-2-(chloromethyl)-2,3-dihydrothieno[3,4-b][1,4]dioxine (36) .	44
2.4.10 ( $\pm$ )-1,3-Dibromo-4a,5,6,7,8,8a-hexahydrobenzo[e]thieno[3,4- b][1,4]dioxine (37).....	44
2.5 Polymer synthesis .....	45
2.5.1 Solid state polymerization (SSP) .....	45
2.5.1.1 PEDOT from SSP (38).....	45
2.5.1.2 Poly (2,3-dihydrothieno[3,4-b]-1,4-dioxin-2-yl methanol).....	46
2.5.1.3 Poly ((2,3-dihydrothieno[3,4-b][1,4]dioxin-2-yl)methyl 4'- methylbenzenesulfonate) (40).....	46

2.5.1.4 Poly ((2,3-dihydrothieno[3,4-b][1,4]dioxin-2-yl)methyl 2'-chloroacetate) (41).....	47
2.5.1.5 Poly ((±)-4a,5,6,7,8,8a-hexahydrobenzo[e]thieno[3,4-b][1,4]dioxine) (42) .....	47
2.5.2 Chemical polymerization .....	47
2.5.2.1 PEDOT from chemical polymerization (38c).....	48
2.5.2.2 Poly bis((2,3-dihydrothieno[3,4-b]dioxin-2-yl)methyl [1',4']benzene dicarboxylate (44) .....	48
2.5.2.3 Poly (bis((2,3-dihydrothieno[3,4-b][1,4]dioxin-2-yl)methyl malonate) (45) .....	48
2.5.2.4 Poly (tris((2,3-dihydrothieno[3,4-b][1,4]dioxin-2-yl)methyl benzene-1,3,5-tricarboxylate) (46).....	49
2.5.2.5 Copolymer of (PEDOT + 5% polymer 44).....	50
CHAPTER III RESULTS AND DISCUSSION.....	51
3.1 Monomer synthesis.....	51
3.1.1 Synthesis of Diethyl 3,4-dihydroxythiophene-2,5-dicarboxylate (14) .....	51
3.1.2 Synthesis of diethyl 2-(hydroxymethyl)-2,3-dihydrothieno[3,4-b]-1,4-dioxine-5,7-dicarboxylate (15).....	54
3.1.3 Synthesis of EDTM by transesterification .....	56
3.1.4 Synthesis of other thiophene derivatives.....	58
3.1.4.1 Synthesis of (2,3-dihydrothieno[3,4-b][1,4]dioxin-2-yl)methyl 4'-methyl benzenesulfonate (17).....	58
3.1.4.2 Synthesis of 2-(azidomethyl)-2,3-dihydrothieno[3,4-b][1,4]dioxine (19).....	58

3.1.4.3 Synthesis of 2-((2,3-dihydrothieno[3,4-b][1,4]dioxin-2-yl)methoxy) acetic acid (21).....	59
3.1.4.4 Synthesis of (2,3-dihydrothieno[3,4-b][1,4]dioxin-2-yl)methyl 2'-chloroacetate (22).....	60
3.1.4.5 Synthesis of 2-(chloromethyl)-2,3-dihydrothieno[3,4-b][1,4]dioxine (26).....	61
3.1.4.6 Synthesis of (±)-4a,5,6,7,8,8a-hexahydrobenzo[e]thieno[3,4b][1,4]dioxine (27).....	61
3.1.5 Synthesis of linked multi thiophene precursor.....	62
3.2 Bromination of monomers.....	63
3.3 Polymerization of monomers.....	67
3.3.1 Solid state polymerization (SSP).....	67
3.3.2 Chemical polymerization.....	68
3.4 Surface area measurement.....	68
3.5 Scanning Electron Microscope (SEM).....	69
3.6 Conductivity measurement.....	69
3.7 UV-Visible spectroscopic study.....	71
CHAPTER IV CONCLUSION.....	73
REFERENCES.....	74
APPENDIX A.....	82
APPENDIX B.....	124
VITA.....	129

## LIST OF FIGURES

Figure	Page
1.1 Structures of some conjugated polymers .....	2
1.2 The delocalized $\pi$ system of conjugated polymers .....	4
1.3 HOMO and LUMO energy levels of oligo and polythiophenes.....	5
1.4 Band energy levels of an insulator, a semiconductor, and a conductor.....	5
1.5 Conductivities of various metals and conjugated polymers.....	7
1.6 A defect in polyacetylene and steric induced structural twisting in poly (3-alkylthiophene).....	8
1.7 Twisting of polythiophene .....	9
1.8 Solid-state polymerization of DBEDOT to PEDOT .....	12
1.9 (a) Calculated energy for dimerization of DBProDOT (b) Proposed mechanism for the autocatalyzed initiation of the SSP of DBProDOT .....	15
1.10 Generation of a 3D conjugated network by electropolymerization of a pseudo-tetrahedral precursor .....	20
1.11 Structure of TriaTh.....	20
1.12 Structure of various range of EDOT attached to bithiophene core .....	21
1.13 Structures of monomers used for the generation of microporous polythiophene networks.....	23
1.14 Structure of contorted conjugated microporous polymers <b>7-9</b> .....	24
1.15 Synthetic pathways toward the polythiophene networks.....	25
3.1 Polymers obtained from solid state polymerization.....	67
3.2 Scanning electron microscope images (x 5000) for the PEDOT (A), Polymer <b>44</b> (B) and PEDOT + 5% polymer <b>44</b> (C).....	69

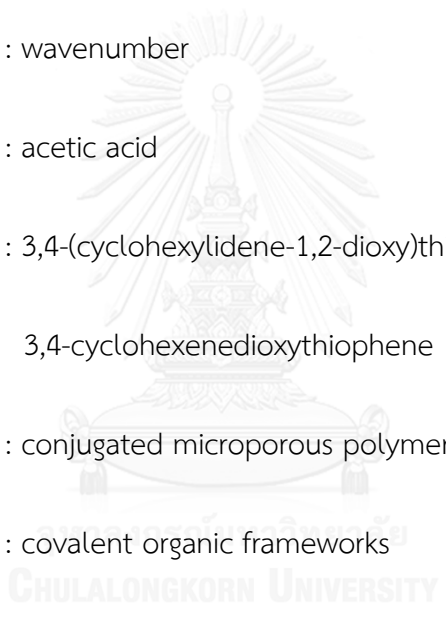
## LIST OF TABLES

Table	Page
1.1 General properties of some conducting polymers.....	2
1.2 Comparison between the chemical and electrochemical synthesis.....	10
1.3 Conductivity of PEDOT polymers. ....	13
1.4 Surface area for poly(aryleneethynylene) network.....	22
3.1 Conditions for the synthesis of diester <b>13</b> .....	52
3.2 Conditions for the synthesis of dihydroxythiophene <b>14</b> .....	54
3.3 Condition for the synthesis of compound <b>15</b> .....	55
3.4 Conditions for transesterification of DMT with glycerol.....	57
3.5 Percentage yields of brominated dioxothiophene monomers synthesis.....	65
3.6 Percentage yields of perbrominated linked multi-thiophenes synthesis.....	66
3.7 Conductivity of the synthesized polymers.....	70
3.8 $\lambda_{\max}$ of polymers from SSP.....	72

## LIST OF SCHEMES

Schemes	Page
3.1 Synthesis of Diethyl 3,4-dihydroxythiophene-2,5-dicarboxylate ( <b>14</b> ).....	51
3.2 Mechanism of Hinsberg reaction .....	53
3.3 Mechanism for substitution on epichlorohydrin .....	54
3.4 Synthesis of compound <b>17</b> .....	58
3.5 Synthesis of compounds <b>18</b> and <b>19</b> .....	58
3.6 Synthesis of compounds <b>20</b> and <b>21</b> .....	59
3.7 Synthesis of compound <b>22</b> .....	60
3.8 Synthesis of compound <b>26</b> .....	61
3.9 Synthesis of compound <b>27</b> .....	61
3.10 Reactions of EDTM with various acid chlorides.....	62
3.11 Bromination reaction on thiophene monomers through radical-initiated mechanism.....	64

## LIST OF ABBREVIATIONS



$^{13}\text{C}$ -NMR	: carbon-13 nuclear magnetic resonance spectroscopy
$^1\text{H}$ -NMR	: proton nuclear magnetic resonance spectroscopy
$\text{AlCl}_3$	: anhydrous aluminum chloride
cm	: centimeter
$\text{cm}^{-1}$	: wavenumber
$\text{CH}_3\text{COOH}$	: acetic acid
CDOT	: 3,4-(cyclohexylidene-1,2-dioxy)thiophene or 3,4-cyclohexenedioxythiophene
CMP	: conjugated microporous polymer
COFs	: covalent organic frameworks
CP	: conjugated polymer
d	: doublet (NMR), day (s)
dd	: doublet of doublet (NMR)
DBCOT	: 2,5-dibromo-3,4-(cyclohexylidene-1,2-dioxy)thiophene or 2,5-dibromo-3,4-cyclohexenedioxythiophene
DBEDOT	: 2,5-dibromo-3,4-ethylenedioxythiophene

DBEDTM	: 2,5-dibromo-3,4-ethylenedioxythiophene methanol
DCM	: dichloromethane
DMAP	: 4-dimethylaminopyridine
DMF	: <i>N,N</i> -dimethylformamide
DMT	: 3,4-dimethoxythiophene
EDOT	: 3,4-ethylenedioxythiophene
EDTM	: 3,4-ethylenedioxythiophene methanol
equiv	: equivalent (s)
EtOAc	: ethyl acetate
EtOH	: ethanol
eV	: electron volt
FeCl <sub>3</sub>	: anhydrous ferric chloride
g	: gram (s)
HH	: head to head
h	: hour (s)
HT	: head to tail
HCl	: hydrochloric acid
HCPs	: hyper-crosslink polymers



HOMO	: highest occupied molecular orbital
HRMS	: high resolution mass spectrometry
Hz	: hertz (s)
IR	: infrared spectroscopy
IUPAC	: international union of pure and applied chemistry
$J$	: coupling constant
LED	: light emitting diode
LUMO	: lowest unoccupied molecular orbital
M	: molar (s)
m	: multiplet (NMR)
MeOH	: methanol
min	: minute
mg	: milligram (s)
mL	: milliliter (s)
mmol	: millimole (s)
$M_n$	: number average molecular weight
mM	: millimolar
MOFs	: metal organic frameworks

MOPs	: microporous organic polymer
m.p.	: melting point
m/z	: mass per charge ratio (s)
MS	: mass spectrometry
Ms	: Methanesulfonyl
NaOH	: sodium hydroxide
NBS	: <i>N</i> -bromosuccinimide
nm	: nanometer (s)
°C	: degree Celsius
PA	: Polyacetylene
PANI	: Polyaniline
ppm	: parts per million (unit of chemical shift)
PPP	: poly( <i>p</i> -phenylene)
PPV	: poly( <i>p</i> -phenylene vinylene)
PPy	: Polypyrrole
PCDOT	: poly(3,4-(cyclohexylidene-1,2-dioxy)thiophene) or poly(3,4-cyclohexenedioxythiophene)
PDMT	: poly(3,4-dimethoxythiophene)

P3AT	: poly(3-alkylthiophene)
P3HT	: poly(3-hexylthiophene)
PT	: polythiophene
q	: quartet (NMR)
rt	: room temperature
s	: singlet (NMR)
st	: stretching vibration (IR)
S	: siemen
SEM	: scanning electron micrographs/microscope
SSP	: solid-state polymerization
PIMs	: polymers of intrinsic microporosity
PTSA	: <i>p</i> -toluenesulfonic acid
TEA	: triethylamine
$T_c$	: crystallization temperature
$T_m$	: melting temperature
TT	: tail to tail
t	: triplet (NMR)
TLC	: thin layer chromatography

Ts	: p-toluenesulfonyl
UV-Vis	: ultra-violet and visible spectroscopy
$\delta$	: chemical shift
$\lambda_{\max}$	: maximum wavelength
XRD	: X-ray powder diffraction



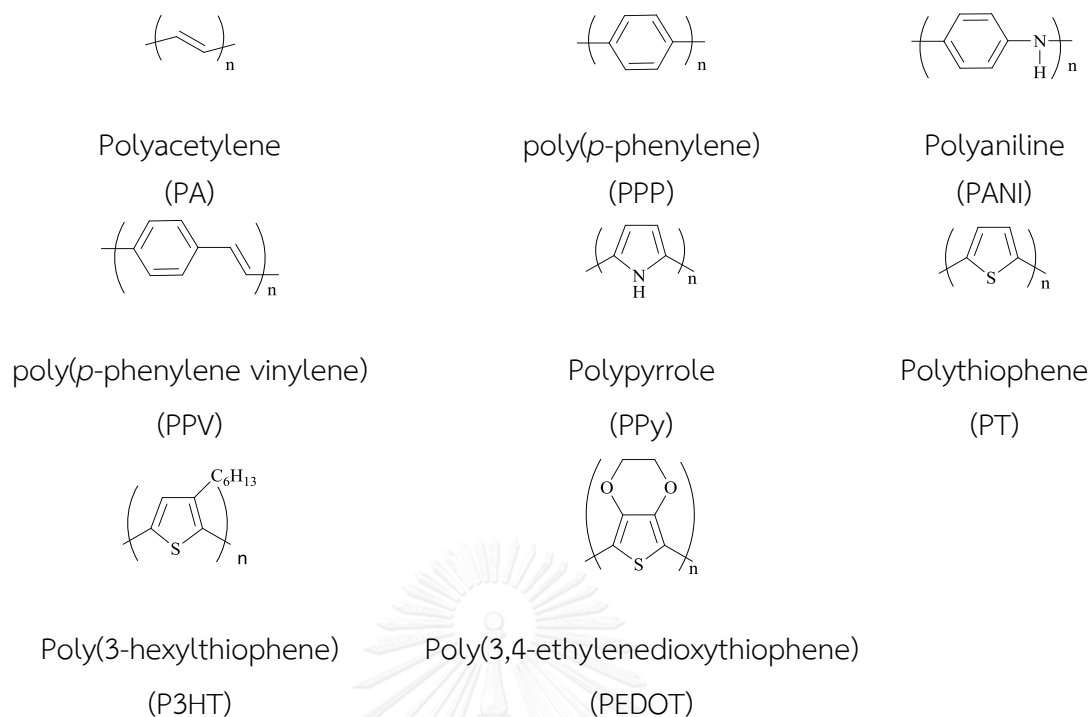
## CHAPTER I

### INTRODUCTION

#### 1.1 Conjugated polymers

In 1977, Shirakawa, MacDiarmid and Heeger found that conductivity of polyacetylene films could be increased by  $10^9$  times under oxidation with halogen vapor [1, 2]. This discovery was awarded the Nobel Prize in Chemistry in 2000 “for the discovery and development of electrically conductive polymers”. Further advance in the development of conjugated poly(heterocycles) was reported in 1979 by Diaz and coworkers with the polypyrrole (PPy) obtained as a free standing film by oxidative electropolymerization of pyrrole [3]. Since then, these conducting polymers were highlighted as interesting technology because of their unique properties [4]. This material has the electronic properties of a semiconductor with mechanical flexibility and potential ease of plastic processing. Moreover, conjugated polymers are suitable materials to be employed in the fabrication of electronic devices because their properties is tunable by chemical synthesis.

In the field of conjugated polymers, polythiophenes and their derivatives have received large attention because of their unique electrical properties, environmental stabilities, ease of derivatization and ability to be polymerized by various methods. Other polymers such as polyaniline, polypyrrole and poly(*p*-phenylene) (**Figure 1.1**) were also well known with inferior stability or conductivity (**Table 1.1**) [5].



**Figure 1.1** Structures of some conjugated polymers

**Table 1.1** General properties of some conducting polymers

Polymer	Conductivity (S/cm)	Stability (doped state)	Processing Possibility
Polyacetylene	$10^3$ - $10^5$	poor	limited
Poly( <i>p</i> -phenylene)	1000	poor	limited
poly( <i>p</i> -phenylene vinylene)	1000	poor	limited
Polypyrrole	100	fair	good
Polythiophene	100	good	excellent
Polyaniline	10	good	good

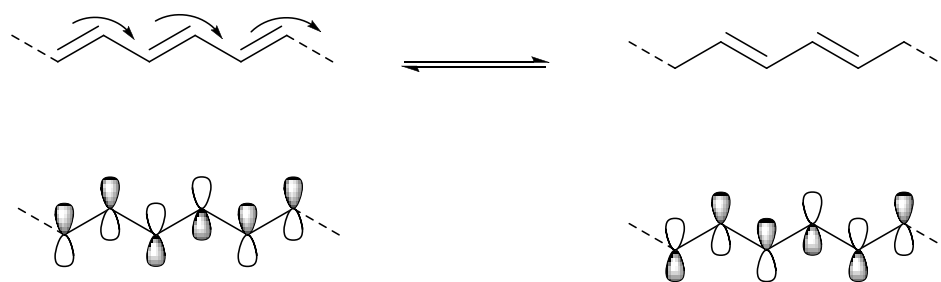
## 1.2 Applications of organic conducting polymers

The tunable and attractive properties of organic conducting polymers lead to their use in many applications such as:

- Applications utilizing the inherent conductivity of polymer : Antistatic coating (metal and polymer), microelectronic devices, naval vessels and stealth material for providing a minimum radar profile for military aircrafts [6]
- Polymer photovoltaics (light-induced charge separation) [7]
- Separation technologies : Novel smart-membrane, selective molecular recognition
- Electromechanical actuators : windows wipers in spacecrafts, Artificial muscles, rehabilitation gloves, bionic ears for deaf patients, electronic Braille screen [8]
- Electrochemical switching, energy storage and conversion : redox supercapacitors, new rechargeable battery,
- Cellular communication : Growth and control of biological cell cultures
- Corrosion protection
- Controlled release devices
- Thin film transistor [9]
- Sensor [10-12]
- Display technologies : Light emitting diode (LED), flat panel displays[13]
- Electrochromic windows or multichromic displays [14, 15]

### 1.3 Conjugated polymers and their conductive properties

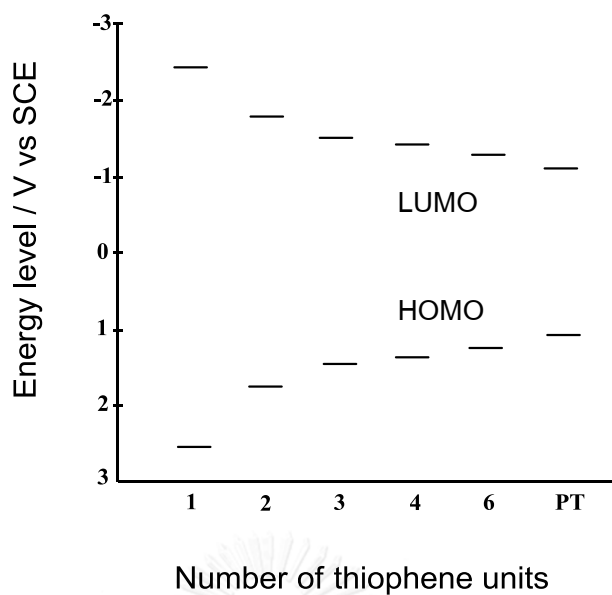
Conjugated polymers can be classified as organic semiconductors [16]. They contain a backbone with alternating single and double bonds between carbon-carbon or carbon-heteroatoms. **(Figure 1.2)** Conjugated polymers are imaged to be linear or rigid rods. In fact, they are not completely straight and flat, but twisted along their backbones. [17] The  $\pi$ -electrons from the  $sp^2$ -hybridized carbons form a delocalized  $\pi$ -system, which yield the semiconducting property.



**Figure 1.2** The delocalized  $\pi$  system of conjugated polymers

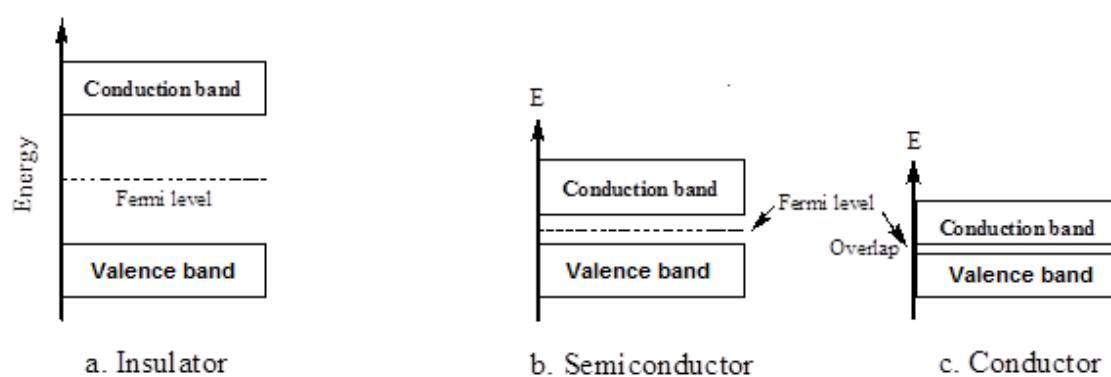
By linking a string of  $\pi$  bonds together, conjugated systems can be created such that the HOMO and LUMO of these extended systems merge into continuous bands similar to those inorganic semiconductors. By taking the  $E_{1/2}$  values for oxidation of thiophene oligomers and their onset of absorption from UV-Vis experiments, a plot of the position of the HOMO and LUMO can be shown in **Figure 1.3** [18, 19]. Thiophene can be oxidized at 2.07 V vs SCE and has a HOMO-LUMO separation of 5.0 eV based on UV-Vis experiments. Addition of a second thiophene ring to create bithiophene extends the conjugation and results in a lowering of both the energy gap and oxidation potential to 3.5 eV and 1.31 V, respectively [20]. As the  $\pi$ -system is extended further to sexithiophene, the values approach a saturation point with oxidation occurring at 0.83 V and an energy gap of 2.5 eV. Further extension leads to intractable solids and, at this point, addition of thiophene units results in properties that are “polythiophene-like.” Polythiophene (PT) oxidizes at 0.7 V, and its energy gap (or band gap) is 2.0 eV. [21, 22]





**Figure 1.3** HOMO and LUMO energy levels of oligo and polythiophenes

Materials may be placed in one of three categories depicted in **Figure 1.4** [23]. The valence band is defined as the total sum of all HOMOs, and is therefore lower in energy. The conduction band is made up of LUMOs and is consequently higher in energy.



**Figure 1.4** Band energy levels of an insulator, a semiconductor, and a conductor

Common molecular compounds are insulators. The band gap ( $E_g$ ) in these materials is too wide (over 3-4 eV) for any excitation of charge carriers to occur. The reason is that the valence band is made up of completely filled bonding orbitals, while the conduction band is constructed of anti-bonding orbitals of much higher energy. If a charge is injected into an insulator, it has no energetically favorable way to travel within the material. Semiconductors have a narrow bandgap (under 3 eV), which allows some excitation of charge carriers to the conduction band. Since the overlap between the two bands is not very efficient, semiconductors usually have conductivities much lower than true conductors. When the temperature of a semiconductor is lowered, the probability of thermal excitation to the conduction band is diminished, which explains why conductivity of semiconductors decrease with decreasing temperature.

Conductors have either an incomplete valence band which is the case for all transition metals with unoccupied d-orbitals, or a near-zero bandgap between the valence band and the conduction band. Both these situations lead to a continuous and partially filled band. Conductors have a very large number of charge carriers but are instead limited by a relatively low mobility. Thermal excitation leads to scattering of charges, which makes it less probable for them to move ideally along the current axis, hence lowering the conductivity. This explains why conductivity decreases with increasing temperature in metallic conductors.

#### 1.4 Doping process

Doping means the introduction of impurities into a semiconductor crystal that induce modification in conductivity. The modification of electrical conductivity of conducting polymers can be accomplished either by chemical or electrochemical doping. Both *n-type* (electron donating) and *p-type* (electron accepting) dopants have been used to induce an insulator-to-conductor transition in polymers. Unlike substitutional doping that occurs in conventional semiconductors, the dopants are interstitially positioned between  $\pi$ -conjugated polymers chain, and donate charges to or accept charges from the polymer backbone. In this case, the counter ion is not covalently bound to the polymer, but only attracted to it by the Coulombic force. In

self-doping cases, these dopants are covalently bound to the polymer backbone [24]. The strong coupling between electrons and phonons near the doped charges causes distortions of the bond lengths. For degenerate ground state polymers, doped charges at low doping levels are stored in charged solitons whereas nondegenerate systems, they are stored as charged polarons or bipolarons [25-28]. High doping nondegenerate polymers form a polaron lattice or electrically conducting partially filled energy band [29, 30]. Bipolarons or pairs of polarons are formed in less ordered regions of doped polymers [31].

### 1.5 Conductive Processes

In order for a polyheterocycle to exhibit metallic conductivity, it must be doped in high level. Intermediate doping results in charge carriers called polarons. There are unpaired spin in polaron, and they are radical cations or radical anions. They exhibit an EPR signal and are delocalized over four to five heterocycle rings. High doping levels result in formation of non spin dication bipolarons [16].

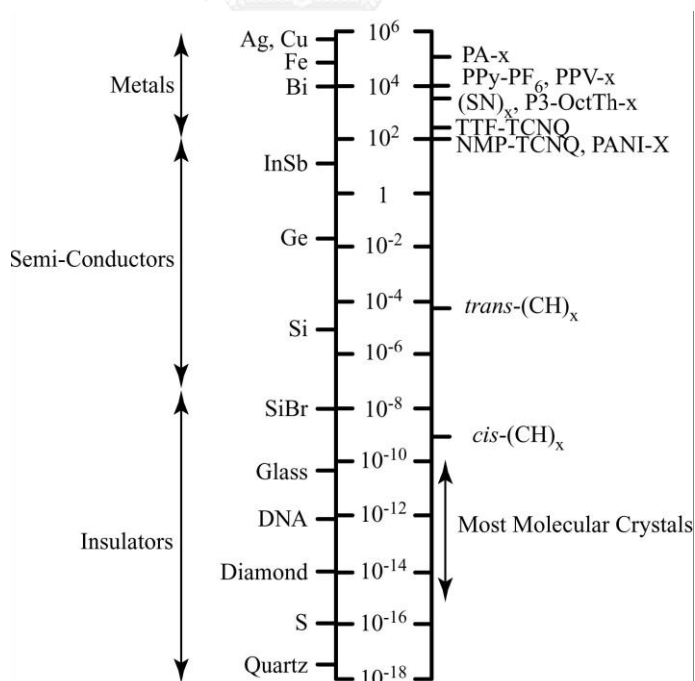


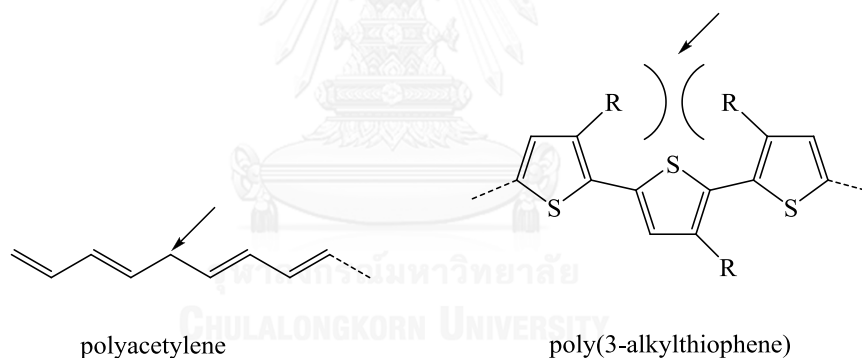
Figure 1.5 Conductivities of various metals and conjugated polymers

## 1.6 Effective conjugation length (ECL)

Ideal conducting polymers have totally delocalized  $\pi$  electrons in the conjugated unsaturated bonds along the whole chain. This requirement usually does not occur due to the following:

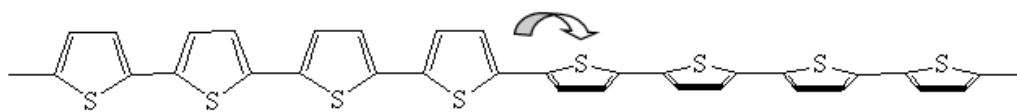
- i) defects in polymer chain
- ii) Twisting of planar structure

Examples of those two reasons above are shown in **Figure 1.6**. Formation of a defect in polyacetylene which is the saturated  $sp^3$ -hybridized methylene caused the disruptive effect to the electrons flow on polymer chain. In another case, the steric incumbent between adjacent R groups on HH thienyl units in irregular poly(3-alkylthiophene) brought about the twisting of the thienyl ring planes out of coplanarity, causing an increase of energy required to allow the flow of electrons through the polymer chain, which make the polymer chain less conductive.



**Figure 1.6** A defect in polyacetylene and steric induced structural twisting in poly (3-alkylthiophene)

Another reason might be the twisting of polymer chain, which randomly occur at the single bonds and divided the polymer into separated sections with their own coplanarity (**Figure 1.7**). This polymer chain twisting would also cause the reduction of conjugation in the polymer.



**Figure 1.7** Twisting of polythiophene

## 1.7 Polythiophene

Polythiophene composes of repeating five-membered sulfur heterocyclic monomeric units. It is also considered one of the most interested classes of conducting polymers in many applications [32]. It has environmental stability, structural versatility which allows their electrochemical and electronic properties to be modified by chemical means, and non-degenerate ground states in aromatic and quinoidal forms [33, 34]. For these reasons, polythiophene has been reported to be used in applications with the following characters:

- The electrical properties of the doped conducting state, (antistatic coating, EMI shielding, radiation detector, gas sensors, and corrosion protective films)
- The electrical properties of the neutral semiconducting state (non-linear optics and photovoltaic cell)
- The reversibility of electrochemical properties in the transition between the doped and the undoped states (new rechargeable battery, modified electrode, electrochemical sensor, and display devices) [34].

## 1.8 Synthesis of polythiophene

Initially, polythiophene can be obtained from electrochemical polymerization of thiophene monomers [35]. The yield of polymers prepared from electrochemical polymerization is moderate to low, and their structures are not well-defined and polymer film that produced at the anode surface after electropolymerization, are not easy to process further.

Compared to other chemical and electrochemical syntheses of conducting polymers (**Table 1.2**), the anodic electropolymerization of the monomer shows several advantages such as no presence of catalysts, easy control of the film thickness by deposition charge, possibility for doped conducting polymer to be

directly grafted onto the electrode surface and in situ characterization for the growing process of the polymer by electrochemical and/or spectroscopic techniques.

**Table 1.2** Comparison between the chemical and electrochemical synthesis

Polymerization Approach	Advantages	Disadvantages
Chemical Polymerization	Large scale production possible	Difficult to make thin film
	Post-covalent modification of bulk conjugated polymer (CP) possible	Complicated Synthesis
	More options to modify CP Backbone covalently	
Electrochemical Polymerization	Thin film synthesis possible	Difficult to remove film from electrode surface
	Ease of synthesis	
	Entrapment of molecules in CP	Post-covalent modification of bulk CP is difficult
	Doping is simultaneous	

Although electrochemical polymerization is a very useful method for preparing polymers such as polythiophene, poly(3-methylthiophene), and poly(3-phenylthiophene), the obtained polymers are infusible and insoluble, and their powder cannot be processed into a film or other useable forms [36]. Furthermore polythiophene is unstable at the potentials used for the electrochemical polymerization of thiophene. Consequently, the deposited thiophene on the anode at the earlier stage of the polymerization is overoxidized and damaged, while the process continues to produce new polymer.

The yield of polythiophene prepared from the oxidative polymerization with iron (III) chloride is relatively higher than the polymer prepared by electrochemical polymerization. Moreover, the molecular weight of polymer synthesized by this method is sufficiently high to be cast into a film. There are examples of polymers obtained from this method that are soluble in common organic solvents and their films can be formed by simply casting its solution on a solid substrate.

The study of the polymerization mechanism and polymerization conditions have been made by Amou and coworkers [37]. They discovered that lower concentration and temperature increased the HT coupling. Niemi and coworkers [38] performed a detailed study on the polymerization mechanism of 3-alkylthiophene with iron (III) chloride. The results revealed that only solid iron (III) chloride was active as an oxidative polymerization agent for 3-alkylthiophene while the soluble part of iron (III) chloride was inert. The solubility of iron (III) chloride in chloroform and the consuming effect of evolved hydrogen chloride gas explained the extra amount of iron (III) chloride that was initially necessary to obtain high conversion in polymerization.

Polymerization via the metal-catalyzed cross-coupling technique has been extensively investigated [39, 40]. The reaction proceeds by an oxidative addition of an organic halide with a metal catalyst and then transmetalation between the catalyst complex and a reactive Grignard or other organometallic reagent (or disproportionation), to form a diorganometallic complex. The last step includes reductive elimination of the coupled product with regeneration of the metal catalyst. Numerous organometallic species (including organomagnesium, organozinc, organoboron, organoaluminum, and organotin) have been demonstrated to be used in cross-coupling reactions with organic halides.

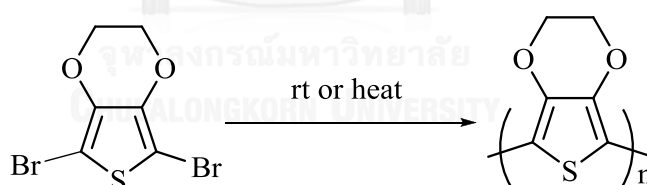
### 1.9 Solid state polymerization

Polymerization of PEDOT via traditional oxidative polymerization of 3,4-ethylenedioxythiophene (EDOT) with  $\text{FeCl}_3$  in organic solvents gives an insoluble blue-black polymer in form of powder. The limitations of traditional polymerization methods can be a serious problem for PEDOT applications as well as for in-depth investigation of molecular order in this conducting polymer. It is generally not possible to obtain a well-defined polymer structure, unless the synthesis of conducting polymers is carried out via pure chemical polymerization routes, without adding any catalyst. The possible solution for this problem lies in a solid-state polymerization of structurally pre-organized crystalline monomer. The first report of solid state polymerization was in 1962 by Magat [41] and was applied to conjugated

polymer in 1970 by Wegner on poly(diacetylenes) [42], and MacDiarmid, Heeger and co-workers on poly(sulfur nitride).[41, 43]

The advantages of solid-state polymerization includes low operating temperatures, which prevent side reactions and thermal degradation of production, while requiring inexpensive equipment, and uncomplicated and environmental friendly. For the solid-state polymerization at low temperatures, rate of the reactions are slow compared to polymerization in the melting phase because of the reduced mobility of the reacting species, and the slow diffusion of the by-products [44].

Meng and coworkers [45, 46] discovered the solid-state polymerization (SSP) of 2,5-dibromo-3,4-ethylenedioxythiophene (DBEDOT) by chance as a result of prolonged storage (2 years) at room temperature or heated (50-80 °C) of the monomer (**Figure 1.8**). The colorless crystalline DBEDOT transformed into a dark blue material while retaining the morphology. Surprisingly, the conductivity of this decomposition product appeared to be very high (up to 80 S/cm) for an organic solid. Indeed, the most likely explanation for the observed transformation was polymerization with formation of bromine-doped PEDOT.



**Figure 1.8** Solid-state polymerization of DBEDOT to PEDOT

Meng and coworkers have continued to study solid state polymerization (SSP) of other dihalogen-substituted derivatives of 3,4-ethylenedioxythiophene (EDOT), whose halogen atoms are Cl, Br or I, respectively.[45] The results showed that 2,5-dibromo-3,4-ethylenedioxythiophene (DBEDOT) is the most reactive monomer and polymerization reaction occurred via radical cationic polymerization which electron



donating group (3,4-ethylenedioxy group) enhanced the stability of cation intermediate.

The conductivity of different SSP-PEDOT samples was measured by the four point probe technique at room temperature (**Table 1.3**) [46]. The polymer prepared at lowest temperature and longest reaction time, showed the highest in conductivity which may reflect achievement of a higher degree of order. Indeed, heating above the monomer's melting point resulted in dramatically reduced conductivity (0.1 S/cm), which rised up to 5.8 S/cm after doping with iodine, approaching the value of an FeCl<sub>3</sub>-synthesized PEDOT (7.6 S/cm). Not very significant, but certain increase in conductivity of SSP-PEDOT (about 2 times) was found on exposing a sample to iodine vapor.

**Table 1.3** Conductivity of PEDOT polymer

Polymerization method	Conductivity ( $\sigma$ ) (S.cm <sup>-1</sup> )				
	SSP-PEDOT <sup>a</sup>			FeCl <sub>3</sub> -PEDOT <sup>b</sup>	
Reaction temperature (°C)	20	60	80	120	0-5
Reaction time	2 years	24 h	4 h	24 h	24 h
1. Crystal	80	33	20	- <sup>c</sup>	- <sup>c</sup>
2. Pellets as synthesized	30	18	16	0.1	- <sup>d</sup>
3. Pellets after I <sub>2</sub> doping	53	30	27	5.8	7.6

<sup>a</sup> Prepared from solid state polymerization (SSP)

<sup>b</sup> Prepared from oxidative coupling polymerization by FeCl<sub>3</sub>

<sup>c</sup> cannot be obtained

<sup>d</sup> very small value

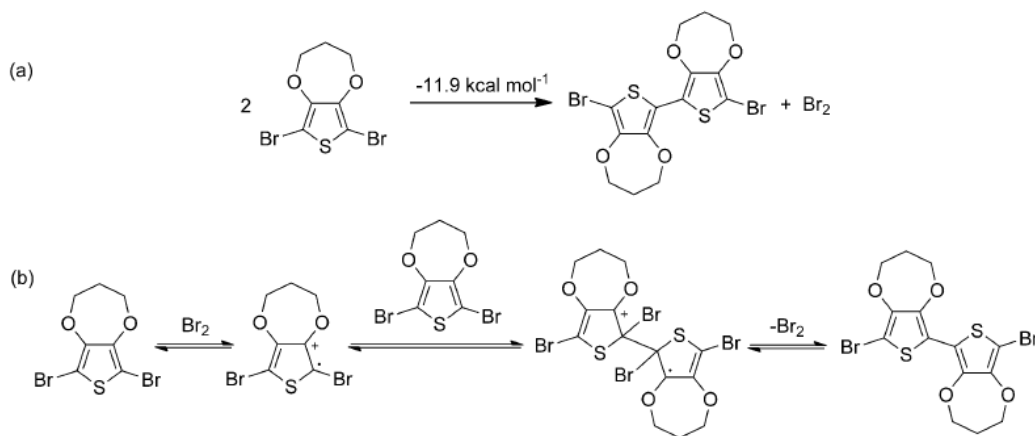
From the experiment, they concluded that heating the solid state DBEDOT resulted in an unprecedented self-coupling reaction which yield highly conductive and relatively well-ordered bromine-doped PEDOT. Furthermore, heating DBEDOT above its melting point resulted in polymer with a lower conductivity.

As a unique derivative of polythiophene, poly(3,4-ethylenedioxythiophene) (PEDOT), possesses several advantageous properties compared with unsubstituted polythiophene and polythiophene derivatives. PEDOT had received considerable

interests attributable to its low band gap, high electrical conductivity, excellent optical transparency in the visible region and good stability. Ether groups at  $\beta, \beta'$  positions of thiophene ring in PEDOT can prevent the formation of  $\alpha\text{-}\beta'$  linkages defect during polymerization process. Thus derivatization of thiophene ring by other substituents such as alkoxy or polyether groups at the  $\beta$  positions could lead to higher solubility and improved physical and chemical properties. Solid state polymerization (SSP) of their new structurally pre-organized crystalline monomers could also result in another well-defined polymer structures with high conductivity. Moreover, this method was uncomplicated, had environmental friendly procedures and less side reactions.

Eunyoung and coworker [47] have studied the solid state polymerization of 2,5-dibromo-3,4-propylenedioxythiophene (DBProDOT) which are another thiophene derivatives that can be prepared by SSP. They found that the result of crystallographic studies revealed a short interplane distance between DBProDOT molecules, which was responsible for polymerization at low temperature with a lower activation energy and higher exothermic reaction than 2,5-dibromo-3,4-ethylenedioxythiophene (DBEDOT) or its derivatives. To elucidate the reaction mechanism, the energy of each structure was calculated by the Gaussian 03 program. The dimerization of DBProDOT was exothermic at 11.9 kcal/mol, releasing more energy than the dimerization of DBEDOT (11.2 kcal/mol) and dibromothiophene (8.3 kcal/mol, **Figure 1.9a**). In radical polymerization in the dark, the homolytic cleavage energy of a C-Br bond in DBProDOT was 87.0 kcal/mol, which barely progresses at room temperature. The electron donating dioxypropylene ring in DBProDOT stabilized the cation of the heterolytic cleavage of the C-Br bond in oxidative polymerization. In **Figure 1.9b**, the first step for the production of a DBProDOT carbocation by bromine requires a high activation energy of 115.2 kcal/mol, which makes it the rate-determining step. Nonetheless, this value is smaller than that for the DBEDOT reaction. The second step for the production of a dimerized carbocation releases 11.0 kcal/mol, and the last step for the release of bromine is exothermic with 116.1 kcal/mol. Thus, SSP for DBProDOT is an energetically favorable process and is autocatalyzed by the bromide ions  $\text{Br}^-$  and  $\text{Br}_3^-$ . Despite the ordered structure

of PProDOT and steric bulkiness, the activation energy of the oligomerized carbocations is less than that of the dimerized carbocations, mainly because of the formation of a stable delocalized structure in the oligomer.



**Figure 1.9** (a) Calculated energy for dimerization of DBProDOT (b) Proposed mechanism for the autocatalyzed initiation of the SSP of DBProDOT

### 1.10 Porous materials

Porous materials play vital roles in many fields of science and technology and have attracted much attention as a useful platform for advanced functional material design. Historically, the skeleton structure of porous material has evolved from the inorganic open framework of zeolite and mesoporous silicates [48] to metal-organic frameworks (MOFs) [49] and recently organic porous materials [50]. Organic porous materials can be constructed by noncovalent and covalent approaches.

Porous polymer is the sub class of organic porous materials. It was defined as polymeric material containing many pores. According to the IUPAC recommendation, [51] microporous polymers are defined as polymeric materials with pore size smaller than 2 nm in diameter, mesoporous polymers with pore size in the range of 2–50 nm, and macroporous polymers with pore size larger than 50 nm. Pores with a smaller size (e.g., micropores) contribute predominantly to the generation of materials with high surface area. In addition to the physical structure of the pores, the functionalities of the polymer framework and pore surface are also important. The framework and pore surface functionalities can be engineered through the use

of functional monomers or by postmodification processes. The ability to control the structure of pores and incorporate desired functionalities into the material has benefited from the great strides being made in the preparation of porous polymers by various synthetic methods. Microporous materials have garnered considerable attention from both the academic and the industrial communities due to their wide range of potential applications in storage, separation, and catalysis [52]. There are several different classes of microporous organic polymer (MOP), such as hypercrosslinked polymers (HCPs) [53], polymers of intrinsic microporosity (PIMs) [54], and covalent organic frameworks (COFs) [55]. MOPs can be classified as either amorphous (HCPs, PIMs) or crystalline (COFs).

There are three distinct strategies for the synthesis of polymers with inherent microporosity. First, excess free volume can be trapped by the formation of an amorphous hypercrosslinked polymer network, which on removal of the included solvent provides a predominantly microporous material. Second, polymers (e.g., polymers of intrinsic microporosity) can be designed to possess macromolecular structures that are both rigid and contorted so as to pack space very inefficiently, resulting in a large amount of interconnected free volume. Such polymers with “intrinsic” microporosity may be a network or a non-network polymer; the former may also trap additional excess free volume, whereas the latter can be soluble and, therefore, solvent processable.

In contrast to traditional syntheses of polymers, where long chains of polymerized monomers are interconnected by ditopic cross-linkers, porous polymers are generally constructed from monomer units that are multitopic (three or more connection points). These multitopic monomeric precursors generate the linkages between polymer chains after polymerization in which each chain is kept far apart by void space near the linkers. The presence of the interchain space leads to the porous materials.

### **1.11 Conjugated microporous polymer**

Conjugated microporous polymers (CMPs) constitute the typical classes of covalently linked organic porous materials and feature high porosity, light weight

elements and strong covalent linkages [56]. Among these covalently linked organic porous materials, CMPs are a class of amorphous materials that permit the linking of building blocks in a  $\pi$ -conjugated fashion and possess three-dimensional (3D) networks. These structural features are unique and are not available in other porous materials, which are typically not  $\pi$ -conjugated, or conventional conjugated polymer, which are nonporous. Since the first discovery of CMP by Jiang and coworkers [57], many chemists and materials scientists have joined this field of study and contributed to the rapid growth of the CMP family. From a molecular design perspective, the most characteristic feature of CMPs is the rather broad diversity of  $\pi$  units. Building blocks ranging from simple phenyl units to extended arenes, heterocyclic aromatic units and large macrocycles have been successfully exploited for the synthesis of CMPs. Because there is less limitation on size, geometry and functional groups, CMPs can be systematically tuned their  $\pi$ -conjugated porous architectures and allowed for the optimization of the skeleton and properties. From a synthetic perspective, chemical reactions for synthesizing linear conjugated polymers, such as the Suzuki cross-coupling reaction, Yamamoto reaction, Sonogashira–Hagihara reaction, oxidative coupling, Schiff-base reaction, cyclotrimerization, phenazine ring fusion reaction and Friedel–Crafts arylation, are effective for the preparation of CMPs. The diversity of building blocks, coupled with the wide availability of different reaction types, make CMPs an invaluable platform for developing new organic porous materials. To construct a conjugated skeleton, the synthetic reaction must covalently link building blocks with a  $\pi$ -conjugated bond. Because building blocks can have different geometries, reactive groups and  $\pi$  systems, this structural diversity significantly enhances the flexibility of the design of both skeletons and pores. CMPs are usually obtained as insoluble powders which is the main obstacle that prevents it from forming thin film product by solution processes.

### 1.12 Application of CMP

CMPs are unique in that they are nanoporous and  $\pi$ -conjugated, whereas their structures can be designed at the molecular level and synthetically controlled.

By virtue of high surface areas and microporous characteristics, CMPs have emerged as a new class of porous materials for gas adsorption and storage applications. The pores provide open space and are accessible to various guest molecules and metal ions, allowing for the construction of supramolecular structures and organic–inorganic hybrids. Most importantly, CMPs allow the complementary utilization of  $\pi$ -conjugated skeletons and nanopores for functional exploration. For examples:

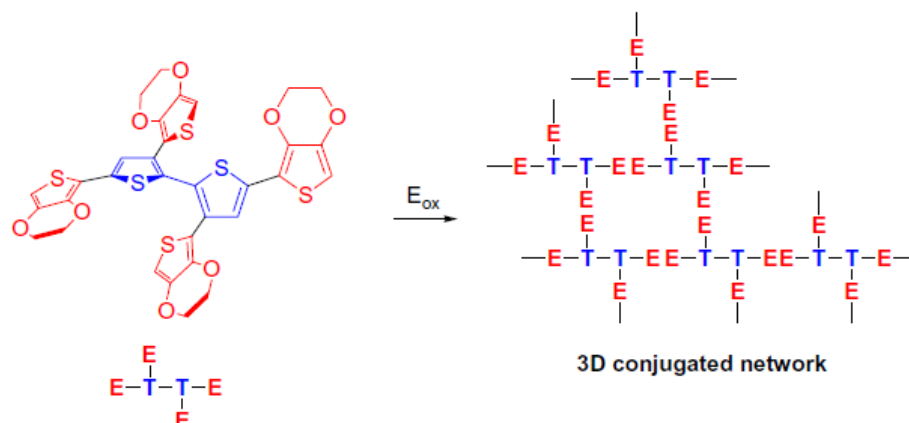
- Gas adsorption and storage: CMPs have been widely explored for the adsorption and storage of gases, such as hydrogen, carbon dioxide and methane. In addition to the control over porosity provided by synthetic methods, the pore environment can be modified by introducing functional units to the wall surface. This surface functionalization is an important and effective way to enhance the capacity and selectivity of a specific gas [58, 59].
- Encapsulation of dyes, solvents and other chemicals: In addition to gases, the pores of CMPs are accessible to toxic chemicals, organic solvents, dyes and fullerenes, expanding the encapsulation scope of CMPs. The introduction of a hydrophobic unit, such as fluorine, endows CMPs with hydrophobic pores, whereas hydrophilic groups can enhance the hydrophilicity of the porous materials [60].
- Heterogeneous catalyst: CMPs are characterized by their capabilities of integrating various functionalities into their skeletons. Introduction of catalytic sites to the skeletons endows CMPs with built-in catalytic sites. Due to their 3D open frameworks, CMPs constitute a new type of nanoreactor that allows the complementary utilization of skeletons and pores [61].
- Light emitter: Extended  $\pi$  conjugation over their 3D skeletons endows CMPs with a high probability of preparing highly efficient luminescent materials [62].
- Chemosensors: Conjugated polymers are fascinating materials with  $\pi$  conjugation and light-emitting properties that allow for the detection of various chemicals. Specific sites that interact with target

compounds can be introduced into conjugated chains to enhance the interaction interface and improve the signaling activity. CMPs are attractive candidates because they possess large surface areas and provide a broad interface for analyte interaction [63].

- Light harvesting and excitation energy transduction: A variety of light-harvesting systems have been studied and attracted much attention due to their potential for artificial photosynthesis. Among them, CMPs that bear conjugated skeletons and inherent micropores are fascinating platforms because CMPs allow for building supramolecular light-harvesting systems by encapsulating energy acceptors within the micropores [64].
- Electrical energy storage and power supply: Supercapacitors are energy storage and power supply devices that are in increasing demand with the broadening of applications such as vehicles and electric devices. Supercapacitive energy storage operates on the electric double layer by accumulation of charges at the electrode/electrolyte interface, where the stored energy is proportional to the capacitance of the electrode. Therefore, a breakthrough in electrode materials holds the key to fundamental advances in supercapacitors [65].

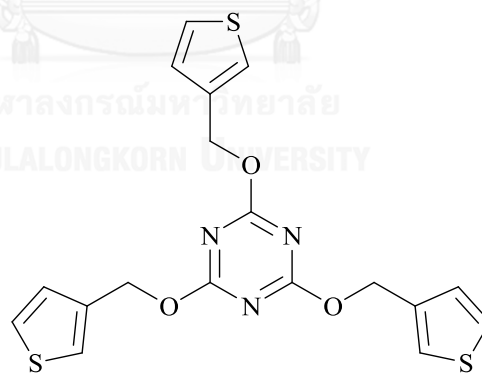
### 1.13 Multitopic thiophene precursors

There are some examples of multitopic thiophene monomer unit. Since the polymerization of those molecules will lead to the formation of CMPs. In 2008 Roncali and coworkers [66] have synthesized first three-dimensional  $\pi$ -conjugated system based on 3,4-ethylenedioxythiophene (EDOT) (**Figure 1.10**) by electro polymerization of the linked multi units of EDOT, but the porous properties of this polymer has not been observed.



**Figure 1.10** Generation of a 3D conjugated network by electropolymerization of a pseudo-tetrahedral precursor

In 2009, Ak and Toppare [67] have synthesized star shaped thiophene functionalized monomer: 2,4,6-tris(4-(1H-pyrrol-1-yl)phenoxy)-1,3,5-triazine (TriaTh). (**Figure 1.11**) Spectroelectrochemical analysis reflected that copolymer films have low  $\pi$  to  $\pi^*$  electronic transitions (386 nm) and high band gap (1.97 eV).



TriaTh

**Figure 1.11** Structure of TriaTh

In 2010, Roncali and coworkers [68] have continued their work on three-dimensional  $\pi$ -conjugated system based on 3,4-ethylenedioxythiophene (EDOT)



(Figure 1.12). Three-dimensional conjugated architectures involving conjugated branches with terminal EDOT groups attached onto a bithiophene core twisted by steric interactions have been synthesized by Stille coupling reactions. The UV-Vis absorption spectra recorded in solution showed complex spectral features that depended on both size and chemical structure of the main conjugated segment and of the conjugated side chains. Thanks to the fixation of the terminal EDOT groups, these compounds undergo straightforward and complete electropolymerization to produce stable electrode materials. The analysis of the electrochemical and optical properties of the polymers by cyclic voltammetry and spectroelectrochemistry suggests that the electrochemical coupling of the terminal EDOT groups leads to the formation of  $\pi$ -conjugated networks the electrochemical and optical properties of which can be tuned through the length and chemical composition of the oligomeric conjugated links.

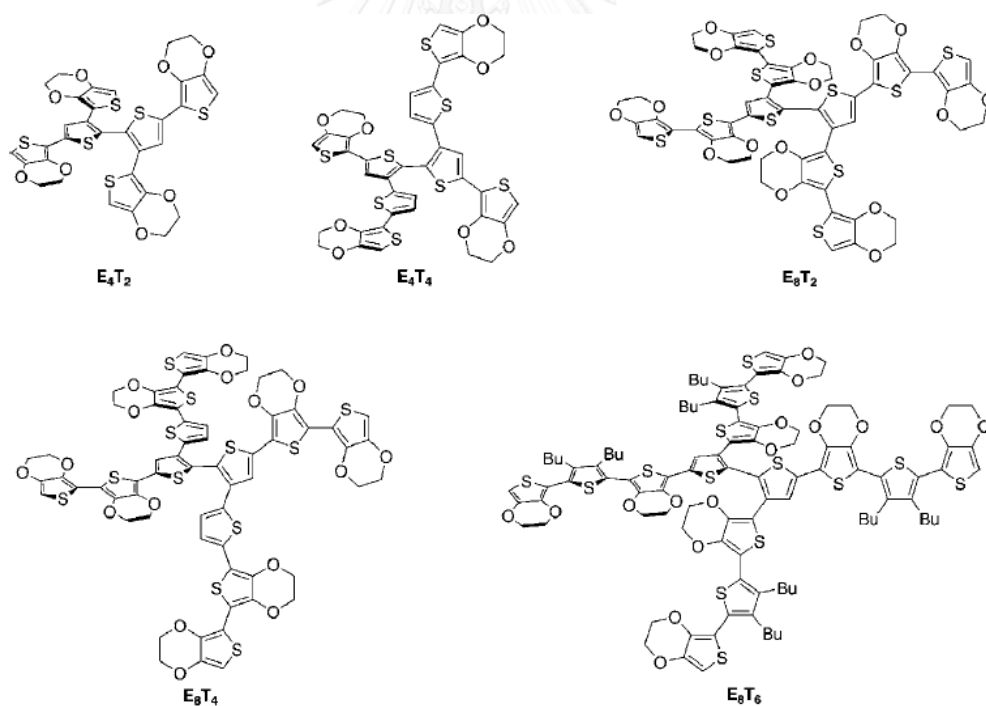
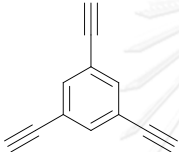

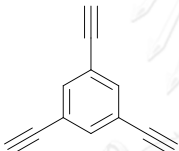
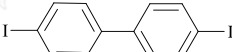
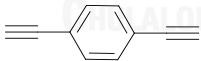
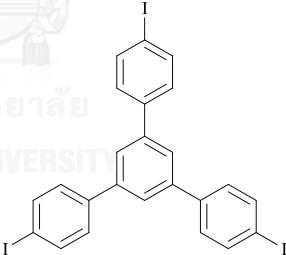
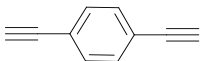
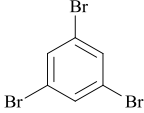


Figure 1.12 Structure of various range of EDOT attached to bithiophene core

### 1.14 Literature review

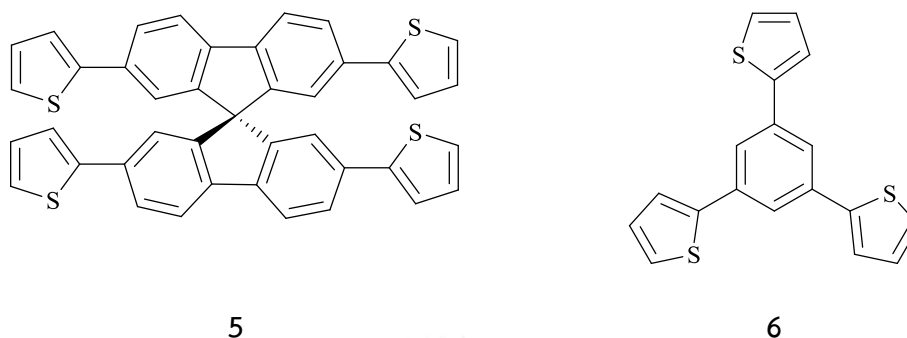
In 2007, Cooper and coworkers [57] have synthesized porous poly(aryleneethynylene) networks using palladium-catalyzed Sonogashira–Hagihara cross-coupling (Table 1.4). They have demonstrated systematic control over micropore size distribution by varying the structure of the monomers. The micropore size was directly correlated to the dimensions and geometry of the precursor molecules.

**Table 1.4** Surface area for poly(aryleneethynylene) network

CMP	Alkyne monomer	Halogen monomer	$S_{\text{BET}}$ [m <sup>2</sup> g <sup>-1</sup> ]
1			834
2			634
3			522
4			744

In 2009, Thomas and coworkers [69] have synthesized a new class of microporous conjugated polymers, namely poly(arylene thienylene)s, based on thiophene linkages. They have synthesized 2,2',7,7'-tetrakis(2-thienyl)-9,9'-spirobifluorene (Compound 5) and 1,3,5-tris(2-thienyl)benzene (compound 6) which

can be polymerized using  $\text{FeCl}_3$ . (**Figure 1.13**) The resulting powders exhibited very high surface areas of 577 and 1060  $\text{m}^2/\text{g}$ , respectively.



**Figure 1.13** Structures of monomers used for the generation of microporous polythiophene networks

In 2010, Cooper and coworkers [70] have synthesized a series of contorted conjugated microporous polymer networks using Sonogashira-Hagihara cross-coupling on a contorted monomer: spiro-bis(2,5-dibromopropylenedioxythiophene). (**Figure 1.14**) The polymers show enhanced surface areas and exhibit a reversibly adsorption of 1.71% hydrogen by mass at 1.13 bar/77 K. While they do not anticipate applications in  $\text{H}_2$  storage by simple physisorption, these polymers are highly porous and represent a new class of cross-linked CMP-containing thiophene in the backbone. These discoveries suggested the possibility for producing composite photovoltaic materials or conducting microporous materials by introducing low band-gap units into the polymer chain.

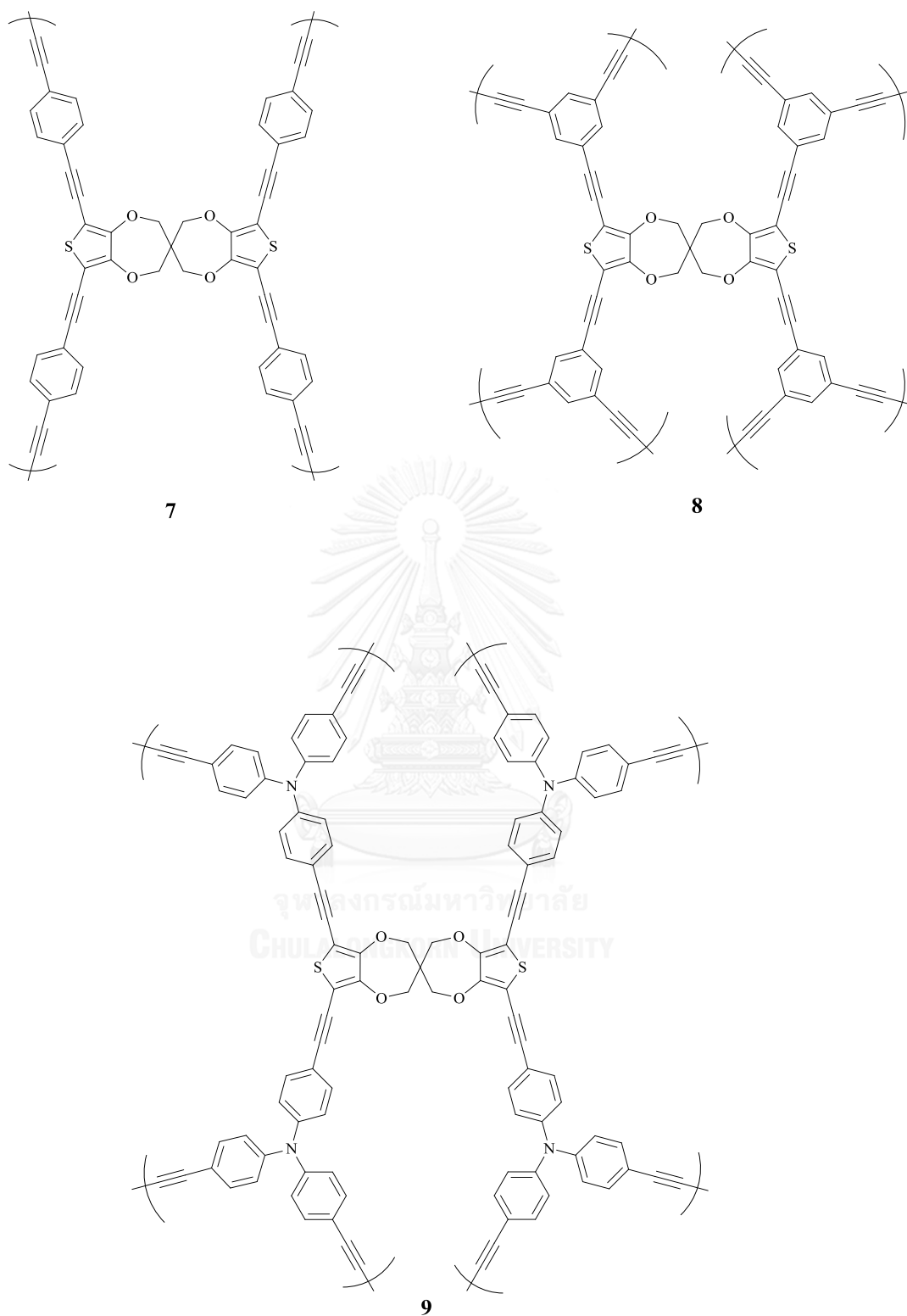
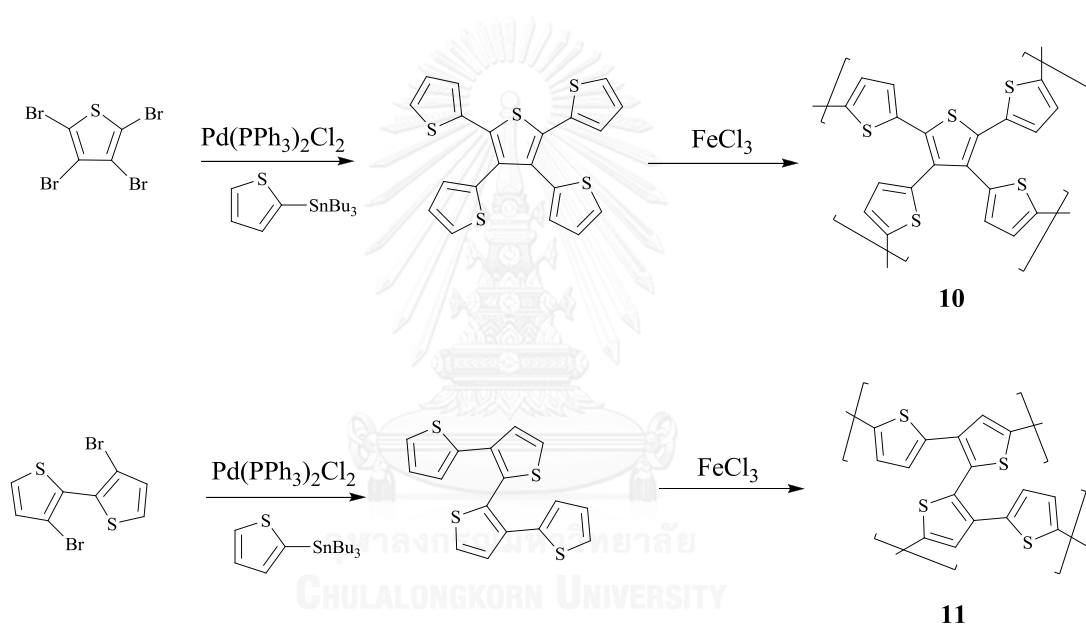


Figure 1.14 Structure of contorted conjugated microporous polymers 7- 9

In 2014, Yang and coworkers [71] have synthesized two conjugated porous polymers with different steric configuration. (**Figure 1.15**) The two polymers have almost equal BET surface areas of 57.72 m<sup>2</sup>/g and 62.97 m<sup>2</sup>/g respectively, but exhibit different CO<sub>2</sub> uptake capacity even with identical chemical constitution. This resulted from the different aggregated morphologies. This work demonstrates that design of initial monomer with specific geometries can change the polymer aggregated morphology, which could influence the gas isotherms enthalpies and adsorption capacity. In other words, the gas adsorption capacity depends not only on the high BET area, but also on the aggregated morphology of the material.



**Figure 1.15** Synthetic pathways toward the polythiophene networks

### 1.15 Statement of the problem and objectives

As only few examples of conjugated microporous polymers (CMP) based on 3,4-dioxythiophenes were reported, the possibilities of creating new porous materials carrying beneficial features of this versatile group of conjugated polymers are still vastly available. The ease and varieties of polymerization methods allow these polythiophenes, especially PEDOT derivatives, to be the prime target. Consequently, the goal of this project is to synthesize new conjugated microporous polymer (CMP)

from multitopic EDOT monomers carrying 2 or more thiophene units that linked together by appropriate linkers. Furthermore, new thiophene derivatives relating to PEDOT are designed and prepared to extend the utility of efficient solid state polymerization (SSP) with the prospect to apply towards constructing new CMP.



## CHAPTER II

### EXPERIMENTS

#### 2.1 Chemicals

Thin layer Chromatography (TLC) was performed on aluminum sheets precoated with silica gel (Merck Kieselgel 60 F<sub>254</sub>, Merck KGaA, Darmstadt, Germany). Column chromatography was performed using 0.063-0.200 mm or 70-230 mesh ASTM silica gel 60 (Merck Kieselgel 60 G, Merck KGaA, Darmstadt, Germany). Solvents used in synthesis were reagent or analytical grades. Solvents used in column chromatography were distilled from commercial grade prior to use. Other reagents were purchased from the following vendors:

- RCI Labscan (Bangkok, Thailand): acetone, acetonitrile, chloroform, dichloromethane, dimethylsulfoxide (DMSO), dimethylformamide (DMF), nitric acid (HNO<sub>3</sub>), sodium hydrogen carbonate (NaHCO<sub>3</sub>)
- Acrös Organics (New Jersey, USA): 1,2-dibromoethane, dimethyl sulfate ((CH<sub>3</sub>)<sub>2</sub>SO<sub>4</sub>), *N*-bromosuccinimide (NBS), *p*-toluenesulfonic acid (PTSA), quinoline,
- Carlo Erba (Milan, Italy): fuming nitric acid, Iodine, sodium azide (NaN<sub>3</sub>), triethylamine (TEA).
- Merck Co. (Darmstadt, Germany): acetic acid (AcOH), chloroacetyl chloride, concentrated hydrochloric acid, concentrated sulfuric acid, diethyl ether (Et<sub>2</sub>O), absolute ethanol (EtOH), glycerol, epichlorohydrin, sodium hydroxide (NaOH).
- Ajax Finechem Pty (Auckland, New Zealand): calcium chloride
- Cambridge Isotope Laboratories (USA): deuterated chloroform (CDCl<sub>3</sub>), deuterated dimethylsulfoxide (DMSO-*d*<sub>6</sub>)
- Aldrich (USA): diethyl oxalate (CO<sub>2</sub>Et)<sub>2</sub>, ethyl chloroacetate, 3,4-dimethoxythiophene (DMT), deuterium oxide (D<sub>2</sub>O), 3,4-ethylene-dioxythiophene (EDOT), malonylchloride, 1,4-phenylene diisocyanate, terephthaloylchloride, *p*-toluene sulfonyl chloride, 1,3,5-benzene tricarbonyl

trichloride, cuprous oxide ( $\text{Cu}_2\text{O}$ ), epichlorohydrin, potassium carbonate ( $\text{K}_2\text{CO}_3$ ), propionyl chloride, sodium metal

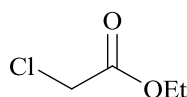
- KENTO (Japan): methanesulfonyl chloride
- TCI-EP (Japan): trans-1,2-cyclohexanediol
- Panreac (Spain): anhydrous magnesium sulfate ( $\text{MgSO}_4$ )

## 2.2 Instruments and equipment

Melting points were determined with a Stuart Scientific Melting Point SMP10 (Bibby Sterlin Ltd., Staffordshire, UK). FT-IR spectra were recorded on a Nicolet 6700 FT-IR spectrometer.  $^1\text{H}$  and  $^{13}\text{C}$  NMR spectra were obtained in deuterated chloroform ( $\text{CDCl}_3$ ), deuterated dimethylsulfoxide ( $\text{DMSO}-d_6$ ) or deuterium oxide ( $\text{D}_2\text{O}$ ) using Varian Mercury NMR spectrometer operated at 400.00 MHz for  $^1\text{H}$  and 100.00 MHz for  $^{13}\text{C}$  nuclei (Varian Company, USA). Mass spectra were recorded on Waters Micromass Quattro micro API ESCi (Waters, USA). Samples were dissolved in EtOAc, MeOH, acetone or water. UV-Vis absorption spectra were recorded on an Agilent 8453E UV-Visible spectroscopy. Conductivity of each polymers were measured by 4-point probe technique using Keithley Semiconductor Characterization System 4200. Surface morphologies of the polymers were analyzed by scanning electron microscope JEM-2100 (JEOL, Tokyo, Japan). High resolution mass spectra were recorded on microTOF-Q II 10335.

## 2.3 Monomer Synthesis

### 2.3.1 Ethyl chloroacetate (12)



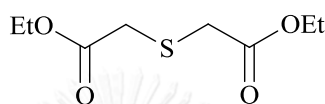
12

50 mL (56.510 g, 0.50 mol) of chloroacetyl chloride was slowly added into 32 mL (25.4 g, 0.55 mol) of EtOH over period of 30 min. The reaction mixture was stirred at 0 °C and then warmed to room temperature and stirred for another 3 h. The mixture was quenched by adding 120 mL of 2 M NaOH. The organic layer was



separated and the aqueous layer was extracted with diethyl ether three times. The combined organic layers were dried over anhydrous  $\text{MgSO}_4$ . The solvent was removed using rotary evaporator to give an almost quantitative yield of **1** as colorless liquid (55 mL, 99%).  $^1\text{H}$  NMR (400 MHz,  $\text{CDCl}_3$ ):  $\delta$  (ppm) 4.24 (q,  $J = 7.2$  Hz, 2H), 4.04 (s, 2H), 1.29 (t,  $J = 7.2$  Hz, 3H) (Figure A.1, Appendix A).  $^{13}\text{C}$  NMR (100 MHz,  $\text{CDCl}_3$ ):  $\delta$  (ppm) 167.3, 62.2, 40.9, 14.0 (Figure A.2, Appendix A).

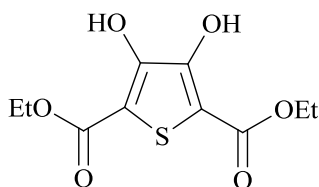
### 2.3.2 Diethyl thiodiglycolate (13)



**13**

Solution of sodium sulfide nonahydrate ( $\text{Na}_2\text{S}\cdot 9\text{H}_2\text{O}$ , 12.0 g, 50 mmol) in water (30 mL) was added dropwise to the solution of compound **12** (13.240 g, 55 mmol) in acetone (50 mL). The reaction was stirred and refluxed for 3 h under nitrogen atmosphere. After cooling back to room temperature, the organic layer was separated and the aqueous layer was extracted with diethyl ether three times. The combined organic layers were dried over anhydrous  $\text{MgSO}_4$  and then evaporated by a rotary evaporator to give compound **2** as a yellow liquid (5.030 g, 45%).  $^1\text{H}$  NMR (400 MHz,  $\text{CDCl}_3$ ):  $\delta$  (ppm) 4.19 (q,  $J = 7.1$  Hz, 4H), 3.37 (s, 4H), 1.28 (t,  $J = 7.2$  Hz, 6H) (Figure A.3, Appendix A).  $^{13}\text{C}$  NMR (100 MHz,  $\text{CDCl}_3$ ):  $\delta$  (ppm) 169.5, 61.1, 33.3, 13.9 (Figure A.4, Appendix A). MS:  $[\text{M}+\text{Na}]^+$   $m/z = 229.05$  (Figure A.5, Appendix A) [72].

### 2.3.3 Diethyl 3,4-dihydroxythiophene-2,5-dicarboxylate (14)

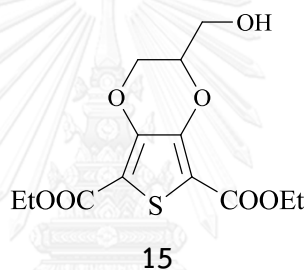


**14**

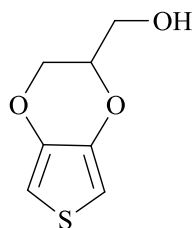
Sodium metal (4.0 g, 0.35 mol) was dissolved in EtOH (75 mL) and then added dropwise to a mixture of compound **2** (4.217 g, 0.021 mol) and diethyl oxalate (7.2 g, 0.05 mol) over 30 min in ice bath. The reaction mixture was refluxed for

additional 3 h under nitrogen, cooled to room temperature, poured into water (400 mL) and acidified by concentrated hydrochloric acid (15 mL) to afford a yellow precipitate. The filtered solid was recrystallized from methanol to give **14** as white needle crystals (3.502 g, 68%). mp. 134-135 °C.  $^1\text{H}$  NMR (400 MHz,  $\text{CDCl}_3$ ):  $\delta$  (ppm) 9.36 (s, 2H), 4.39 (q,  $J = 7.1$  Hz, 4H), 1.38 (t,  $J = 7.1$  Hz, 6H) (Figure A.6, Appendix A).  $^{13}\text{C}$  NMR (100 MHz,  $\text{CDCl}_3$ ):  $\delta$  (ppm) 165.5, 151.6, 107.1, 61.7, 14.0 (Figure A.7, Appendix A). IR (ATR,  $\text{cm}^{-1}$ ): 3305 (-OH st), 2981 (-CH st), 1690 (C=O st), 1663 (C=C st) (Figure A.8, Appendix A). MS:  $[\text{M}+\text{H}]^+$   $m/z = 250.20$  (Figure A.9, Appendix A) [73].

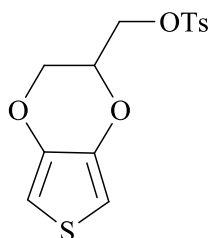
#### 2.3.4 Diethyl 2-(hydroxymethyl)-2,3-dihydrothieno[3,4-*b*]-1,4-dioxine-5,7-dicarboxylate (**15**)



Compound **14** (0.260 g, 1.0 mmol), epichlorohydrin (0.47 mL, 6.0 mmol) and  $\text{K}_2\text{CO}_3$  (0.28 g, 2.0 mmol) were mixed in EtOH (20 mL). The reaction was stirred and refluxed at 80 °C for 72 h under nitrogen atmosphere. The reaction mixture was quenched by 10% hydrochloric acid solution and then extracted twice with chloroform. The combined organic layers were washed by 2 M NaOH, dried over anhydrous  $\text{MgSO}_4$ , and evaporated using rotary evaporator to get yellow solid. The crude mixture was purified by passing through a silica gel column, eluted with hexane:ethyl acetate (2:1) to yield a light yellow solid (0.180 g, 57%).  $^1\text{H}$  NMR (400 MHz,  $\text{CDCl}_3$ ):  $\delta$  (ppm) 4.47 (m, 2H), 4.36 (m, 1H), 4.27 (m, 2H), 3.94 (q,  $J = 12.5$ , 4H), 1.36 (s, 1H), 1.33 (t, 6H) (Figure A.10, Appendix A).  $^{13}\text{C}$  NMR (100 MHz,  $\text{CDCl}_3$ ):  $\delta$  (ppm) 161.0, 160.8, 145.3, 144.7, 112.0, 111.3, 74.8, 74.5, 66.0, 61.4, 60.9, 14.2, 14.2 (Figure A.11, Appendix A). IR (ATR,  $\text{cm}^{-1}$ ): 3539 (-OH st), 2987, 2934 (-CH st), 1702 (C=O st) (Figure A.12, Appendix A) [74].

2.3.5 2,3-Dihydrothieno[3,4-*b*]-1,4-dioxin-2-yl methanol (**16**)**16**

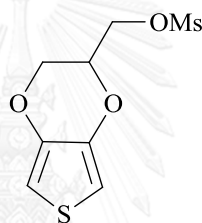
3,4-dimethoxythiophene (0.144 g, 1.0 mmol), glycerol (0.552 g, 6.0 mmol) and *p*-toluenesulfonic acid (PTSA) (0.038 g, 0.2 mmol) was stirred in 15 mL toluene and refluxed at 110 °C for 48 h under nitrogen atmosphere. After completion, the reaction was quenched by adding saturated NaHCO<sub>3</sub> solution. Then the organic layer was separated and the aqueous layer was extracted with ethyl acetate three times. The combined organic layers were dried over anhydrous MgSO<sub>4</sub>. The crude mixture was purified by column chromatography using hexane:ethyl acetate (1:1) as eluent to yield 2,3-dihydrothieno[3,4-*b*]-1,4-dioxin-2-yl methanol (**16**) as yellow oil (0.070 g, 42 %). <sup>1</sup>H NMR (400 MHz, CDCl<sub>3</sub>): δ (ppm) 6.27 (s, 2H), 4.15 (m, 2H), 4.02 (m, 1H), 3.77 (m, 2H), 1.94 (s, 1H) (Figure A.13, Appendix A). <sup>13</sup>C NMR (100 MHz, CDCl<sub>3</sub>): δ (ppm): 141.4, 100.2, 99.8, 74.1, 65.7, 61.6 (Figure A.14, Appendix A). IR (ATR, cm<sup>-1</sup>): 3386 (-OH st), 3114 (-CH st), 2923, 1485 (C=C st), 1183 (-C-O st) (Figure A.15, Appendix A) [74].

2.3.6 (2,3-Dihydrothieno[3,4-*b*][1,4]dioxin-2-yl)methyl-4'-methylbenzene sulfonate (**17**)**17**

Compound **16** (0.086 g, 0.5 mmol) and *p*-toluenesulfonyl chloride (0.191 g, 1.0 mmol) was dissolved in 2 mL of dry dichloromethane, added triethylamine (0.2

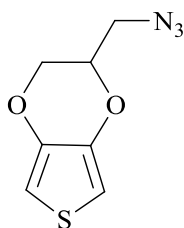
mL, 1.4 mmol) and stirred for 2 days under nitrogen atmosphere at room temperature. The solution was quenched by 5% H<sub>2</sub>SO<sub>4</sub> solution, extracted by dichloromethane, and washed by sat. NaHCO<sub>3</sub>. After purified by column chromatography using EtOAc and hexane in 1:4 ratio as eluent, the product was obtained as white solid in 0.130 g (80% yield). <sup>1</sup>H NMR (400 MHz, CDCl<sub>3</sub>) δ (ppm) 7.80 (d, *J* = 7.9 Hz, 2H), 7.36 (d, *J* = 7.9 Hz, 2H), 6.32 (3.6 Hz, 1H), 6.26 (3.6 Hz, 1H), 4.35 (d, *J* = 5.6 Hz, 1H), 4.15–4.23 (m, 3H), 4.02 (dd, *J* = 11.8, 6.5 Hz, 1H), 2.46 (s, 3H) (**Figure A.16, Appendix A**). <sup>13</sup>C NMR (100 MHz, CDCl<sub>3</sub>) δ 145.3, 141.0, 140.4, 132.5, 130.0, 128.0, 100.2, 100.2, 70.8, 66.9, 65.0, 21.6 (**Figure A.17, Appendix A**) [75].

### 2.3.7 (2,3-Dihydrothieno[3,4-*b*][1,4]dioxin-2-yl)methyl methanesulfonate(18)

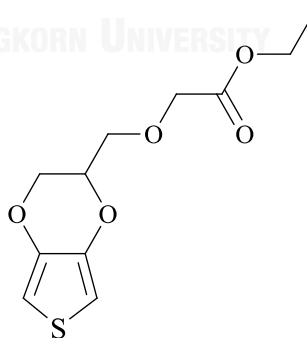


**18**

Compound **16** (0.086 g, 0.5 mmol) was added into dichloromethane 2 mL and NEt<sub>3</sub> 1 mL solution that was stirred in ice bath. Methanesulfonyl chloride (0.092 g, 0.8 mmol) was added dropwise into the solution and then stirred for 24 h. The solution was quenched by 5% H<sub>2</sub>SO<sub>4</sub>. The organic layer was extracted by dichloromethane, washed by sat. NaHCO<sub>3</sub>, dried with anhydrous MgSO<sub>4</sub> and evaporated the solvent to obtain the product as yellow liquid in quantitative yield (0.125 g). <sup>1</sup>H NMR (400 MHz, CDCl<sub>3</sub>) δ 6.37 (s, 2H), 4.43 (m, 3H), 4.25 (d, *J* = 11.8 Hz, 1H), 4.10 (dd, *J* = 11.8, 6.2 Hz, 1H), 3.07 (s, 3H) (**Figure A.18, Appendix A**). <sup>13</sup>C NMR (100 MHz, CDCl<sub>3</sub>) δ 141.0, 140.4, 100.4, 71.1, 66.9, 64.9, 52.6, 37.7, 37.6 (**Figure A.19, Appendix A**) [76].

2.3.8 2-(Azidomethyl)-2,3-dihydrothieno[3,4-*b*][1,4]dioxine (19)**19**

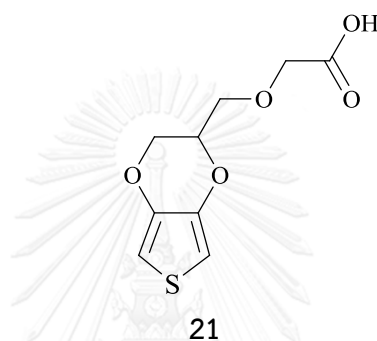
Compound **18** (0.100 g, 0.4 mmol) was added into solution of 2 mL EtOH and 2 mL THF. Sodium azide solution (0.28 g, 0.43 mmol in 1 mL water) was added and the reaction was stirred and heated at 80 °C for 48 h. The reaction was added 10 mL water and extracted by EtOAc. The separated organic layer was concentrated and purified by column chromatography using hexane:ethyl acetate (1:1) as eluent to yield the clear liquid product in 70 % yield (0.055 g). <sup>1</sup>H NMR (400 MHz, CDCl<sub>3</sub>) δ 6.38 (d, *J* = 3.5 Hz, 1H), 6.35 (d, *J* = 3.5 Hz, 1H), 4.36–4.26 (m, 1H), 4.19 (dd, *J* = 11.7, 1.4 Hz, 1H), 4.05 (dd, *J* = 11.7, 6.9 Hz, 1H), 3.53 (ddd, *J* = 18.3, 13.1, 5.6 Hz, 2H) (Figure A.20, Appendix A). <sup>13</sup>C NMR (100 MHz, CDCl<sub>3</sub>) δ 141.1, 140.7, 100.3, 100.1, 72.5, 65.8, 50.6 (Figure A.21, Appendix A) [76].

2.3.9 Ethyl 2-((2,3-dihydrothieno[3,4-*b*][1,4]dioxin-2-yl)methoxy)acetate (20)**20**

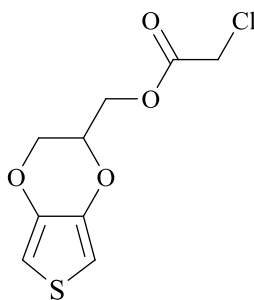
Compound **16** (0.122 g, 0.7 mmol), NaI (0.023 g, 0.15 mmol) and NaH (0.080 g, 2 mmol) were added into 5 mL of dry THF and then stirred for 15 min in ice bath. Ethyl chloroacetate (0.1 mmol, 0.123 g) was added and the solution was stirred at room temperature under nitrogen atmosphere for 24 h. The reaction was added 10 mL water and extracted by EtOAc. The separated organic layer was concentrated and

purified by column chromatography using hexane:ethyl acetate (1:1) as eluent to yield the clear liquid product in 37 % yield (0.040 g).[77]  $^1\text{H}$  NMR (400 MHz,  $\text{CDCl}_3$ )  $\delta$  6.53–6.16 (m, 2H), 4.44 – 4.34 (m, 1H), 4.33–4.20 (m, 3H), 4.20–4.07 (m, 3H), 3.82 (dtd,  $J = 14.5, 10.0, 4.6$  Hz, 2H), 1.31 (t,  $J = 4.8$  Hz, 3H) (Figure A.22, Appendix A).  $^{13}\text{C}$  NMR (101 MHz,  $\text{CDCl}_3$ )  $\delta$  170.0, 141.5, 141.3, 99.8, 99.7, 72.6, 69.9, 68.9, 65.9, 61.0, 14.2 (Figure A.23, Appendix A).

#### 2.3.10 2-((2,3-Dihydrothieno[3,4-b][1,4]dioxin-2-yl)methoxy)acetic acid (21)

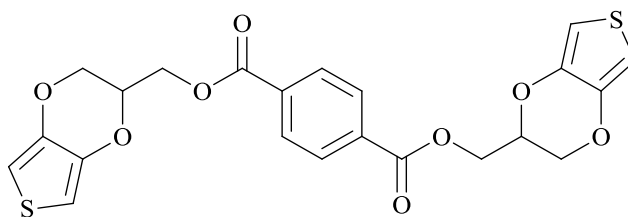


Compound **20** (0.069 g, 0.27 mmol) was dissolved in 2 mL THF. 2 mL of 2 M NaOH solution was added and stirred for 4 h. Excess THF was removed and the mixture was acidified by 10% HCl to pH 2. The mixture was extracted by 10 mL EtOAc twice. The combined organic layer was evaporated to obtain product as clear liquid in 92 % yield (0.057 g). [77]  $^1\text{H}$  NMR (400 MHz,  $\text{CDCl}_3$ )  $\delta$  6.28 (d,  $J = 3.7$  Hz, 1H), 6.26 (d,  $J = 3.7$  Hz, 1H), 4.34 – 4.25 (m, 1H), 4.22–4.17 (m, 1H), 4.16 (s, 2H), 4.08–4.00 (m, 1H), 3.82–3.69 (m, 2H) (Figure A.24, Appendix A).  $^{13}\text{C}$  NMR (101 MHz,  $\text{CDCl}_3$ )  $\delta$  174.6, 141.4, 141.1, 100.0, 99.9, 72.6, 70.1, 68.4, 65.8 (Figure A.25, Appendix A).

2.3.11 (2,3-Dihydrothieno[3,4-*b*][1,4]dioxin-2-yl)methyl 2'-chloroacetate (22)

22

Compound **16** (0.086 g, 0.5 mmol),  $K_2CO_3$  (0.207 g, 1.5 mmol) and DMAP (0.012 g, 0.1 mmol) were added into 5 mL DCM. Chloroacetyl chloride (0.16 mL, 2 mmol) was added into the solution and then stirred for 24 h. The reaction was quenched by sat.  $NaHCO_3$  and extracted twice with 10 mL DCM. The separated organic layer was concentrated and purified by column chromatography using hexane:ethyl acetate (1:1) as eluent to yield the clear liquid product in quantitative yield (0.124 g).  $^1H$  NMR (400 MHz,  $CDCl_3$ )  $\delta$  6.30 (d,  $J = 3.7$  Hz, 1H), 6.29 (d,  $J = 3.7$  Hz, 1H), 4.38–4.32 (m, 3H), 4.20–4.13 (m, 1H), 4.07–3.96 (m, 3H) (Figure A.26, Appendix A).  $^{13}C$  NMR (101 MHz,  $CDCl_3$ )  $\delta$  167.0, 141.1, 140.8, 100.3, 100.2, 71.1, 65.3, 63.8, 40.5 (Figure A.27, Appendix A) [78].

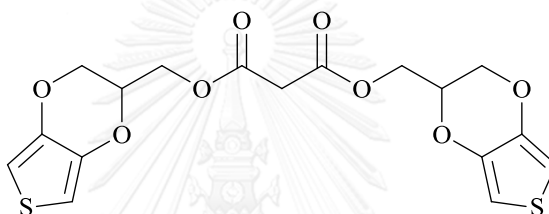
2.3.12 Bis((2,3-dihydrothieno[3,4-*b*]dioxin-2-yl)methyl) [1',4']benzene dicarboxylate (23)

23

Compound **16** (0.172 g, 1 mmol) was dissolved in 20 mL dry dichloromethane with potassium carbonate (0.138 g, 1 mmol) and terephthaloyl chloride (0.122 g, 0.6 mmol). Then, catalytic amount of DMAP was added (0.024 g, 0.02 mmol). The reaction was stirred at room temperature for 48 h. After washed by sat.  $NaHCO_3$  solution, the organic phase was purified by column chromatography with 1:1 EtOAc

and hexane as mobile phase. The product was obtained as white solid in 0.133 g (56% yield). mp. 158.2-158.5 °C; HRMS  $m/z$ : 497.0325  $[M + Na]^+$ . Calcd for  $C_{22}H_{18}O_8S_2Na$ : 497.0341 (**Figure A.28, Appendix A**).  $^1H$  NMR (400 MHz,  $CDCl_3$ )  $\delta$  (ppm) 8.10 (s, 4H), 6.39 (d,  $J = 3.6$  Hz, 2H), 6.36 (d,  $J = 3.6$  Hz, 2H), 4.66–4.46 (m, 6H), 4.32 (dd,  $J = 11.7, 1.8$  Hz, 2H), 4.16 (dd,  $J = 11.7, 6.7$  Hz, 2H) (**Figure A.29, Appendix A**).  $^{13}C$  NMR (100 MHz,  $CDCl_3$ )  $\delta$  (ppm) 166.3, 165.4, 141.1, 133.6, 129.8, 100.2, 71.4, 65.6, 63.4 (**Figure A.30, Appendix A**). IR (ATR,  $cm^{-1}$ ) 3105 (-CH st), 1715 (C=O st), 1474 (C=C st), 1171 (-C-O st) (**Figure A.31, Appendix A**) [78].

### 2.3.13 Bis((2,3-dihydrothieno[3,4-*b*][1,4]dioxin-2-yl)methyl) malonate (24)

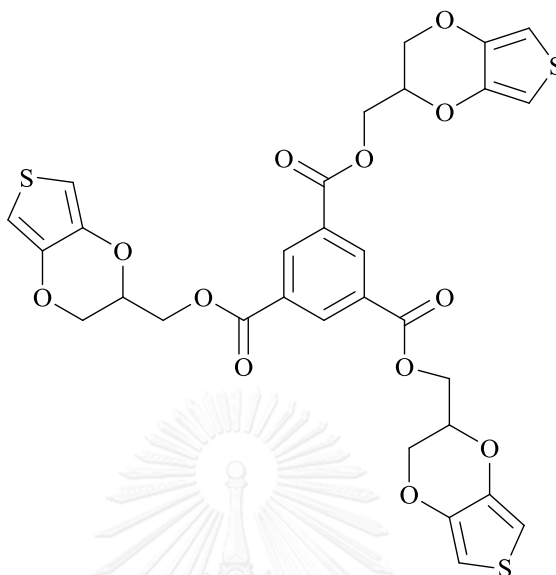


24

Compound **16** (0.172 g, 1 mmol) was added into 10 mL of dry dichloromethane and potassium carbonate (0.138 g, 1 mmol) under nitrogen atmosphere at 0 °C. Malonyl chloride (0.085 g, 0.6 mmol) in 10 mL dry dichloromethane was added dropwise for 30 min, followed by DMAP (0.024 g, 0.02 mmol). The reaction was stirred at room temperature for 30 min before being quenched by sat.  $NaHCO_3$  solution. The mixture was extracted twice with 10 mL dichloromethane. The combined organic phase was purified by column chromatography eluted with EtOAc and obtained pale yellow liquid as the product in 0.811 g (88 %yield). HRMS  $m/z$ : 435.0185  $[M + Na]^+$  Calcd for  $C_{17}H_{16}O_8S_2Na$ : 435.0184 (**Figure A.32, Appendix A**).  $^1H$  NMR (400 MHz,  $CDCl_3$ )  $\delta$  (ppm) 6.39–6.31 (m, 4H), 4.45–4.32 (m, 6H), 4.26–4.17 (m, 2H), 4.09–3.99 (m, 2H), 3.50 (s, 2H) (**Figure A.33, Appendix A**).  $^{13}C$  NMR (100 MHz,  $CDCl_3$ )  $\delta$  (ppm) 165.7, 141.1, 140.8, 106.0, 100.2, 100.1, 71.2, 65.4, 63.3, 41.0 (**Figure A.34, Appendix A**). IR (ATR,  $cm^{-1}$ ) 3109 (-CH st), 1733 (C=O st), 1478 (C=C st), 1171 (-C-O st) (**Figure A.35, Appendix A**) [78].

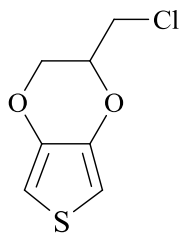


2.3.14 Tris((2,3-dihydrothieno[3,4-b][1,4]dioxin-2-yl)methyl) benzene-1',3',5'-tricarboxylate (25)



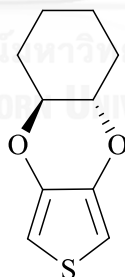
25

Compound **16** (0.103 g 0.6 mmol) was dissolved in 10 mL dichloromethane and the solution was added  $K_2CO_3$  (0.083 g, 0.6 mmol) and benzene-1,3,5-tricarbonyl trichloride (0.054 g, 0.2 mmol), followed by DMAP (0.003 g, 0.025 mmol). The reaction was stirred at room temperature under nitrogen atmosphere for 48 h. After washed by sat.  $NaHCO_3$  solution, the organic phase was separated, concentrated and purified by column chromatography using 1:1 EtOAc and hexane as mobile phase. The product was obtained as white solid in 0.082 g (61 %yield).  $^1H$  NMR (400 MHz,  $CDCl_3$ )  $\delta$  8.85 (s, 3H), 6.38 (d,  $J$  = 3.6 Hz, 3H), 6.36 (d,  $J$  = 3.6 Hz, 3H), 4.65–4.60 (m, 6H), 4.55 (td,  $J$  = 6.6, 2.2 Hz, 3H), 4.32 (dd,  $J$  = 11.7, 2.1 Hz, 3H), 4.19–4.10 (m, 3H) (Figure A.36, Appendix A).  $^{13}C$  NMR (100 MHz,  $CDCl_3$ )  $\delta$  164.3, 141.1, 140.9, 135.1, 130.9, 100.3, 100.2, 71.3, 65.5, 63.7 (Figure A.37, Appendix A). IR (ATR,  $cm^{-1}$ ) 3110 (-CH st), 1712 (C=O st), 1481 (C=C st), 1165 (-C-O st) (Figure A.38, Appendix A) [78].

2.3.15 2-(Chloromethyl)-2,3-dihydrothieno[3,4-*b*][1,4]dioxine (26)

26

3,4-Dimethoxythiophene (0.288 g, 2 mmol) was mixed with 3-chloro-1,2-propanediol (0.5 mL, 6 mmol) and PTSA (0.080 g, 0.4 mmol) in 10 mL dry toluene. The mixture was stirred at 100 °C under nitrogen atmosphere for 24 h. The reaction mixture was washed by sat. NaHCO<sub>3</sub> and then extracted twice with 10 mL EtOAc. The combined organic layer was evaporated to obtain product as colorless liquid in quantitative yield (0.381 g). <sup>1</sup>H NMR (400 MHz, CDCl<sub>3</sub>) δ 6.44–6.25 (m, 2H), 4.37 (tdd, *J* = 7.3, 5.3, 2.2 Hz, 1H), 4.28 (dd, *J* = 11.7, 2.2 Hz, 1H), 4.20–4.09 (m, 1H), 3.78–3.60 (m, 2H) (Figure A.39, Appendix A). <sup>13</sup>C NMR (101 MHz, CDCl<sub>3</sub>) δ 141.2, 140.7, 100.2, 72.9, 65.6, 41.3 (Figure A.40, Appendix A) [79].

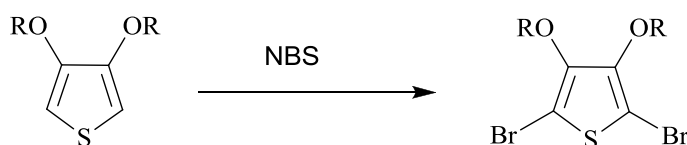
2.3.16 (±)-4a,5,6,7,8,8a-Hexahydrobenzo[*e*]thieno[3,4-*b*][1,4]dioxine (27)

27

3,4-Dimethoxythiophene (0.144 g, 1 mmol) was mixed with (±) trans-1,2-cyclohexanediol (0.233 g, 2 mmol) and PTSA (0.020 g, 0.1 mmol) in 10 mL dry toluene. The mixture was stirred at 100 °C under nitrogen atmosphere for 72 h. The reaction mixture was washed by sat. NaHCO<sub>3</sub> and then extracted twice with EtOAc. Using column chromatography eluted by hexane/dichloromethane (3:2), 3,4-cyclohexenedioxythiophene (CDOT) was obtained as white solid crystal in 0.197 g (86% yield). mp. 142.1–142.5 °C; <sup>1</sup>H NMR (400 MHz, CDCl<sub>3</sub>) δ (ppm) 6.30 (s, 2H), 3.78–

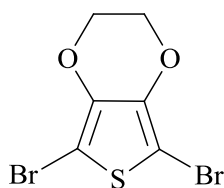
3.68 (m, 2H), 2.20 (d,  $J = 11.8$  Hz, 2H), 1.84 (dd,  $J = 6.2, 2.7$  Hz, 2H), 1.49–1.24 (m, 4H) (Figure A.41, Appendix A).  $^{13}\text{C}$  NMR (100 MHz,  $\text{CDCl}_3$ )  $\delta$  (ppm) 142.4, 99.0, 77.1, 30.1, 23.8 (Figure A.42, Appendix A) [80].

## 2.4 Brominations of thiophene derivatives



**General procedure:** 2.5 equivalents of *N*-bromosuccinimide (NBS) were added to a stirred solution of a thiophene precursor (1.0 mmol) in chloroform (10 mL) at room temperature. After completion, the reaction mixture was quenched by adding saturated  $\text{NaHCO}_3$  solution. The organic layer was separated and the aqueous layer was extracted with dichloromethane three times. Then the combined organic layers were washed with 2 M  $\text{NaOH}$  three times. After drying over anhydrous  $\text{MgSO}_4$ , the solution was evaporated using rotary evaporator and then purified by column chromatography to obtain the corresponding dibromothiophene.[81]

### 2.4.1 2,5-Dibromo-3,4-ethylenedioxythiophene (28)

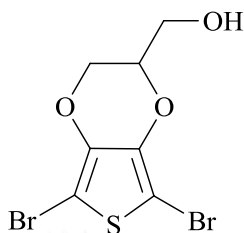


28

Following the general procedure, 3,4-ethylenedioxythiophene (EDOT) (0.142 g, 1.0 mmol) and NBS (0.4450 g, 2.5 mmol) in chloroform (10 mL) were mixed for 2 min. The crude mixture was purified by column chromatography, eluted with 3:2 mixture of hexane and ethyl acetate to get a light yellow solid (0.290 g, 98%). Mp. 96–97 °C.  $^1\text{H}$  NMR (400 MHz,  $\text{CDCl}_3$ ):  $\delta$  (ppm) 4.27 (s, 4H) (Figure A.43, Appendix A).  $^{13}\text{C}$  NMR

(100 MHz, CDCl<sub>3</sub>):  $\delta$  (ppm) 139.7, 85.5, 64.9 (Figure A.44, Appendix A). IR (ATR, cm<sup>-1</sup>): 2923 (-CH st), 1505 (C=O st), 1080 (-C-O st) (Figure A.45, Appendix A). MS: [M+H]<sup>+</sup> m/z = 299.20 (Figure A.46, Appendix A) [81].

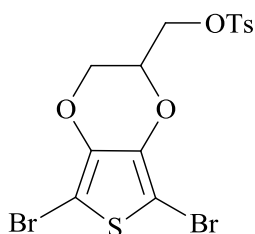
#### 2.4.2 (5,7-dibromo-2,3-dihydrothieno[3,4-*b*][1,4]dioxin-2-yl)methanol (29)



29

Following the general procedure, compound **16** (0.172 g, 1.0 mmol) and NBS (0.4450 g, 2.5 mmol) in chloroform (10 mL) were mixed for 1 min. The crude mixture was purified by column chromatography, eluted with ethyl acetate to get a pale yellow liquid (0.250 g, 77%). <sup>1</sup>H NMR (400 MHz, CDCl<sub>3</sub>):  $\delta$  (ppm) 4.24 (m, 2H), 4.10 (m, 1H), 3.84 (m, 2H), 1.99 (s, 1H) (Figure A.47, Appendix A). <sup>13</sup>C NMR (100 MHz, CDCl<sub>3</sub>):  $\delta$  (ppm) 139.5, 85.6, 85.5, 74.6, 65.1, 61.4 (Figure A.48, Appendix A). MS: [M+H]<sup>+</sup> m/z = 329.09 (Figure A.49, Appendix A) [82].

#### 2.4.3 (5,7-Dibromo-2,3-dihydrothieno[3,4-*b*][1,4]dioxin-2-yl)methyl 4'-methylbenzenesulfonate (30)

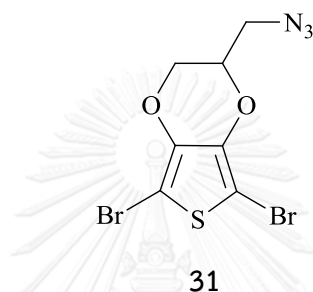


30

Following the general procedure, compound **17** (0.163 g, 0.5 mmol) and NBS (0.223 g, 1.25 mmol) in chloroform (10 mL) were stirred for 1 min. The crude mixture was purified by column chromatography, eluted with ethyl acetate to get a white

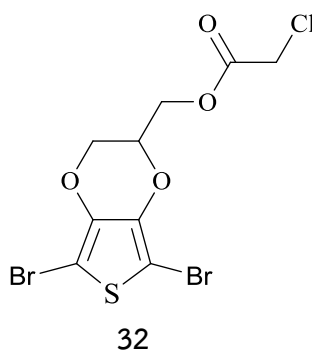
solid product (0.219 g, 90.4 %)  $^1\text{H}$  NMR (400 MHz,  $\text{CDCl}_3$ )  $\delta$  7.81 (d,  $J = 8.3$  Hz, 2H), 7.37 (d,  $J = 8.1$  Hz, 2H), 4.52–4.34 (m, 1H), 4.26 (ddd,  $J = 9.9, 6.2, 3.7$  Hz, 2H), 4.20 (dd,  $J = 11.1, 5.9$  Hz, 1H), 4.08 (dd,  $J = 12.1, 6.7$  Hz, 1H), 2.46 (s, 3H) (Figure A.50, Appendix A).  $^{13}\text{C}$  NMR (100 MHz,  $\text{CDCl}_3$ )  $\delta$  145.5, 139.0, 138.5, 132.2, 130.1, 130.0, 128.0, 86.1, 71.3, 66.3, 65.3, 29.6, 21.7 (Figure A.51, Appendix A). HRMS  $m/z$ : 504.8374  $[\text{M} + \text{Na}]^+$  Calcd for  $\text{C}_{14}\text{H}_{12}\text{Br}_2\text{O}_5\text{S}_2\text{Na}$ : 504.8391 (Figure A.52, Appendix A).

#### 2.4.4 2-(Azidomethyl)-5,7-dibromo-2,3-dihydrothieno[3,4-*b*][1,4]dioxine (31)



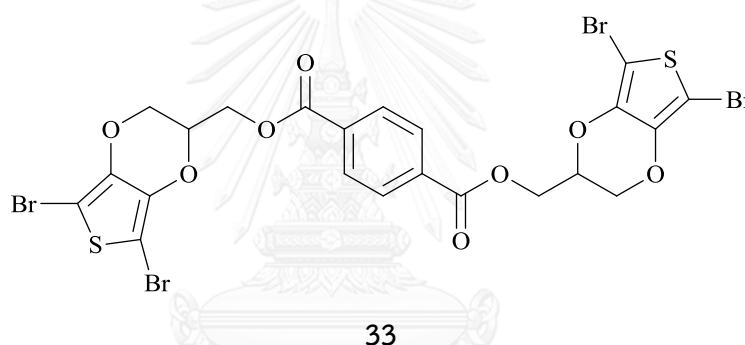
Following the general procedure, compound **19** (0.099 g, 0.5 mmol) and NBS (0.223 g, 1.25 mmol) in chloroform (10 mL) were stirred for 1 min. The crude mixture was purified by column chromatography, eluted with ethyl acetate to get a yellow liquid (0.124 g, 70%)  $^1\text{H}$  NMR (400 MHz,  $\text{CDCl}_3$ )  $\delta$  4.37 (td,  $J = 7.4, 2.1$  Hz, 1H), 4.28 (dd,  $J = 11.9, 2.1$  Hz, 1H), 4.19–4.04 (m, 1H), 3.67–3.48 (m, 2H) (Figure A.53, Appendix A).  $^{13}\text{C}$  NMR (100 MHz,  $\text{CDCl}_3$ )  $\delta$  139.1, 138.8, 86.2, 86.0, 73.0, 66.1, 50.2 (Figure A.54, Appendix A).

#### 2.4.5 (5,7-Dibromo-2,3-dihydrothieno[3,4-*b*][1,4]dioxin-2-yl)methyl 2'-chloroacetate (32)



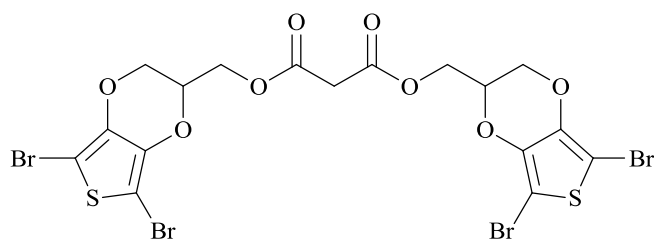
Following the general procedure, compound **22** (0.125 g, 0.5 mmol) and NBS (0.223 g, 1.25 mmol) in chloroform (10 mL) were stirred for 1 min. The crude mixture was purified by column chromatography, eluted with ethyl acetate to get a white solid product (0.148 g, 73%).  $^1\text{H}$  NMR (400 MHz,  $\text{CDCl}_3$ )  $\delta$  4.46–4.30 (m, 3H), 4.25 (dd,  $J$  = 11.9, 2.1 Hz, 1H), 4.11–4.02 (m, 3H) (**Figure A.55, Appendix A**).  $^{13}\text{C}$  NMR (101 MHz,  $\text{CDCl}_3$ )  $\delta$  166.9, 139.1, 138.8, 86.1, 86.0, 71.5, 65.6, 63.2, 40.5, 28.7 (**Figure A.56, Appendix A**). HRMS  $m/z$ : 426.8050  $[\text{M} + \text{Na}]^+$  Calcd for  $\text{C}_9\text{H}_7\text{Br}_2\text{ClO}_4\text{SNa}$ : 426.8018 (**Figure A.57, Appendix A**).

#### 2.4.6 Bis((5,7-dibromo-2,3-dihydrothieno[3,4-*b*][1,4]dioxin-2-yl)methyl)terephthalate (**33**)



Following the general procedure, compound **23** (0.119 g, 0.25 mmol) and NBS (0.223 g, 1.25 mmol) in chloroform (10 mL) were stirred for 3 min. The crude mixture was purified by column chromatography, eluted with ethyl acetate to get clear liquid product (0.188 g, 95%).  $^1\text{H}$  NMR (400 MHz,  $\text{CDCl}_3$ )  $\delta$  8.10 (s, 4H), 4.70–4.56 (m, 6H), 4.40 (dd,  $J$  = 11.9, 2.0 Hz, 2H), 4.24 (dd,  $J$  = 11.9, 6.0 Hz, 2H) (**Figure A.58, Appendix A**).  $^{13}\text{C}$  NMR (100 MHz,  $\text{CDCl}_3$ )  $\delta$  165.1, 139.0, 133.5, 129.9, 86.0, 71.8, 65.9, 62.9 (**Figure A.59, Appendix A**).

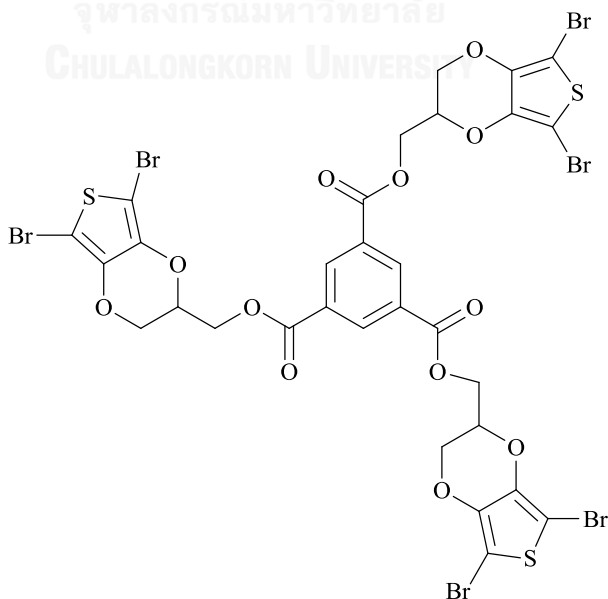
2.4.7 Bis((5,7-dibromo-2,3-dihydrothieno[3,4-*b*][1,4]dioxin-2-yl)methyl) malonate (34)



34

Following the general procedure, compound **24** (0.103 g, 0.25 mmol) and NBS (0.223 g, 1.25 mmol) in chloroform (10 mL) were stirred for 2 min. The crude mixture was purified by column chromatography, eluted with dichloromethane and hexane in 3:1 ratio to get clear liquid product (0.124 g, 68%).  $^1\text{H}$  NMR (400 MHz,  $\text{CDCl}_3$ )  $\delta$  4.53–4.41 (m, 4H), 4.42–4.34 (m, 2H), 4.31 (d,  $J = 11.6$  Hz, 2H), 4.18–4.05 (m, 2H), 3.53 (d,  $J = 8.9$  Hz, 2H) (Figure A.60, Appendix A).  $^{13}\text{C}$  NMR (101 MHz,  $\text{CDCl}_3$ )  $\delta$  165.6, 139.1, 138.9, 86.0, 71.6, 71.6, 65.6, 62.8, 62.8, 41.1, 40.9 (Figure A.61, Appendix A).

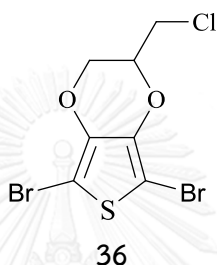
2.4.8 Tris((5,7-dibromo-2,3-dihydrothieno[3,4-*b*][1,4]dioxin-2-yl)methyl) benzene-1',3',5'-tricarboxylate (35)



35

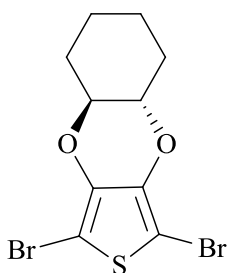
Following the general procedure compound **25** (0.067 g, 0.10 mmol) and NBS (0.134 g, 0.75 mmol) in chloroform (10 mL) were stirred for 3 min. The crude mixture was purified by column chromatography, eluted with ethyl acetate to get a clear liquid product (0.095 g, 83 % yield).  $^1\text{H}$  NMR (400 MHz,  $\text{CDCl}_3$ )  $\delta$  8.85 (s, 3H), 4.75–4.66 (m, 3H), 4.63 (dd,  $J = 9.0, 3.6$  Hz, 6H), 4.39 (dt,  $J = 20.0, 10.0$  Hz, 3H), 4.24 (dd,  $J = 11.9, 5.9$  Hz, 3H) (Figure A.62, Appendix A).

#### 2.4.9 5,7-Dibromo-2-(chloromethyl)-2,3-dihydrothieno[3,4-*b*][1,4]dioxine (36)



Following the general procedure, compound **26** (0.191 g, 1.0 mmol) and NBS (0.445 g, 2.5 mmol) in chloroform (10 mL) were mixed for 1 min. The crude mixture was purified by column chromatography, eluted with ethyl acetate to get a pale yellow liquid product (0.296 g, 85%).  $^1\text{H}$  NMR (400 MHz,  $\text{CDCl}_3$ )  $\delta$  4.46–4.39 (m, 1H), 4.29 (ddd,  $J = 18.2, 11.9, 4.3$  Hz, 2H), 3.82–3.63 (m, 2H) (Figure A.63, Appendix A).  $^{13}\text{C}$  NMR (101 MHz,  $\text{CDCl}_3$ )  $\delta$  139.2, 138.8, 95.0, 86.0, 73.4, 66.0, 40.7 (Figure A.64, Appendix A).

#### 2.4.10 ( $\pm$ )-1,3-Dibromo-4a,5,6,7,8,8a-hexahydrobenzo[*e*]thieno[3,4-*b*][1,4]dioxine (37)

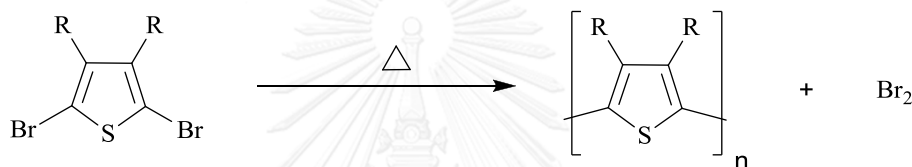




Following the general procedure, compound **27** (0.098 g, 0.5 mmol) and NBS (0.223 g, 1.25 mmol) in chloroform (10 mL) were stirred for 2 min. The crude mixture was purified by column chromatography, eluted with dichloromethane and hexane in 2:3 ratio to get white needle crystal of the product (0.166 g, 94%). mp. 127.5-128 °C  $^1\text{H}$  NMR (400 MHz,  $\text{CDCl}_3$ )  $\delta$  3.79–3.65 (m, 2H), 2.28 (d,  $J$  = 13.1 Hz, 2H), 1.85 (d,  $J$  = 9.0 Hz, 2H), 1.55–1.28 (m, 4H). (**Figure A.65, Appendix A**).  $^{13}\text{C}$  NMR (100 MHz,  $\text{CDCl}_3$ )  $\delta$  140.4, 84.8, 77.7, 29.9, 23.7. (**Figure A.66, Appendix A**).

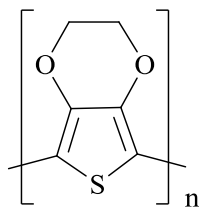
## 2.5 Polymer synthesis

### 2.5.1 Solid state polymerization (SSP)



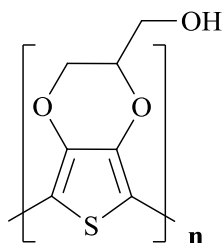
**General procedure:** 0.5 mmol of brominated monomer was placed in a round bottom flask and heated at 80 °C for 24 h. During this period the brominated monomer would turn into dark blue solid polymer. The resulted polymer was washed by dichloromethane to remove the non-polymerized monomer and afforded the corresponding bromine-doped polymer after being dried in dessicator [46].

#### 2.5.1.1 PEDOT from SSP (**38**)

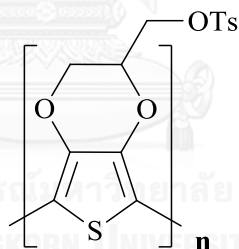


**38**

Following the general procedure, compound **28** (0.150 g, 0.5 mmol) was turned into insoluble doped PEDOT **38** in 0.115 g (> 100%). IR (ATR,  $\text{cm}^{-1}$ ): 1476 (C=C st), 1165 (-C-O st) (**Figure A.67, Appendix A**).[83]

2.5.1.2 Poly (2,3-dihydrothieno[3,4-*b*]-1,4-dioxin-2-yl methanol) (39)**39**

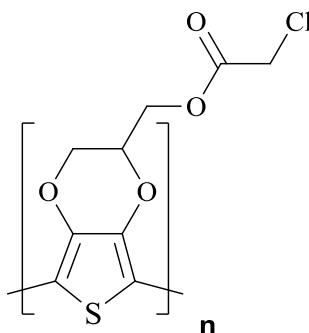
Following the general procedure, compound **29** (0.165 g, 0.5 mmol) was turned into insoluble polymer **39** in 0.122 g (> 100%). IR (ATR,  $\text{cm}^{-1}$ ): 3425 (-O-H st), 1502 (C=C st), 1135 (-C-O st) (Figure A.69, Appendix A).

2.5.1.3 Poly ((2,3-dihydrothieno[3,4-*b*][1,4]dioxin-2-yl)methyl 4'-methylbenzenesulfonate) (40)**40**

Following the general procedure compound **30** (0.242 g, 0.5 mmol) was turned into insoluble polymer **40** in 0.183 g (> 100%). IR (ATR,  $\text{cm}^{-1}$ ): 1485 (C=C st), 1290 (S=O st), 1125 (-C-O st) (Figure A.71, Appendix A).

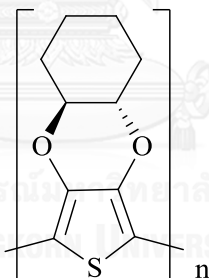
2.5.1.4 Poly ((2,3-dihydrothieno[3,4-*b*][1,4]dioxin-2-yl)methyl 2'-chloroacetate)

(41)



41

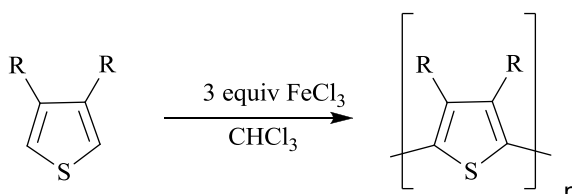
Following the general procedure, compound **32** (0.203 g, 0.5 mmol) was turned into insoluble polymer **41** in 0.146 g (> 100%). IR (ATR,  $\text{cm}^{-1}$ ): 1735 (C=O st), 1481 (C=O st), 1134 (-C-O st) (Figure A.73, Appendix A).

2.5.1.5 Poly ((±)-4a,5,6,7,8,8a-hexahydrobenzo[*e*]thieno[3,4-*b*][1,4]dioxine) (42)

42

Following the general procedure compound **37** (0.177 g, 0.5 mmol) was turned into insoluble polymer **42** in 0.135g. (> 100%). IR (ATR,  $\text{cm}^{-1}$ ): 1431 (C=C st), 1102 (-C-O st) (Figure A.75, Appendix A).

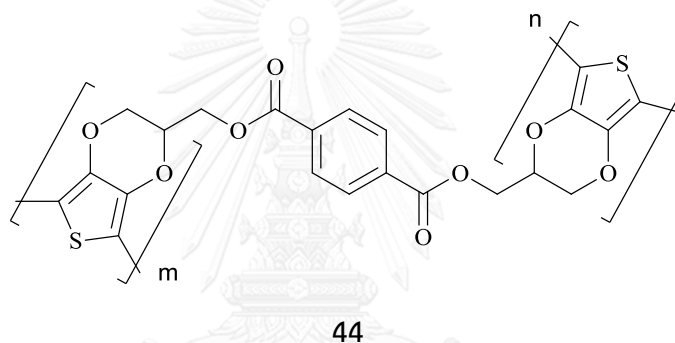
## 2.5.2 Chemical polymerization



### 2.5.2.1 PEDOT from chemical polymerization (38c)

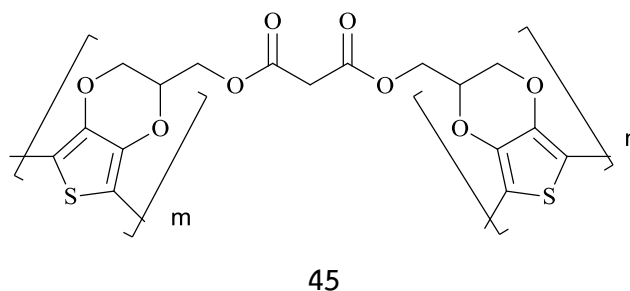
Solution of EDOT (2.840 g, 20 mmol) in 20 mL chloroform was added dropwise to well stirred suspension of  $\text{FeCl}_3$  (9.72 g, 60 mmol) in 100 mL chloroform. After being stirred for 24 h, methanol (20 mL) was added and filtered solid product. The remaining  $\text{FeCl}_3$  was removed by soxhlet extraction with methanol for 72 h to obtain insoluble dark blue polymer (1.846 g, 65%). IR (ATR,  $\text{cm}^{-1}$ ): 1477 (C=C st), 1157 (-C-O st) (Figure A.77, Appendix A). [83, 84]

### 2.5.2.2 Poly bis((2,3-dihydrothieno[3,4-*b*]dioxin-2-yl)methyl) [1',4']benzene dicarboxylate (44)



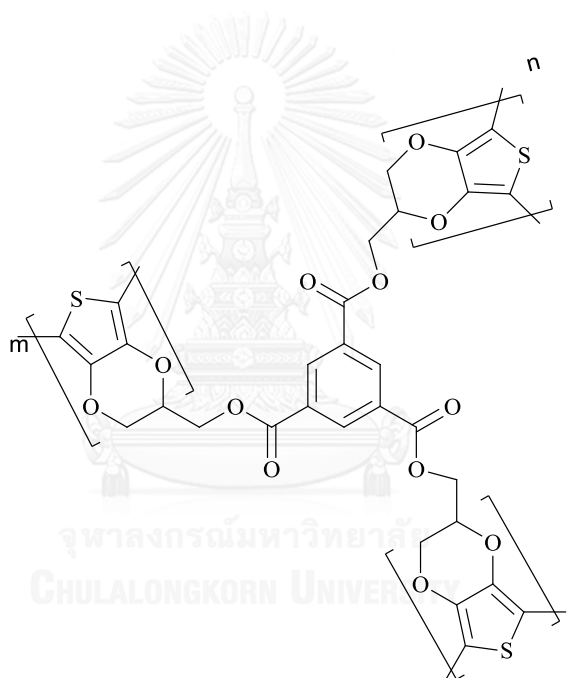
Solution of compound **23** (0.237 g, 0.5 mmol) in 10 mL chloroform was added dropwise to well stirred suspension of  $\text{FeCl}_3$  (0.488 g, 3 mmol) in 20 mL chloroform. After being stirred for 24 h, methanol (20 mL) was added and filtered the solid product. The remaining  $\text{FeCl}_3$  was removed by soxhlet extraction with methanol for 72 h to obtain insoluble dark blue polymer (0.149 g, 63%). IR (ATR,  $\text{cm}^{-1}$ ): 1708 (C=O st), 1432 (C=C st), 1085 (-C-O st) (Figure A.78, Appendix A).

### 2.5.2.3 Poly (bis((2,3-dihydrothieno[3,4-*b*][1,4]dioxin-2-yl)methyl) malonate) (45)



Solution of compound **24** (0.206 g, 0.5 mmol) in 10 mL chloroform was added dropwise to well stirred suspension of  $\text{FeCl}_3$  (0.488 g, 3 mmol) in 20 mL chloroform. After being stirred for 24 h, methanol (20 mL) was added and filtered solid product. The remaining  $\text{FeCl}_3$  was removed by soxhlet extraction with methanol for 72 h to obtain insoluble dark blue polymer (0.126 g, 61%). IR (ATR,  $\text{cm}^{-1}$ ): 1721 (C=O st), 1459 (C=C st), 1094 (-C-O st) (**Figure A.79, Appendix A**).

#### 2.5.2.4 Poly (tris((2,3-dihydrothieno[3,4-*b*][1,4]dioxin-2-yl)methyl) benzene-1,3,5-tricarboxylate) (**46**)



#### 46

Solution of compound **25** (0.134 g, 0.2 mmol) in 10 mL chloroform was added dropwise to well stirred suspension of  $\text{FeCl}_3$  (0.292 g, 1.8 mmol) in 20 mL chloroform. After being stirred for 24 h, methanol (20 mL) was added and filtered solid product. The remaining  $\text{FeCl}_3$  was removed by soxhlet extraction with methanol for 72 h to obtain insoluble dark blue polymer (0.090 g, 67%). IR (ATR,  $\text{cm}^{-1}$ ): 1712 (C=O st), 1481 (C=C st), 1090 (-C-O st) (**Figure A.80, Appendix A**).

### 2.5.2.5 Copolymer of (PEDOT + 5% polymer 44)

The copolymer of PEDOT + 5% polymer **44** was prepared from the mixture of compound **23** (0.475 g, 1 mmol) and EDOT (2.698 g, 19 mmol) in chloroform (20 mL), which was added dropwise into 100 mL chloroform containing stirred suspension of  $\text{FeCl}_3$  (9.732 g, 60 mmol). The mixture underwent the same chemical polymerization procedure as in 2.5.2.1 to obtain 1.843 g (58%) of the corresponding insoluble copolymer (**Figure A.81, Appendix A**).

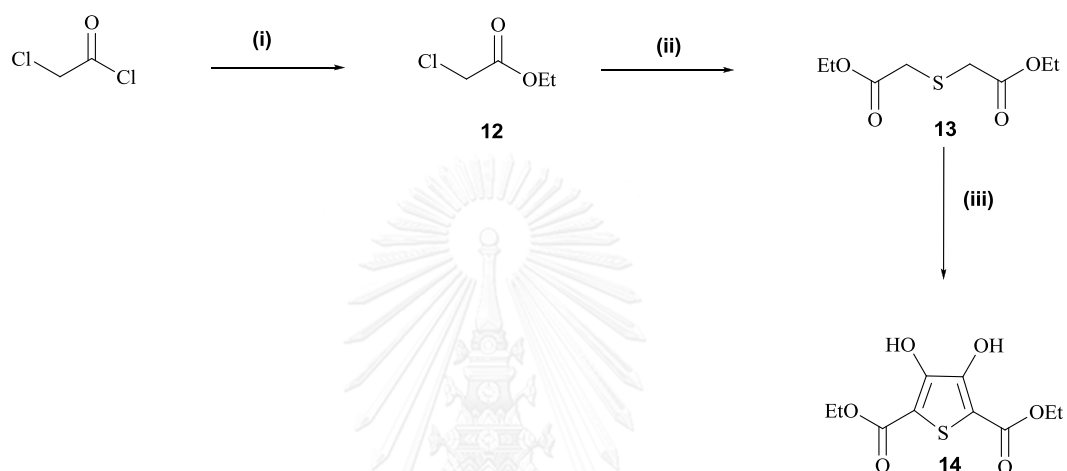


## CHAPTER III

### RESULTS AND DISCUSSION

#### 3.1 Monomer synthesis

##### 3.1.1 Synthesis of Diethyl 3,4-dihydroxythiophene-2,5-dicarboxylate (**14**)



Reagents and conditions: (i) absolute EtOH, rt; (ii) Na<sub>2</sub>S·9H<sub>2</sub>O, acetone, 60 °C, 3 h; (iii) NaOEt, 0.5 h, 0 °C, (CO<sub>2</sub>Et)<sub>2</sub>, then reflux in EtOH, 1 h

**Scheme 3.1** Synthesis of Diethyl 3,4-dihydroxythiophene-2,5-dicarboxylate (**14**)

The reaction of chloroacetyl chloride and ethanol obtained compound **12** as colorless liquid in 99 %yield. This reaction underwent the bimolecular nucleophilic acyl substitution. The characteristic quartet and triplet signals of the newly added ethyl group of compound **12** clearly appeared at  $\delta$  4.21, 1.23 ppm in <sup>1</sup>H NMR spectrum (**Figure A.1, Appendix A**) and  $\delta$  62.2, 14.1 ppm in <sup>13</sup>C NMR spectrum (**Figure A.2, Appendix A**).

An acetone solution of ethyl chloroacetate **12** was treated through the S<sub>N</sub>2 fashion with sodium sulfide, giving diethyl thioglycolate **13** in 50 %yield (**Entry 2, Table 3.1**), which was much better than ambient atmosphere, possibly due to less

sulfide air oxidation (**Entry 1**). Longer reaction time gave only slight increase of the product yield. The reactant may nearly be used up after 3 h. (**Entry 3**).

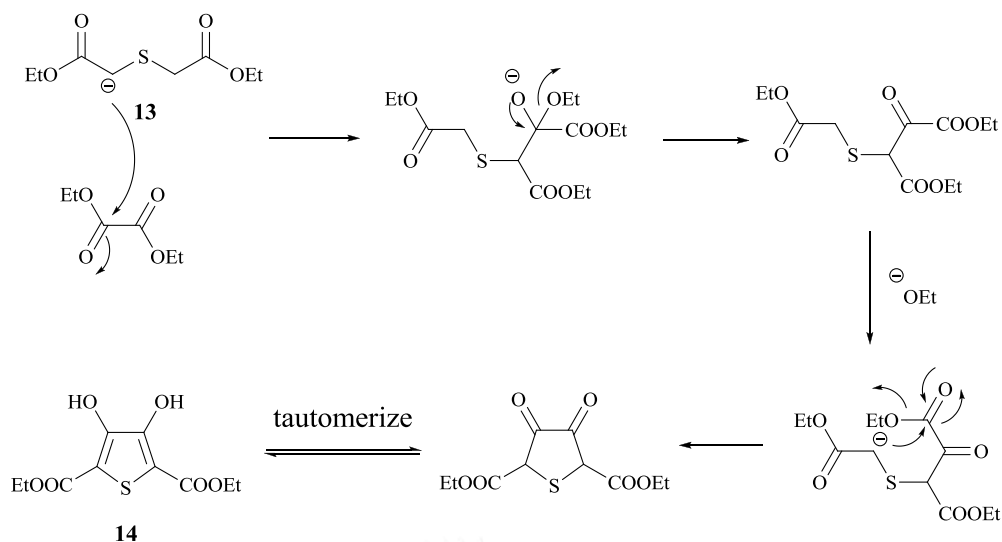
**Table 3.1** Conditions for the synthesis of diester **13**

Entry	Conditions	Time (h)	%yield
1	60 °C, air	3	25
2	60 °C, N <sub>2</sub>	3	50
3	60 °C, N <sub>2</sub>	24	55

The <sup>1</sup>H NMR showed the singlet methylene signal at 3.32 ppm and the quartet and triplet ethyl signals at 4.13 and 1.23 ppm respectively (**Figure A.3, Appendix A**). In the <sup>13</sup>C NMR spectrum, the carbonyl carbon appeared at 169.5 ppm (**Figure A.4, Appendix A**). Finally, the formation of **13** was supported by the mass value from MS in the positive mode at 229.05 amu [M+Na]<sup>+</sup> [85] (**Figure A.5, Appendix A**).

The synthesis of diethyl 3,4-dihydroxythiophene-2,5-dicarboxylate **14** followed the Hinsberg reaction [86], which is a condensation of diethyl thioglycolate **13** with diethyl oxalate under basic conditions [87]. The mechanism of this reaction as shown in **Scheme 3.2** is generally understood to consist of subsequent Claisen condensation reactions to produce a diketone intermediate, which readily tautomerizes to the fully conjugated dihydroxythiophene [73, 88].

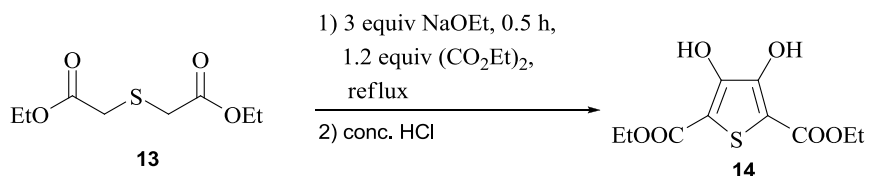




**Scheme 3.2** Mechanism of Hinsberg reaction

The preparation of dihydroxythiophene **14** was optimized in various reaction conditions as shown in **Table 3.2**. The diester **13** was condensed with diethyl oxalate to give the dihydroxythiophene product in good yield (70%) (**Entry 2**). No erosion of the yield was observed with the scale-up reaction (**Entry 3**). Longer reaction time seemed to give poorer results probably due to further reaction of product **14** (**Entry 6**).

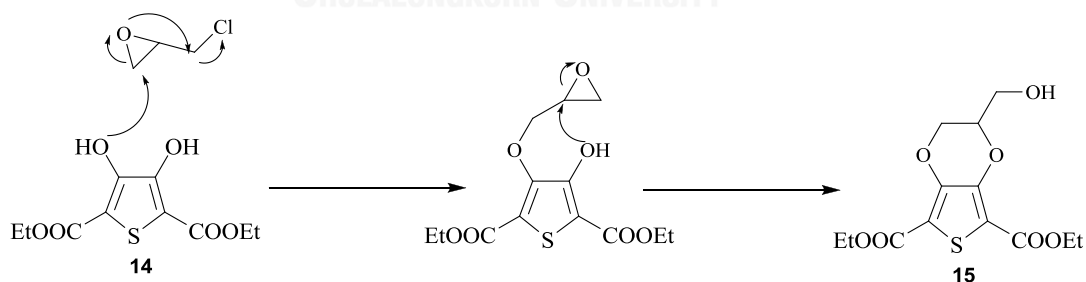
The  $^1\text{H}$  NMR showed a broad singlet OH peak at 9.36 ppm (**Figure A.6, Appendix A**). In the  $^{13}\text{C}$  NMR the carbonyl carbon appeared at 165.5 ppm and the two carbons of the thiophene ring at 107.1 and 151.6 ppm (**Figure A.7, Appendix A**). IR spectrum showed very strong broad OH stretching appeared at  $3293\text{ cm}^{-1}$  and the double bond region at  $1661$  and  $1508\text{ cm}^{-1}$  (**Figure A.8, Appendix A**). In the mass spectrum, the molecular ion peak appeared in the positive mode at  $259.20\text{ amu}$   $[\text{M}-\text{H}]^+$  (**Figure A.9, Appendix A**).

**Table 3.2** Conditions for the synthesis of dihydroxythiophene **14**

Entry	mmol of <b>13</b>	Time (h)	%yield
1	5	1	55
2	10	1	70
3	30	1	68
4	10	2	55
5	30	2	48
6	5	24	41

### 3.1.2 Synthesis of diethyl 2-(hydroxymethyl)-2,3-dihydrothieno[3,4-*b*]-1,4-dioxine-5,7-dicarboxylate (**15**)

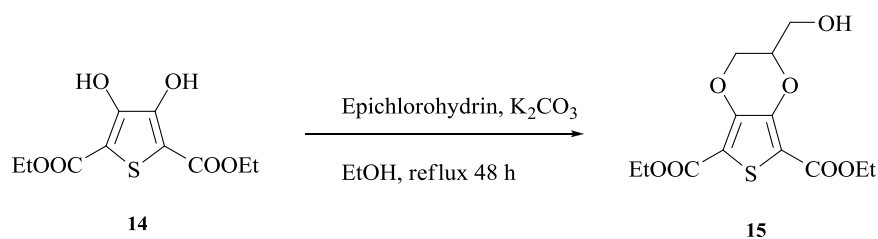
To prepare compound **15**, diethyl 3,4-dihydroxythiophene-2,5-dicarboxylate **14** reacted with excess epichlorohydrin by double  $S_N2$  mechanism as shown in **Scheme 3.3**. The reaction consists of substitution reactions twice on epoxide ring.

**Scheme 3.3** Mechanism for substitution on epichlorohydrin

The synthesis of compound **15** was optimized in various conditions as shown in **Table 3.3**. The reaction gave only unidentified side product when ethanol was

used as solvent (**Entries 1-2**). Most conditions yielded the crude mixture of compounds that could not be purified.

**Table 3.3** Condition for the synthesis of compound **15**



Entry	Solvent	Base	Epichlorohydrin (equiv)	Time (h)	Product	%yield
1	EtOH	K <sub>2</sub> CO <sub>3</sub>	1.2	72	Brown crude oil	-
2	EtOH	K <sub>2</sub> CO <sub>3</sub>	2.0	48	Brown crude oil	-
3	DMF	TEA	1.2	48	White solid	10%
4	DMF	TEA	2.0	72	White solid	20%
5	DMF	K <sub>2</sub> CO <sub>3</sub>	2.0	72	White solid	40%
6	DMF	K <sub>2</sub> CO <sub>3</sub>	3.0	72	White solid coated with brown crude oil	- <sup>a</sup>

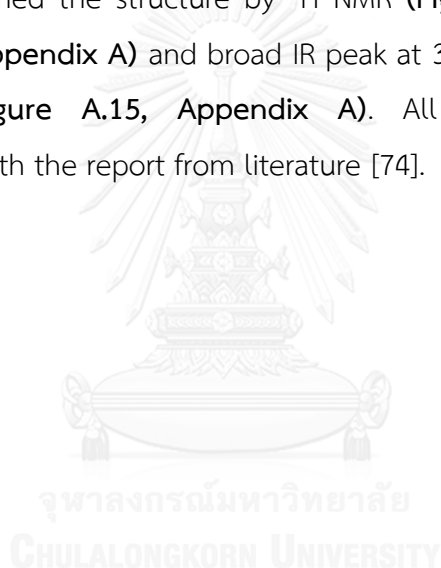
<sup>a</sup> Since the product was still a mixture, %yield could not be calculated.

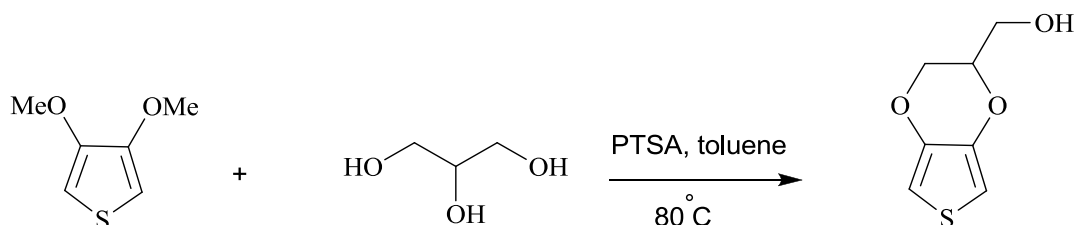
We assumed that the brown crude liquid product probably resulted from self-polymerization of the excess epichlorohydrin. Changing the solvent to DMF successfully yielded the desired product. The <sup>1</sup>H NMR showed the signal at δ 4.2–4.5 ppm which related to the newly constructed structure of compound **15** (**Figure A.10, Appendix A**). In the <sup>13</sup>C NMR, the new 3 carbon signals appeared at 74.8, 74.5 and 66.0 ppm (**Figure A.11, Appendix A**). K<sub>2</sub>CO<sub>3</sub> seemed to be more efficient base for this reaction than TEA (**Entries 4 and 5**). Increase the equivalence of epichlorohydrin seemed to improve the process, but also generated more side product and complicated the subsequent purification (**Entry 6**). Overall, the best condition we found so far still yielded the product in only 40 %. The use of

epichlorohydrin in stead of the originally used epibromohydrin might be the cause of this ineffectiveness.[74] The reactions also often generated brown oil side product that required tedious purifications and further lowered the yields. These lack of efficiency and difficulties led us to discontinue this synthetic route towards EDTM.

### 3.1.3 Synthesis of EDTM by transesterification

Transesterification reaction with glycerol using 3,4-dimethoxythiophene (DMT) as the starting material was applied on EDTM synthesis [89-91]. We optimized the reaction condition as shown in **Table 3.4**. This reaction yielded EDTM as yellow oil which can be confirmed the structure by  $^1\text{H}$  NMR (**Figure A.13, Appendix A**),  $^{13}\text{C}$  NMR (**Figure A.14, Appendix A**) and broad IR peak at  $3386\text{ cm}^{-1}$  of O-H stretching of hydroxyl group (**Figure A.15, Appendix A**). All the characterization data corresponded well with the report from literature [74].



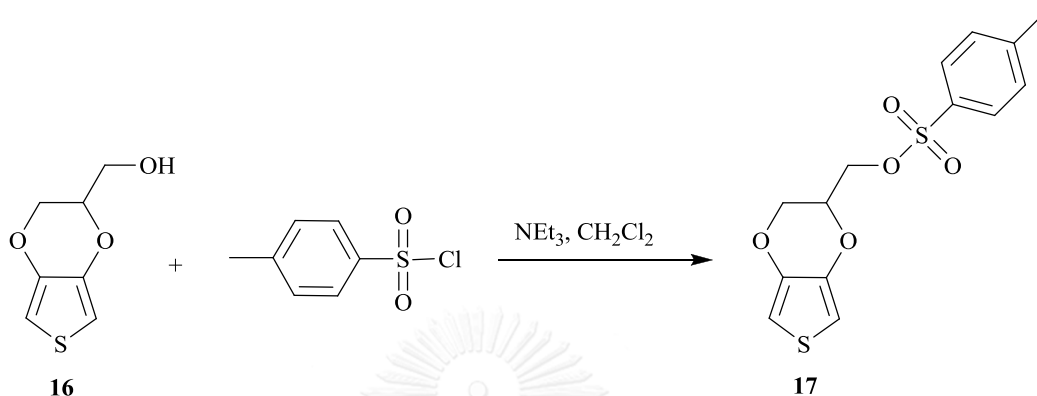
**Table 3.4** Conditions for transesterification of DMT with glycerol

Entry	DMT (mmol)	Glycerol (mmol)	PTSA (mmol)	Time (h)	% conversion	% yield
1	1	6	0.2	30	56	45
2	1	6	0.2	48	61	63
3	1	6	0.2	72	63	34
4	1	6	0.2	168	73	25
5	0.5	3	0.05	48	52	32
6	0.5	3	0.15	48	62	71
7	0.5	3	0.3	48	62	50
8	0.5	3	0.5	48	87	16
9	1	6	0.1	48	63	34
10	1	6	0.3	48	70	53
11	1	6	0.6	48	72	32

From the above table, the optimum time for this reaction is 48 h (**Entry 2**), Longer reaction time increased the conversion of DMT but decreased the amount of EDTM obtained, which might result from partial decomposition of EDTM. The reason for this ineffective transesterification may be because the presence of appreciable amount of water in glycerol interferes the reaction by competitively exchanging with product or reactant. The suitable amount of PTSA for this reaction seemed to be approximately 0.2-0.3 equivalents to DMT (**Entries 6 and 10**). In this reaction moreover, smaller scale gave better % yield of the product (**Entry 6**).

### 3.1.4 Synthesis of other thiophene derivatives

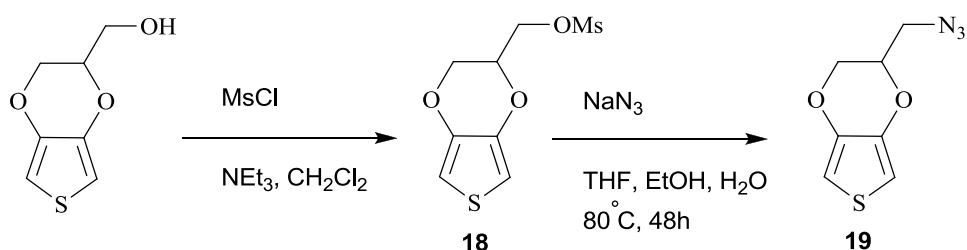
#### 3.1.4.1 Synthesis of (2,3-dihydrothieno[3,4-b][1,4]dioxin-2-yl)methyl 4'-methyl benzenesulfonate (17)



**Scheme 3.4** Synthesis of compound 17

The reaction was carried out based on a relevant report, which yielded compound 17 in 80 %yield [10]. The presence of the tosylate group was characterized by <sup>1</sup>H NMR showing the 2 aromatic ArH signals and the methyl group in addition to the signals of EDTM (Figure A.16, Appendix A). These signals of aromatic ring and methyl group were also present in <sup>13</sup>C NMR at 140.4, 132.5, 130.0, 128.0 and 21.6 ppm (Figure A.17, Appendix A).

#### 3.1.4.2 Synthesis of 2-(azidomethyl)-2,3-dihydrothieno[3,4-b][1,4]dioxine (19)

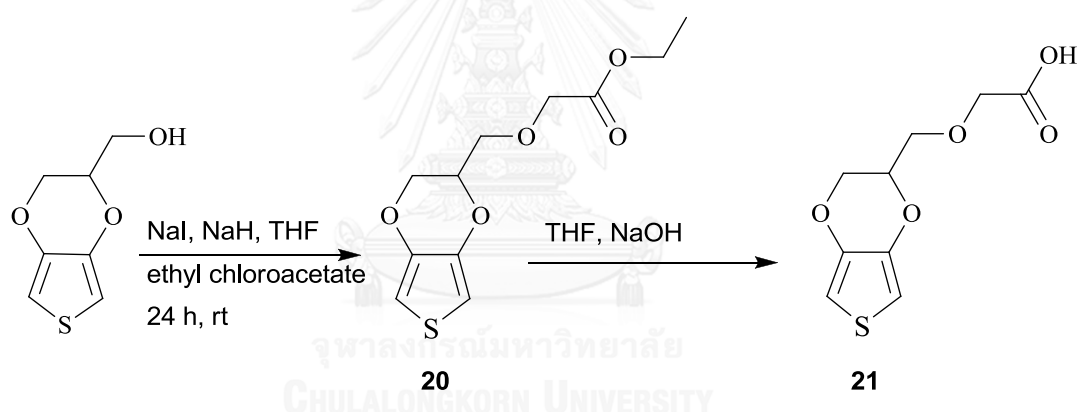


**Scheme 3.5** Synthesis of compounds 18 and 19

EDTM was used as nucleophile in substitution reaction with methanesulfonyl chloride. The product was obtained in quantitative yield and confirmed the structure by  $^1\text{H}$  NMR singlet signal of methanesulfonate group at 3.07 ppm (Figure A.18, Appendix A) and  $^{13}\text{C}$  NMR signal at 37.6 ppm (Figure A.19, Appendix A).

Compound **18** was used as the starting material in the subsequent substitution reaction with azide [76]. The product **19** was obtained as clear liquid in 70 %yield.  $^1\text{H}$  NMR showed similar pattern of signals to EDTM except the exocyclic methylene group that shifted downfield to 3.53 ppm (Figure A.20, Appendix A). The position of this signal in  $^{13}\text{C}$  NMR was at 50.6 ppm (Figure A.21, Appendix A).

### 3.1.4.3 Synthesis of 2-((2,3-dihydrothieno[3,4-b][1,4]dioxin-2-yl)methoxy) acetic acid (**21**)

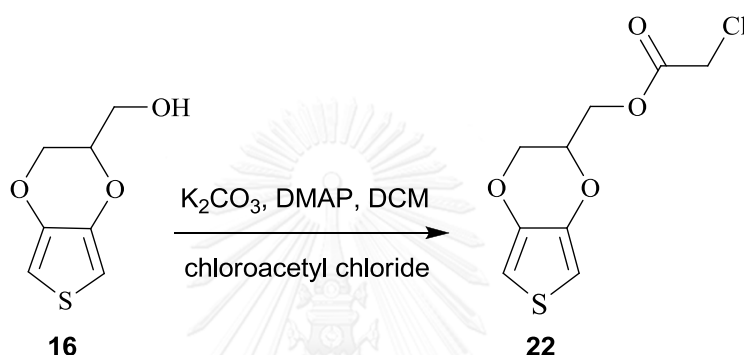


Scheme 3.6 Synthesis of compounds **20** and **21**

The deprotonated EDTM was used as nucleophile in substitution reaction with ethyl chloroacetate with NaI as catalyst to obtain compound **20** in 37 %yield. The efficiency of this reaction may be increased by using more reactive reagent such as ethyl bromoacetate. The structure of the product was confirmed by  $^1\text{H}$  NMR showing the presence of ethoxy acetate group at 4.18, 4.20-4.33 and 1.28-1.35 ppm (Figure A.22, Appendix A). These signals also presented in  $^{13}\text{C}$  NMR at 14.2, 61.0 for ethyl group, 65.9 for  $\alpha$ -carbon and 170.0 ppm for carbonyl carbon (Figure A.23, Appendix A).

Compound **20** was hydrolyzed by NaOH to obtain compound **21** in quantitative yield. The structure of compound **21** was confirmed from the absence of the ethyl group of the original ester in  $^1\text{H}$  NMR (Figure A.24, Appendix A) and  $^{13}\text{C}$  NMR spectra (Figure A.25, Appendix A).

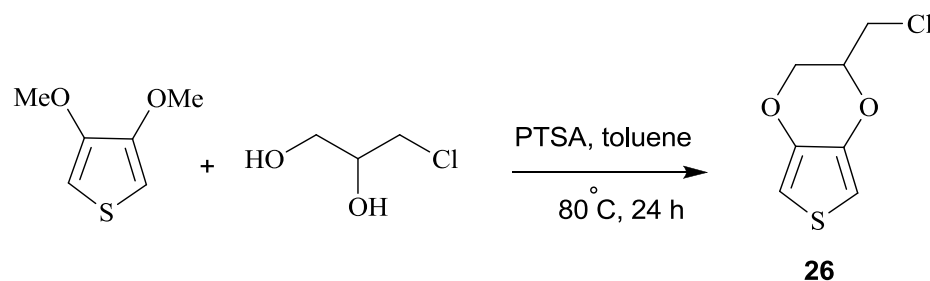
#### 3.1.4.4 Synthesis of (2,3-dihydrothieno[3,4-b][1,4]dioxin-2-yl)methyl 2'-chloroacetate (**22**)



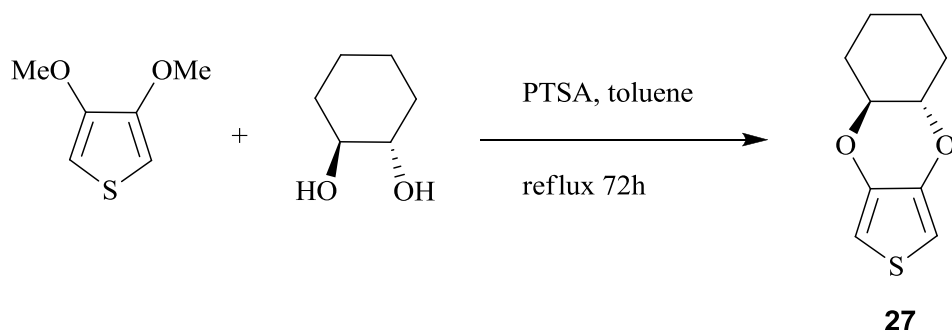
Scheme 3.7 Synthesis of compound **22**

EDTM was used as nucleophile in substitution reaction with chloroacetyl chloride. Using DMAP as catalyst, the reaction obtained the product in quantitative yield. The structure of the product was confirmed by  $^1\text{H}$  NMR showing the presence of additional 2H signal compared to EDTM structure at 4.38-4.32 ppm (Figure A.26, Appendix A) and the presence of carbonyl group in  $^{13}\text{C}$  NMR at 167.0 ppm (Figure A.27, Appendix A).



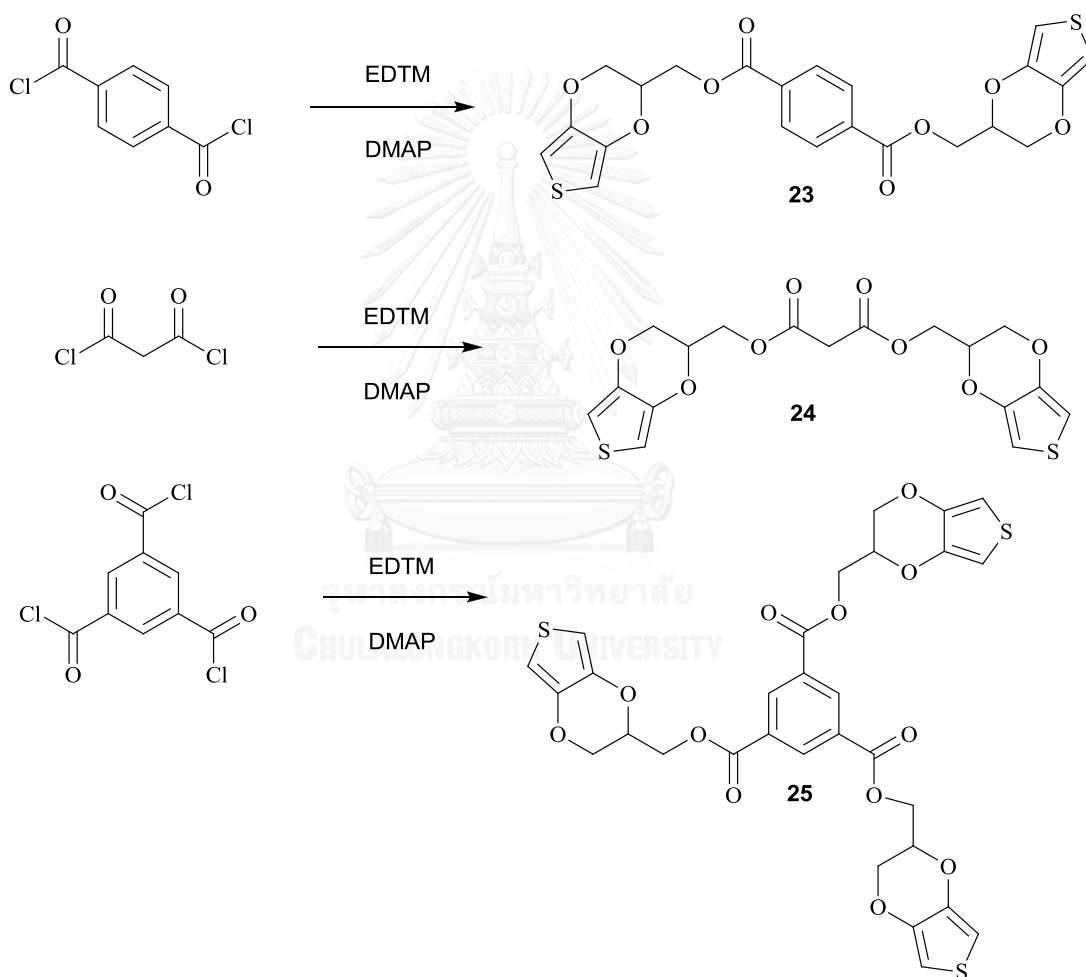
3.1.4.5 Synthesis of 2-(chloromethyl)-2,3-dihydrothieno[3,4-*b*][1,4]dioxine (**26**)Scheme 3.8 Synthesis of compound **26**

DMT was used as the starting material in transesterification reaction with 3-chloro-1,2-propanediol to obtain compound **26** in quantitative yield. The reason that this reaction give better yield compared with the earlier ether exchange with glycerol is because of no interfering moisture in the reagent. The structure of compound **26** was confirmed by  $^1\text{H}$  NMR showing splitting pattern similar to EDTM at 4.37, 4.28, 4.20-4.09 and 3.78-3.60 ppm (Figure A.39, Appendix A) and  $^{13}\text{C}$  NMR showing the new carbon signals at 72.9, 65.6 and 41.3 (Figure A.40, Appendix A) [79].

3.1.4.6 Synthesis of ( $\pm$ )-4a,5,6,7,8,8a-hexahydrobenzo[*e*]thieno[3,4*b*][1,4]dioxine (**27**)Scheme 3.9 Synthesis of compound **27**

EDTM was used as the starting material in transesterification reaction with ( $\pm$ )trans-1,2-cyclohexanediol to synthesize compound **27** in 86 %yield [80]. The structure of compound **27** was confirmed by  $^1\text{H}$  NMR, showing the signals of cyclohexane ring at 1.24–2.20 ppm with the signal of thiophene ring at 6.30 ppm (Figure A.41, Appendix A). In  $^{13}\text{C}$  NMR, the signals of cyclohexane ring appeared at 77.1, 30.1 and 23.8 ppm (Figure A.42, Appendix A).

### 3.1.5 Synthesis of linked multi thiophene precursor



Scheme 3.10 Reactions of EDTM with various acid chlorides

EDTM was used as the pre-polymerizing unit to be linked as the precursor for multi strand polymers. The hydroxyl group of EDTM was the nucleophile in substitution reactions with multi-acid chlorides using DMAP as the catalyst in anhydrous condition. The presumably incomplete substitution products were washed away with base during workup. In the reaction of EDTM with terephthaloyl chloride and benzene-1,3,5-tricarbonyl trichloride resulted in similar % yields of products (56% and 61%). The higher %yield was found in reaction with malonyl chloride (88%) which has higher reactivity.

The character of compound **23** was confirmed with high resolution mass spectrometry (**Figure A.28, Appendix A**) and NMR, IR spectroscopy. The singlet aromatic signal at 8.10 ppm of the linker appeared in  $^1\text{H}$  NMR spectrum (**Figure A.29, Appendix A**), and also at 133.6 and 129.8 ppm with the carbonyl carbon at 165.4 ppm in  $^{13}\text{C}$  NMR spectrum (**Figure A.30, Appendix A**). The IR peak of C=O stretching was present at  $1715\text{ cm}^{-1}$  (**Figure A.31, Appendix A**).

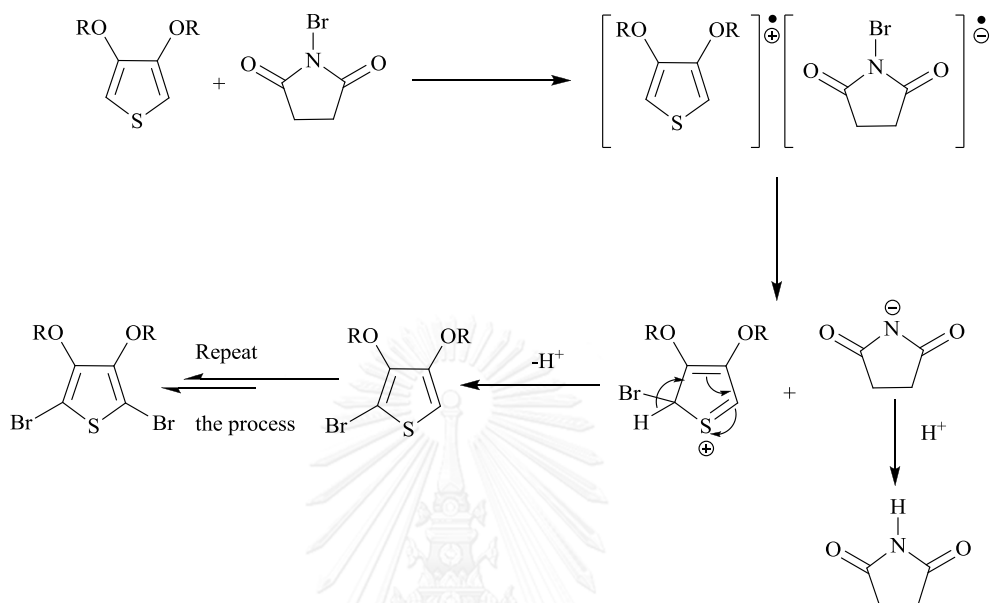
Compound **24** was also characterized by high resolution mass spectrometry (**Figure A.32, Appendix A**) and NMR, IR spectroscopy.  $^1\text{H}$  NMR of this compound showed the singlet methylene hydrogen signal at 3.50 ppm (**Figure A.33, Appendix A**). The signal of carbonyl carbon was found in  $^{13}\text{C}$  NMR at 165.7 ppm with methylene carbon at 41 ppm (**Figure A.34, Appendix A**). The C=O stretching appeared at  $1733\text{ cm}^{-1}$  in IR spectrum (**Figure A.35, Appendix A**).

The structure of compound **25** was confirmed from the presence of singlet aromatic signal in  $^1\text{H}$  NMR at 8.85 ppm (**Figure A.36, Appendix A**) and the carbonyl carbon in  $^{13}\text{C}$  NMR at 164.3 ppm (**Figure A.37, Appendix A**). This carbonyl signal also presented in IR at  $1712\text{ cm}^{-1}$  (**Figure A.38, Appendix A**).

### 3.2 Bromination of monomers

The  $\alpha$ -positions of thiophene ring are generally very reactive towards electrophiles or radicals. Substitutions of these  $\alpha$ -hydrogens by halogenation reactions were mostly facile and efficient [81]. Most thiophene derivatives could be quickly brominated using *N*-bromosuccinimide (NBS), and provided the corresponding relatively pure 2,5-dibromothiophenes. We discovered that high yields of

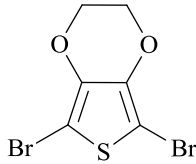
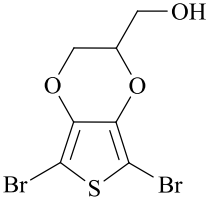
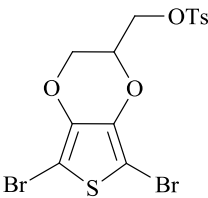
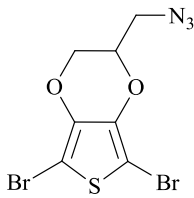
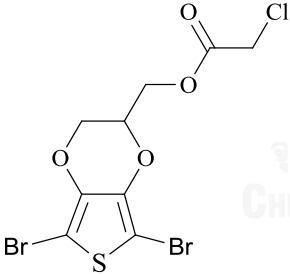
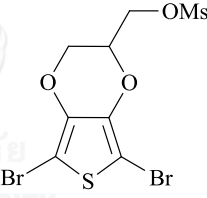
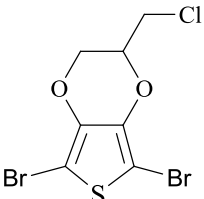
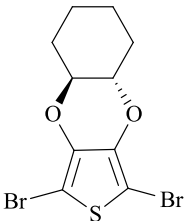
bromination of EDOT-related derivatives could simply be obtained when treated with NBS in a few minutes at room temperature in ambient atmosphere. The possible mechanism of this bromination procedure was shown in **Scheme 3.11**.



**Scheme 3.11** Bromination reaction on thiophene monomers through radical-initiated mechanism

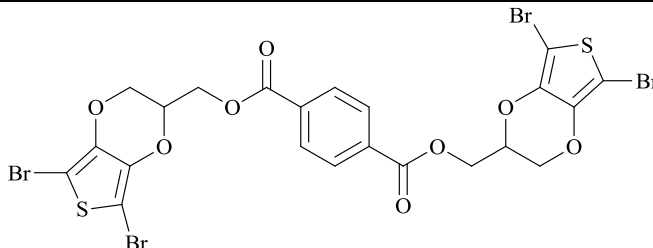
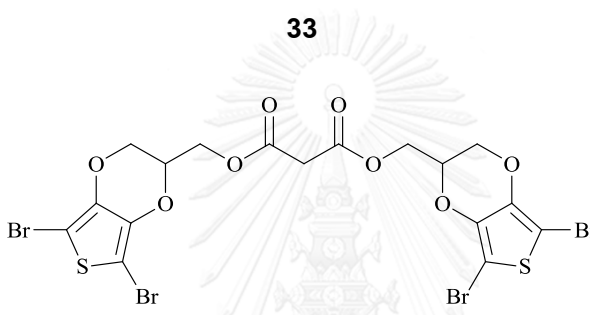
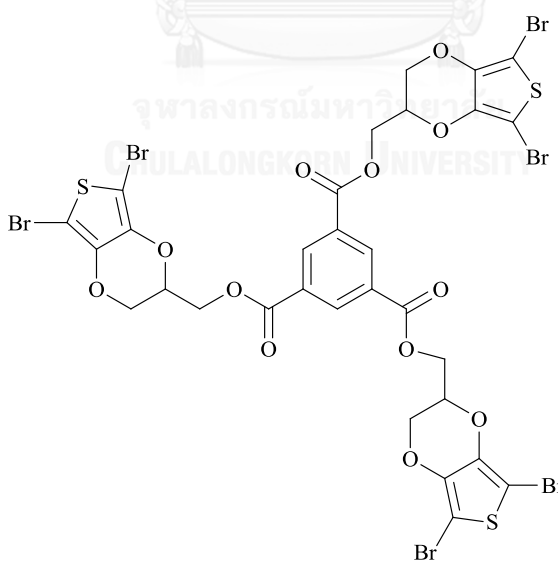
Most bromination processes yielded the corresponding brominated products in high to excellent yields (**Table 3.5**). All brominated products were characterized by the absence of  $\alpha$ -hydrogens signals of thiophene rings in  $^1\text{H}$  NMR. For the compound **48**, the liquid product was quite reactive and perhaps quickly underwent polymerization even in concentrated solution yielding insoluble dark blue solid. This sudden change made it impossible to purify and firmly identify this compound.

**Table 3.5** Percentage yields of brominated dioxithiophene monomers synthesis

Product	%yield	Product	%yield
 <b>28</b>	98	 <b>29</b>	77
 <b>30</b>	90.4	 <b>31</b>	70
 <b>32</b>	94	 <b>48</b>	- <sup>a</sup>
 <b>36</b>	73	 <b>37</b>	94

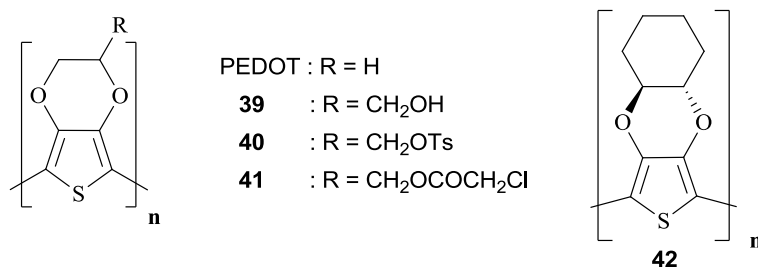
<sup>a</sup>The product can't be purified or identified.

**Table 3.6** Percentage yields of perbrominated linked multi-thiophenes synthesis

Product	%yield
 <b>33</b>	95
 <b>34</b>	68
 <b>35</b>	83

### 3.3 Polymerization of monomers

#### 3.3.1 Solid state polymerization (SSP)



**Figure 3.1** Polymers obtained from solid state polymerization

Among the prepared brominated compounds, only **28**, **30**, **32** and **37** are solid at room temperature and have sufficiently high melting points to be used as the precursors for solid state polymerizations to give polymers PEDOT, **40**, **41** and **42**. Nevertheless, the liquid **29** was also successfully turned into the corresponding polymer **39** under the same polymerization condition. Compounds **29**, **30** and **32** are the first examples of unsymmetric monomers that could be polymerized by this method [45, 46]. The reaction of compound **29** was so facile that the dark blue polymer **39** was possibly obtained even from the warm concentrated solution. These polymers were insoluble in all common solvents, which limited them from being fully characterized. Although the IR spectra of these compounds still carry the structural information of their corresponding monomers (**Figures A.67, A.69, A.71, A.73, and A.75, Appendix A**). The reason for the % yield values higher than 100 in solid state polymerization is because some bromine gas generated as co-product still remained doped within the polymer and significantly increased the total weights of the products.

Unfortunately the perbrominated linked bithiophene precursors **33**, **34** and **35** were liquid at room temperature and did not turn into polymer after being heated. The orientations of the molecules of these precursors in liquid state might

not be suitable for polymerization, in which each monomeric unit was probably kept too far apart from each other by the linker.

### 3.3.2 Chemical polymerization

Due to the unsuccessful attempts on SSP of their brominated derivatives, compounds **23**, **24** and **25** were instead polymerized by oxidative chemical polymerization method using  $\text{FeCl}_3$ . The remaining  $\text{FeCl}_3$  reagent was removed by soxhlet extraction yielding the corresponding insoluble dark blue polymers **44**, **45** and **46** in 63, 61 and 67 %yields respectively [92]. The IR spectra of these compounds contained structural information that were well correlated to the spectra of their monomers. (Figures A.78-80, Appendix A)

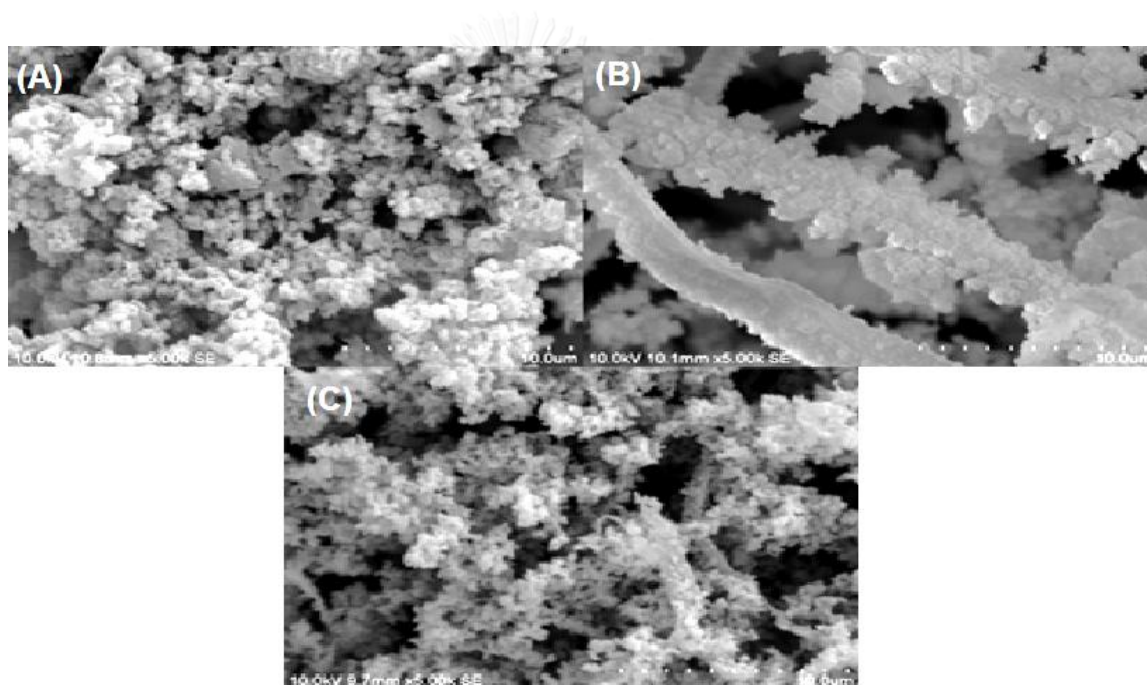
### 3.4 Surface area measurement

To determine if the polymers containing linked bithiophene derivatives could affect the porous property of the PEDOT, a mixture of EDOT combining with 5% of compound **23** was chemically polymerized by  $\text{FeCl}_3$  to obtain the dark blue copolymer mixture (PEDOT + 5% of polymer **44**) and measured its surface area by BET nitrogen adsorption technique. In comparison to pure PEDOT obtained from chemical polymerization, the result showed that the surface area of PEDOT increased from  $238.65 \text{ m}^2/\text{g}$  to  $423.72 \text{ m}^2/\text{g}$  in copolymer with similar average pore size closed to 2 nm, the boundary of mesoporous materials. This porous properties made this copolymeric material to be classified as an example of conjugated microporous polymer (CMP) [69]. It could be noted that the presence of the linked bithiophene polymer **44** even at only 5% incorporation into PEDOT can significantly increase the surface area of the resulted polymer mixture due to the void space generated among polymer chains. Higher ratios of linked bithiophene within the copolymer may create porous polythiophene based materials with even higher surface area, suitable for further developments into sensors and related applications.



### 3.5 Scanning Electron Microscope (SEM)

Scanning electron microscope was used to observe the surface images of chemically polymerized PEDOT and its mixture with polymer **44** (Figure 3.2). Pure PEDOT has a character of amorphous aggregated clusters on its surface while the polymer **44** showed the fibrous-like structure. Although the copolymer, which contained 5% of **44** showed quite similar surface image to that of pure PEDOT, some fibrous structure and relatively larger void space among the aggregates could be visually noticed, supporting the earlier result on higher surface area of the copolymer.



**Figure 3.2** Scanning electron microscope images (x 5000) for the PEDOT (A), Polymer **44** (B) and PEDOT + 5% polymer **44** (C)

### 3.6 Conductivity measurement

Electrical conductivity measurement was carried out using four-point probe technique [93] (Table B.1, Appendix B). A compressed thin polymer pellet of each polymer sample was measured its surface conductivity immediately after being doped by  $I_2$  vapor for 24 h. The results were shown in Table 3.7.

**Table 3.7** Conductivity of the synthesized polymers

Entry	Polymer	Polymerization method	Reaction temperature (°C) <sup>a</sup>	Conductivity (S/cm)
1	PEDOT ( <b>38c</b> )	chemical	30	3.62
2	PEDOT ( <b>38</b> )	SSP <sup>b</sup>	80	5.91
3	<b>39</b>	SSP <sup>b</sup>	80	44.5
4	<b>40</b>	SSP <sup>b</sup>	80	19.0
5	<b>41</b>	SSP <sup>b</sup>	80	1.08
6	<b>42</b>	SSP <sup>b</sup>	80	0.313
7	<b>42</b>	SSP <sup>b</sup>	120	129
8	<b>44</b>	chemical	30	$4.45 \times 10^{-5}$
9	<b>45</b>	chemical	30	$3.34 \times 10^{-2}$
10	PEDOT + 5% <b>44</b>	chemical	30	6.32

<sup>a</sup> The reaction time was limited to 24 h.

<sup>b</sup> Use the corresponding  $\alpha, \alpha'$ -dibromo derivatives as the monomers

From the conductivity data, although PEDOT film obtained from SSP of compound **28** (Entry **2**) showed higher value than that obtained from chemical polymerization, (Entry **1**) the difference margin was not as high as what has been previously reported [45]. The possible reason could be due to the reaction time that was limited to 24 h. We observed that all polymer film obtained from SSP process still contained some unreacted monomers in various amounts. Their conductivity values were found to continue to increase from further SSP of these remaining monomers after being heated or kept for longer period of time. Much higher conductivity of polymer **39** and its tosylate derivative **40** (Entries **3** and **4**) indicated that SSP of these derivatives were more facile, possibly because of polar interactions among the side chains of the monomers help situate them towards suitable arrangements for effective SSP. In fact, the monomer **29** was quite difficult to purify as it kept turning blue upon standing at room temperature or being concentrated from a solution. The more slowly polymerized **32** that turned into polymer **41** (Entry

5) showed lower conductivity than SSP-PEDOT. This exemplified the incomplete polymerization due to limited reaction time used.

The less polar compound **37** correspondingly produced the less conductive polymer **42**. (**Entry 6**) But since this monomer has a relatively high melting point at 128 °C, the attempt on its SSP was repeated at higher temperature. (**Entry 7**) After the same period of 24 h, the conductivity of the resulted polymer **42** soared up to 129 S/cm, reflecting on its much more advanced stage of the reaction progress and the intrinsic efficiency of this class of conjugated polymers that could be achieved by SSP. This value surpasses that of PEDOT and is currently the highest among this group of polymers.[46]

The polymer of linked bithiophene precursor, polymer **44** and **45** (**Entries 8 and 9**) showed very low conductivity values. It is possible that the polymers were formed with less degree of polymerization due to small number of monomers per mole, which were also kept far apart by the linker. The large space within the polymer structure could also reduce the possibilities to transmit electrons between the polymer chains. However, when just 5% of compound **23** was mixed with EDOT and polymerized, the conductivity of the copolymer has restored to the level comparable to pure PEDOT (**Entry 10**). This result revealed that while small blending of the linked bithiophene could significantly increase the surface area of the PEDOT copolymeric film, it had little or no detrimental effect on the conductive property of the film.

### 3.7 UV-Visible spectroscopic study

All polymers obtained by SSP were measured the absorbance by solid state UV. The result showed broad signals with  $\lambda_{\text{max}}$  around 500-650 nm. (**Table 3.8**) (**Figures A.68, A.70, A.72, A.74 and A.76, Appendix A**). Polymer **39** obtained with the most facile SSP process (**Entry 2**) showed highest  $\lambda_{\text{max}}$ , which corresponded higher conjugation length compared with other polymers that was polymerized within the same limited time. These results correlated well to the results of conductivity measurements.

**Table 3.8**  $\lambda_{\max}$  of polymers from SSP

Entry	Polymer	$\lambda_{\max}$ (nm)
1	PEDOT	602.0
2	<b>39</b>	653.0
3	<b>40</b>	549.5
4	<b>41</b>	540.0
5	<b>42</b>	499.5



## CHAPTER IV

### CONCLUSION

The synthesis of compounds **26** and **27** were achieved via ether exchange reactions in good yields. Although the reaction was not yet completed for compound **27**, prolonged reaction only worsened the result. Compound **27** could be brominated to **37**, and subjected to heat-activated SSP, which successfully yielded the expected polymer **42**. Compounds **16**, **17** and **22** could also be similarly brominated and subsequently underwent SSP. The polymer derived from those compounds became the first unsymmetric examples obtained from this method.

Three derivatives of linked bithiophenes were obtained from esterifications of EDTM (**16**) and diacid chlorides. Unfortunately the perbrominated forms of these precursors, compounds **23**, **24** and **25** were liquid at room temperature and did not polymerize by simple heating. The unbrominated precursors could instead be turned into the corresponding polymers by chemical polymerizations using FeCl<sub>3</sub>. Incorporating just 5% of the polymer of **23** into PEDOT gave a significant increase in surface area but had small or no effect on the morphology and conductive property. This result has opened a new way to create a porous conductive material based on polythiophenes.

Finally, the conductivity data from the polymers obtained at 24 h reaction time revealed that compounds **29** and **30** could be polymerized via SSP more efficiently than DBEDOT and became better conductive polymers. Compound **37** could be similarly polymerized at much slower rate. However, its higher melting point allowed SSP to be carried out at higher temperature, which yielded the corresponding polymer **42** with much higher conductivity than all other derivatives. As for the polymers obtained from the linked bithiophene derivatives, the large space within the polymer structure might be the reason for the low electron transmission and hence low conductivity.

## REFERENCES

- [1] Chiang, C.K., Fincher, C.R., Jr., Park, Y.W., Heeger, A.J., Shirakawa, H., Louis, E.J., Gau, S.C., and MacDiarmid, A.G. Electrical conductivity in doped polyacetylene. Physical Review Letters 39(17) (1977): 1098-1101.
- [2] Shirakawa, H., Louis, E.J., MacDiarmid, A.G., Chiang, C.K., and Heeger, A.J. Synthesis of electrically conducting organic polymers: halogen derivatives of polyacetylene, (CH)<sub>x</sub>. Journal of the Chemical Society, Chemical Communications (16) (1977): 578-580.
- [3] Diaz, A., Kanazawa, K.K., and Gardini, G.P. Electrochemical polymerization of pyrrole. Journal of the Chemical Society, Chemical Communications (14) (1979): 635-636.
- [4] Forrest, S.R. The path to ubiquitous and low-cost organic electronic appliances on plastic. Nature 428(6986) (2004): 911-918.
- [5] Saxena, V. and Malhotra, B. Prospects of conducting polymers in molecular electronics. Current Applied Physics 3(2) (2003): 293-305.
- [6] Jonas, F. and Morrison, J. 3, 4-polyethylenedioxythiophene (PEDT): Conductive coatings technical applications and properties. Synthetic Metals 85(1) (1997): 1397-1398.
- [7] Coakley, K.M. and McGehee, M.D. Conjugated polymer photovoltaic cells. Chemistry of Materials 16(23) (2004): 4533-4542.
- [8] Kaneto, K., Kaneko, M., Min, Y., and MacDiarmid, A.G. "Artificial muscle": Electromechanical actuators using polyaniline films. Synthetic Metals 71(1) (1995): 2211-2212.
- [9] Halls, J.M., Walsh, C.A., Greenham, N.C., Marseglia, E.A., Friend, R.H., Moratti, S.C., and Holmes, A.B. Efficient photodiodes from interpenetrating polymer networks. Nature 376 (1995): 498-500.
- [10] Albert, K.J., Lewis, N.S., Schauer, C.L., Sotzing, G.A., Stitzel, S.E., Vaid, T.P., and Walt, D.R. Cross-reactive chemical sensor arrays. Chemical Reviews 100(7) (2000): 2595-2626.
- [11] McQuade, D.T., Pullen, A.E., and Swager, T.M. Conjugated polymer-based chemical sensors. Chemical Reviews 100(7) (2000): 2537-2574.
- [12] Lange, U., Roznyatovskaya, N.V., and Mirsky, V.M. Conducting polymers in chemical sensors and arrays. Analytica Chimica Acta 614(1) (2008): 1-26.
- [13] Friend, R.H., Gymer, R.W., Holmes, A.B., Burroughes, J.H., Marks, R.N., Taliani, C., Bradley, D.D.C., Dos Santos, D.A., Brédas, J.L., Lögdlund, M., and Salaneck,

- W.R. Electroluminescence in conjugated polymers. Nature 397(6715) (1999): 121-128.
- [14] De Paoli, M.A. and Gazotti, W.A. Electrochemistry, polymers and opto-electronic devices: a combination with a future. Journal of the Brazilian Chemical Society 13(4) (2002): 410-424.
- [15] Zhou, E., Tan, Z.A., Huo, L., He, Y., Yang, C., and Li, Y. Effect of branched conjugation structure on the optical, electrochemical, hole mobility, and photovoltaic properties of polythiophenes. The Journal of Physical Chemistry B 110(51) (2006): 26062-26067.
- [16] Bunz, U.H. Poly (aryleneethynylene)s: syntheses, properties, structures, and applications. Chemical reviews 100(4) (2000): 1605-1644.
- [17] Skotheim, T.A., Elsenbaumer, R. L. and Reynolds, J. R. Handbook of Conducting Polymers. 2<sup>nd</sup> ed. New York: Marcel Dekker, 1998.
- [18] Streitwieser, A., Jr. Molecular Orbital Theory for Organic Chemists. New York: Wiley, 1961.
- [19] Dubois, C.J. Donor-acceptor Methods for Band Gap Control in Conjugated Polymer. Ph.D. Dissertation, University of Florida, USA, 2003.
- [20] Chadwick, J.E. and Kohler, B.E. Optical spectra of isolated s-cis-and s-trans-bithiophene: torsional potential in the ground and excited states. The Journal of Physical Chemistry 98(14) (1994): 3631-3637.
- [21] DiCésare, N., Belletête, M., Marrano, C., Leclerc, M., and Durocher, G. Intermolecular interactions in conjugated oligothiophenes. 1. Optical spectra of terthiophene and substituted terthiophenes recorded in various environments. The Journal of Physical Chemistry A 103(7) (1999): 795-802.
- [22] DiCésare, N., Belletête, M., Garcia, E.R., Leclerc, M., and Durocher, G. Intermolecular interactions in conjugated oligothiophenes. 3. Optical and photophysical properties of quaterthiophene and substituted quaterthiophenes in various environments. The Journal of Physical Chemistry A 103(20) (1999): 3864-3875.
- [23] Heeger, A.J. Semiconducting and metallic polymers: the fourth generation of polymeric materials. The Journal of Physical Chemistry B 105(36) (2001): 8475-8491.
- [24] Greenham, N.C., Friend, R.H. Physics of conjugated polymers. New York: Academic Press, 1995.
- [25] Su, W.P., Schrieffer, J., and Heeger, A.J. Solitons in polyacetylene. Physical Review Letters 42(25) (1979): 1698-1701.

- [26] Brazovskii, S.A. Fröhlich Conductivity at Temperatures Excitations in the Peierls-Fröhlich State. Soviet Physics JETP Letters 28 (1978): 606-609.
- [27] Rice, M.J. Charged  $\pi$ -phase kinks in lightly doped polyacetylene. Physics Letters A 71(1) (1979): 152-154.
- [28] Campbell, D. and Bishop, A. Soliton excitations in polyacetylene and relativistic field theory models. Nuclear Physics B 200(2) (1982): 297-328.
- [29] Epstein, A.J., Ginder, J.M., Zuo, F., Bigelow, R.W., Woo, H.S., Tanner, D.B., Richter, A.F., Huang, W.S., MacDiarmid, A.G. Very Low Temperature Nuclear Spin Diffusion in trans-Polyacetylene. Synthetic Metals 18 (1987): 303-309.
- [30] Gebhard, F. and Vollhardt, D. Correlation functions for Hubbard-type models: the exact results for the Gutzwiller wave function in one dimension. Physical Review Letters 59(13) (1987): 1472-1475.
- [31] Pinto, N., Shah, P., Kahol, P., and McCormick, B. Conducting state of polyaniline films: Dependence on moisture. Physical Review B 53(16) (1996): 10690-10694.
- [32] Bowden, M.J., Turner, S. R. . Electronic and Photonic Applications of Polymers. ACS Advances in Chemistry Series 210. Washington DC: American Chemical Society, 1998.
- [33] Bredas, J.L. and Street, G.B. Polarons, bipolarons, and solitons in conducting polymers. Accounts of Chemical Research 18(10) (1985): 309-315.
- [34] Roncali, J. Conjugated poly (thiophenes): synthesis, functionalization, and applications. Chemical Reviews 92(4) (1992): 711-738.
- [35] Pomerantz, M., Tseng, J.J., Zhu, H., Sproull, S.J., Reynolds, J.R., Uitz, R., Amott, H.J., and Haider, M.I. Processable polymers and copolymers of 3-alkylthiophenes and their blends. Synthetic Metals 41(3) (1991): 825-830.
- [36] Wang, S., Takahashi, H., Yoshino, K., Tanaka, K., and Yamabe, T. Dependence of poly (3-alkylthiophene) film properties on electrochemical polymerization conditions and alkyl chain length. Japanese Journal of Applied Physics 29(4) (1990): 772-775.
- [37] Amou, S., Haba, O., Shirato, K., Hayakawa, T., Ueda, M., Takeuchi, K., and Asai, M. Head-to-tail regioregularity of poly (3-hexylthiophene) in oxidative coupling polymerization with  $\text{FeCl}_3$ . Journal of Polymer Science Part A: Polymer Chemistry 37(13) (1999): 1943-1948.
- [38] Niemi, V., Knuutila, P., Österholm, J.-E., and Korvola, J. Polymerization of 3-alkylthiophenes with  $\text{FeCl}_3$ . Polymer 33(7) (1992): 1559-1562.



- [39] Tamao, K., Kiso, Y., Sumitani, K., and Kumada, M. Alkyl group isomerization in the cross-coupling reaction of secondary alkyl Grignard reagents with organic halides in the presence of nickel-phosphine complexes as catalysts. Journal of the American Chemical Society 94(26) (1972): 9268-9269.
- [40] Negishi, E., Takahashi, T., Baba, S., Van Horn, D., and Okukado, N. Palladium- or nickel-catalyzed reactions of alkenylmetals with unsaturated organic halides as a selective route to arylated alkenes and conjugated dienes: Scope, limitations, and mechanism. Journal of the American Chemical Society 109(8) (1987): 2393-2401.
- [41] Magat, M. Polymerization in the solid state. Polymer 3 (1962): 449-469.
- [42] Wegner, G. Topochemical reactions of monomers with conjugated triple-bonds. IV. Polymerization of bis-(p-toluene sulfonate) of 2,4-hexadien-1,6-diol. Die Makromolekulare Chemie 145(1) (1971): 85-94.
- [43] Walatka, V., Jr., Labes, M., and Perlstein, J.H. Polysulfur Nitride—a One-Dimensional Chain with a Metallic Ground State. Physical Review Letters 31(18) (1973): 1139-1141.
- [44] McCullough, R.D. and Williams, S.P. Toward tuning electrical and optical properties in conjugated polymers using side-chains: highly conductive head-to-tail, heteroatom functionalized polythiophenes. Journal of the American Chemical Society 115(24) (1993): 11608-11609.
- [45] Meng, H., Perepichka, D.F., Bendikov, M., and Wudl, F. Solid-state synthesis of a conducting polythiophene via an unprecedented heterocyclic coupling reaction. Journal of the American Chemical Society 125(49) (2003): 15151-15162.
- [46] Meng, H., Perepichka, D.F., and Wudl, F. Facile Solid-State Synthesis of Highly Conducting Poly (ethylenedioxythiophene). Angewandte Chemie International Edition 42(6) (2003): 658-661.
- [47] Kim, B., Koh, J.K., Kim, J., Chi, W.S., Kim, J.H., and Kim, E. Room Temperature Solid-State Synthesis of a Conductive Polymer for Applications in Stable I<sup>2</sup>-Free Dye-Sensitized Solar Cells. ChemSusChem 5(11) (2012): 2173-2180.
- [48] Barrer, R.M. Zeolites and their synthesis. Zeolites 1(3) (1981): 130-140.
- [49] Zhu, Q.-L. and Xu, Q. Metal-organic framework composites. Chemical Society Reviews 43 (2014): 5468-5512.
- [50] Wu, D., Xu, F., Sun, B., Fu, R., He, H., and Matyjaszewski, K. Design and preparation of porous polymers. Chemical Reviews 112(7) (2012): 3959-4015.

- [51] Sing, K.S. Reporting physisorption data for gas/solid systems with special reference to the determination of surface area and porosity (Recommendations 1984). Pure and Applied Chemistry 57(4) (1985): 603-619.
- [52] Silverstein, M.S., Cameron, N. R., Hillmyer, M. A. Porous Polymers. New Jersey: John Wiley & Sons, 2010.
- [53] Wood, C.D., Tan, B., Trewin, A., Niu, H., Bradshaw, D., Rosseinsky, M.J., Khimyak, Y.Z., Campbell, N.L., Kirk, R., Stöckel, E., and Cooper, A.I. Hydrogen storage in microporous hypercrosslinked organic polymer networks. Chemistry of Materials 19(8) (2007): 2034-2048.
- [54] McKeown, N.B. Polymers of intrinsic microporosity. International Scholarly Research Networks 2012 (2012): 1-16.
- [55] Cote, A.P., Benin, A.I., Ockwig, N.W., O'Keeffe, M., Matzger, A.J., and Yaghi, O.M. Porous, crystalline, covalent organic frameworks. Science 310(5751) (2005): 1166-1170.
- [56] Liu, Q., Tang, Z., Wu, M., and Zhou, Z. Design, preparation and application of conjugated microporous polymers. Polymer International 63(3) (2014): 381-392.
- [57] Jiang, J.X., Su, F., Trewin, A., Wood, C.D., Campbell, N.L., Niu, H., Dickinson, C., Ganin, A.Y., Rosseinsky, M.J., Khimyak, Y.Z., and Cooper, A.I. Conjugated microporous poly(aryleneethynylene) networks. Angewandte Chemie International Edition 46(45) (2007): 8574-8578.
- [58] Jiang, J.X., Su, F., Niu, H., Wood, C.D., Campbell, N.L., Khimyak, Y.Z., and Cooper, A.I. Conjugated microporous poly (phenylene butadiynylene)s. Chemical Communication (4) (2008): 486-488.
- [59] Dawson, R., Adams, D.J., and Cooper, A.I. Chemical tuning of CO<sub>2</sub> sorption in robust nanoporous organic polymers. Chemical Science 2(6) (2011): 1173-1177.
- [60] Li, A., Sun, H.X., Tan, D.Z., Fan, W.J., Wen, S.H., Qing, X.J., Li, G.X., Li, S.Y., and Deng, W.Q. Superhydrophobic conjugated microporous polymers for separation and adsorption. Energy & Environmental Science 4(6) (2011): 2062-2065.
- [61] Chen, L., Yang, Y., and Jiang, D. CMPs as scaffolds for constructing porous catalytic frameworks: a built-in heterogeneous catalyst with high activity and selectivity based on nanoporous metalloporphyrin polymers. Journal of the American Chemical Society 132(26) (2010): 9138-9143.

- [62] Jiang, J.X., Trewin, A., Adams, D.J., and Cooper, A.I. Band gap engineering in fluorescent conjugated microporous polymers. Chemical Science 2(9) (2011): 1777-1781.
- [63] Liu, X., Xu, Y., and Jiang, D. Conjugated microporous polymers as molecular sensing devices: microporous architecture enables rapid response and enhances sensitivity in fluorescence-on and fluorescence-off sensing. Journal of the American Chemical Society 134(21) (2012): 8738-8741.
- [64] Chen, L., Honsho, Y., Seki, S., and Jiang, D. Light-harvesting conjugated microporous polymers: rapid and highly efficient flow of light energy with a porous polyphenylene framework as antenna. Journal of the American Chemical Society 132(19) (2010): 6742-6748.
- [65] Kou, Y., Xu, Y., Guo, Z., and Jiang, D. Supercapacitive Energy Storage and Electric Power Supply Using an Aza-Fused  $\pi$ -Conjugated Microporous Framework. Angewandte Chemie International Edition 50 (2011): 8753-8757.
- [66] Piron, F., Leriche, P., Mabon, G., Grosu, I., and Roncali, J. Electropolymerization of three-dimensional  $\pi$ -conjugated system based on 3, 4-ethylenedioxythiophene (EDOT). Electrochemistry Communications 10(10) (2008): 1427-1430.
- [67] Ak, M. and Toppare, L. Synthesis of star-shaped pyrrole and thiophene functionalized monomers and optoelectrochemical properties of corresponding copolymers. Materials Chemistry and Physics 114(2) (2009): 789-794.
- [68] Piron, F., Leriche, P., Grosu, I., and Roncali, J. Electropolymerizable 3D  $\pi$ -conjugated architectures with ethylenedioxythiophene (EDOT) end-groups as precursors of electroactive conjugated networks. Journal of Materials Chemistry 20(45) (2010): 10260-10268.
- [69] Schmidt, J., Weber, J., Epping, J.D., Antonietti, M., and Thomas, A. Microporous conjugated poly(thienylene arylene) networks. Advanced Materials 21(6) (2009): 702-705.
- [70] Jiang, J.X., Laybourn, A., Clowes, R., Khimyak, Y.Z., Bacsá, J., Higgins, S.J., Adams, D.J., and Cooper, A.I. High surface area contorted conjugated microporous polymers based on spiro-bipropylendioxythiophene. Macromolecules 43(18) (2010): 7577-7582.
- [71] Qiao, S., Du, Z., Huang, W., and Yang, R. Influence of aggregated morphology on carbon dioxide uptake of polythiophene conjugated organic networks. Journal of Solid State Chemistry 212 (2014): 69-72.

- [72] Overberger, C., Mallon, H.J., and Fine, R. Cyclic Sulfones. II. The Polymerization of Styrene in the Presence of 3, 4-Diphenylthiophene-1-dioxide and 3, 4-Di-(p-chlorophenyl)-thiophene-1-dioxide. Journal of the American Chemical Society 72(11) (1950): 4958-4961.
- [73] Wynberg, H. and Kooreman, H. The Mechanism of the Hinsberg Thiophene Ring Synthesis. Journal of the American Chemical Society 87(8) (1965): 1739-1742.
- [74] Lima, A., Schottland, P., Sadki, S., and Chevrot, C. Electropolymerization of 3, 4-ethylenedioxythiophene and 3, 4-ethylenedioxythiophene methanol in the presence of dodecylbenzenesulfonate. Synthetic Metals 93(1) (1998): 33-41.
- [75] Skompska, M., Vorotuntsev, M.A., Refczynska, M., Goux, J., Lesniewska, E., Boni, G., and Moise, C. Electrosynthesis and properties of poly (3, 4-ethylenedioxythiophene) films functionalized with titanocene dichloride complex. Electrochimica Acta 51(11) (2006): 2108-2119.
- [76] Tansil, N.C., Yu, H., Kantchev, E.A.B., Ying, J.Y. Naphthalenetetracarboxyl Diimide-Grafted Poly(3,4-ethylenedioxythiophene)s. Polymer Preprints 48 (2007): 74-75.
- [77] Luo, S.C., Ali, E.M., Tansil, N.C., Yu, H.H., Gao, S., Kantchev, E.A.B., and Ying, J.Y. Poly(3, 4-ethylenedioxythiophene) (PEDOT) nanobiointerfaces: thin, ultrasmooth, and functionalized PEDOT films with in vitro and in vivo biocompatibility. Langmuir 24(15) (2008): 8071-8077.
- [78] Berry, D.J., DiGiovanna, C.V., and Murugan, R. Catalysis by 4-dialkylaminopyridines. Arkivoc 2 (2001): 944-964.
- [79] Segura, J.L., Gómez, R., Reinold, E., and Bäuerle, P. Synthesis and electropolymerization of a perylenebisimide-functionalized 3, 4-ethylenedioxythiophene (EDOT) derivative. Organic Letters 7(12) (2005): 2345-2348.
- [80] Caras-Quintero, D. and Bäuerle, P. Synthesis of the first enantiomerically pure and chiral, disubstituted 3, 4-ethylenedioxythiophenes (EDOTs) and corresponding stereo-and regioregular PEDOTs. Chemical Communications (8) (2004): 926-927.
- [81] Kellogg, R.M., Schaap, A.P., Harper, E.T., and Wynberg, H. Acid-catalyzed brominations, deuterations, rearrangements, and debrominations of thiophenes under mild conditions. The Journal of Organic Chemistry 33(7) (1968): 2902-2909.

- [82] Zhao, H., Liu, C.Y., Luo, S.C., Zhu, B., Wang, T.H., Hsu, H.F., and Yu, H.H. Facile Syntheses of Dioxythiophene-Based Conjugated Polymers by Direct C–H Arylation. *Macromolecules* 45(19) (2012): 7783-7790.
- [83] Jonas, F., Heywang, G., Schmidberg, W. Preparation of (alkylenedioxy) thiophene polymers for use as antistatic agents. German Patent DE 38 13 589 A: 1988.
- [84] Corradi, R. and Armes, S. Chemical synthesis of poly(3, 4-ethylenedioxythiophene). *Synthetic metals* 84(1) (1997): 453-454.
- [85] Guo, K., Hao, J., Zhang, T., Zu, F., Zhai, J., Qiu, L., Zhen, Z., Liu, X., and Shen, Y. The synthesis and properties of novel diazo chromophores based on thiophene conjugating spacers and tricyanofuran acceptors. *Dyes and Pigments* 77(3) (2008): 657-664.
- [86] Pei, Q., Zuccarello, G., Ahlskog, M., and Inganäs, O. Electrochromic and highly stable poly(3, 4-ethylenedioxythiophene) switches between opaque blue-black and transparent sky blue. *Polymer* 35(7) (1994): 1347-1351.
- [87] Pope, J., Buttry, D., White, S., and Corcoran, R. Single component sulfur-based cathodes for lithium-ion batteries. United States Patent US6869729 B1: 2005.
- [88] Li, J.J. Name Reactions in Heterocyclic Chemistry. New York: Wiley, 2004.
- [89] Roquet, S., Leriche, P., Perepichka, I., Joussetme, B., Levillain, E., Frère, P., and Roncali, J. 3, 4-Phenylenedioxythiophene (PheDOT): a novel platform for the synthesis of planar substituted  $\pi$ -donor conjugated systems. *Journal of Materials Chemistry* 14(9) (2004): 1396-1400.
- [90] Perepichka, I.F., Roquet, S., Leriche, P., Raimundo, J.M., Frère, P., and Roncali, J. Electronic Properties and Reactivity of Short-Chain Oligomers of 3, 4-Phenylenedioxythiophene (PheDOT). *Chemistry-A European Journal* 12(11) (2006): 2960-2966.
- [91] Gaupp, C.L., Welsh, D.M., and Reynolds, J.R. Poly (ProDOT-Et<sub>2</sub>): A High-Contrast, High-Coloration Efficiency Electrochromic Polymer. *Macromolecular Rapid Communications* 23(15) (2002): 885-889.
- [92] Sugimoto, R.-I., Takeda, S., Gu, H., and Yoshino, K. Preparation of soluble polythiophene derivatives utilizing transition metal halides as catalysts and their property. *Chemistry Express* 1(11) (1986): 635-638.
- [93] Smits, F. Measurement of Sheet Resistivities with the Four-Point Probe. *Bell System Technical Journal* 37(3) (1958): 711-718.

APPENDIX A

The logo of Chulalongkorn University, featuring a central emblem with a sunburst and a tiered base, set within a circular frame.

จุฬาลงกรณ์มหาวิทยาลัย  
CHULALONGKORN UNIVERSITY

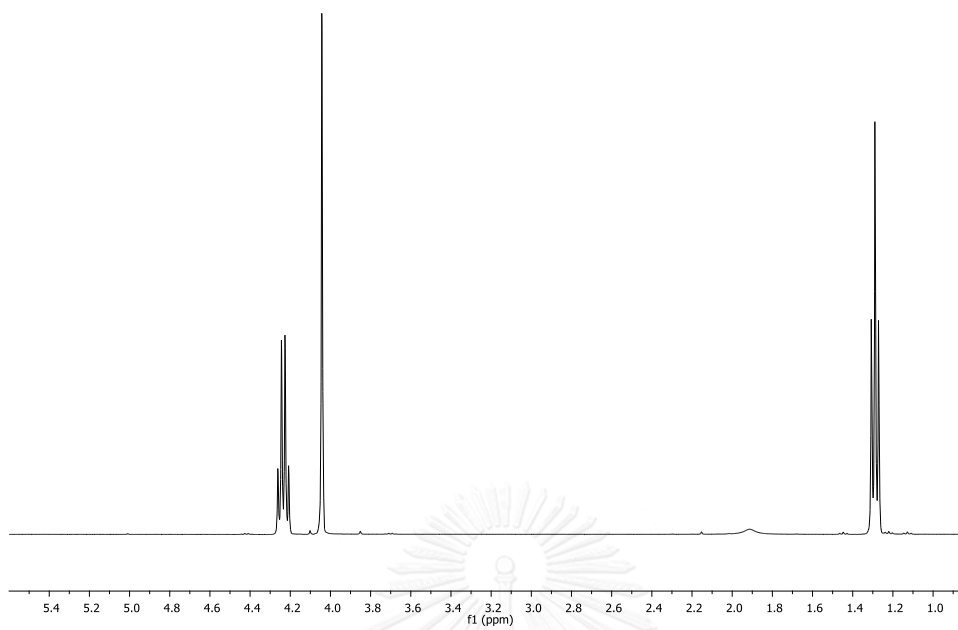


Figure A.1  $^1\text{H}$  NMR ( $\text{CDCl}_3$ ) spectrum of compound 12

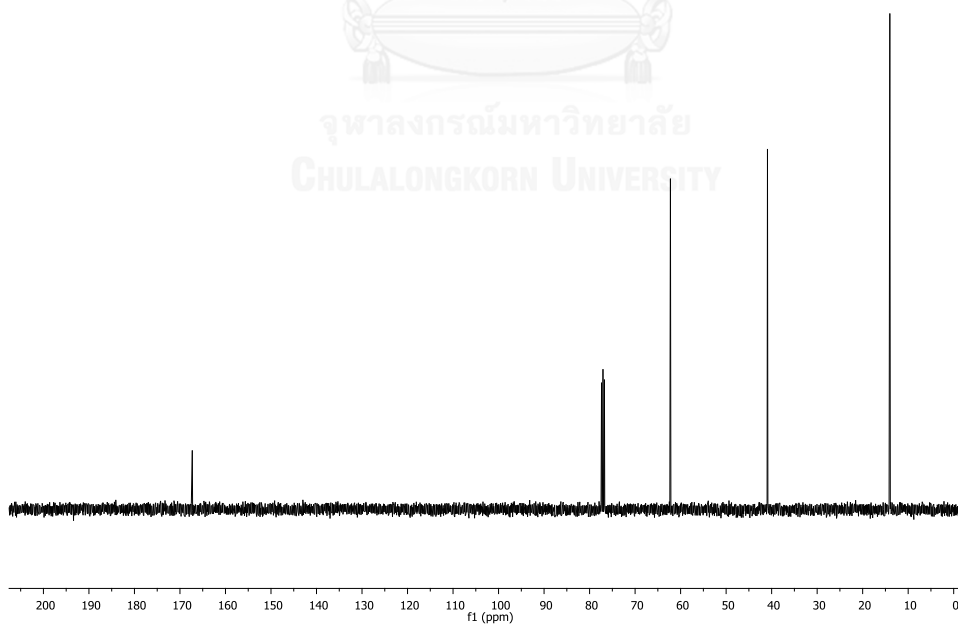


Figure A.2  $^{13}\text{C}$  NMR ( $\text{CDCl}_3$ ) spectrum of compound 12

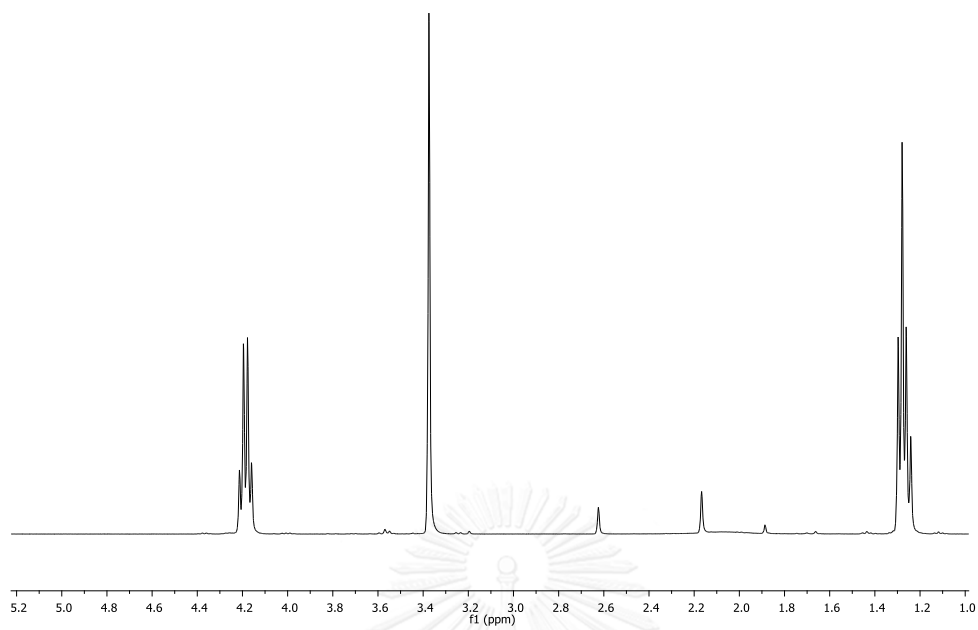


Figure A.3  $^1\text{H}$  NMR ( $\text{CDCl}_3$ ) spectrum of compound **13**

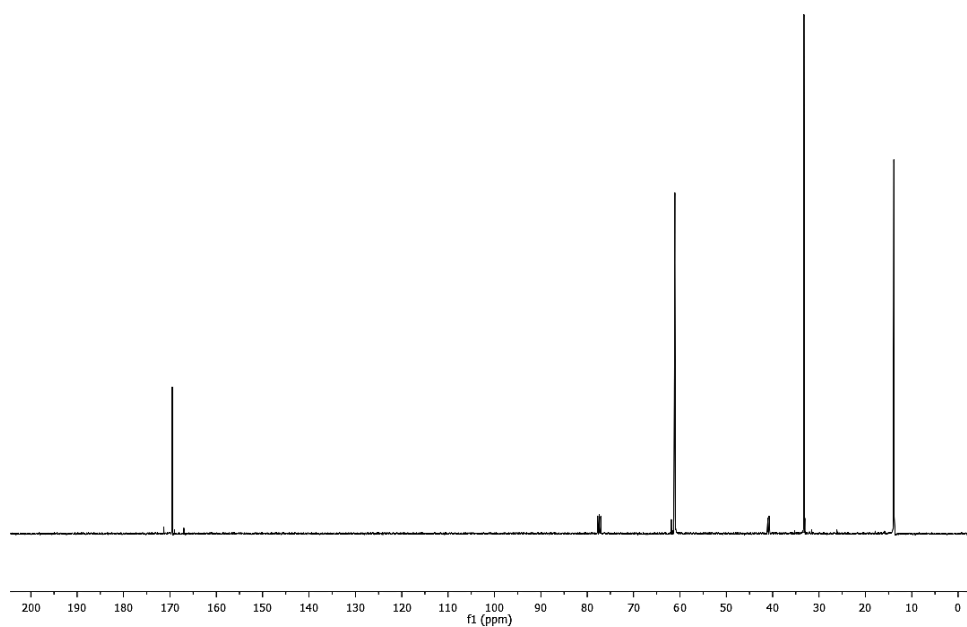


Figure A.4  $^{13}\text{C}$  NMR ( $\text{CDCl}_3$ ) spectrum of compound **13**



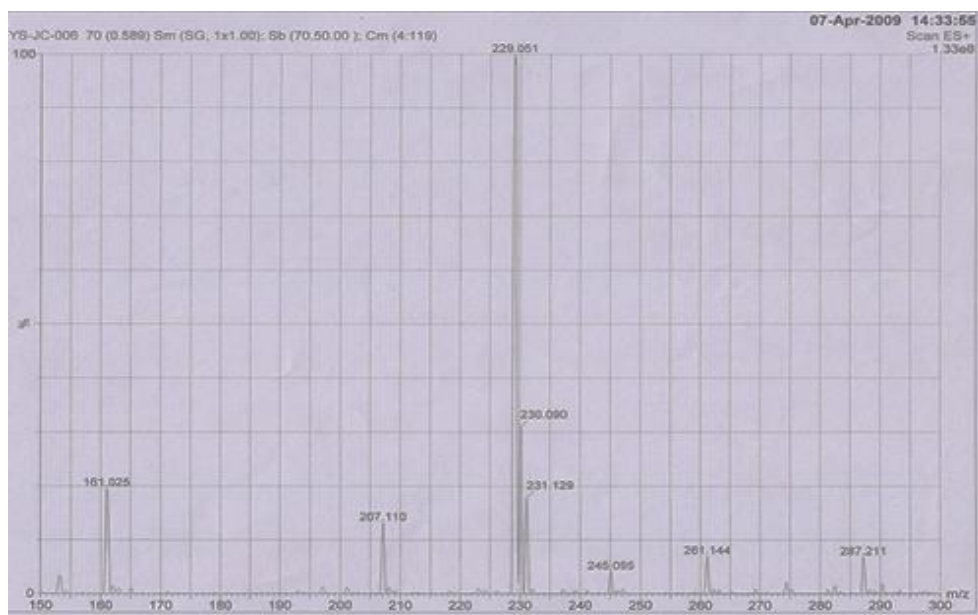


Figure A.5 Mass spectrum of compound 13

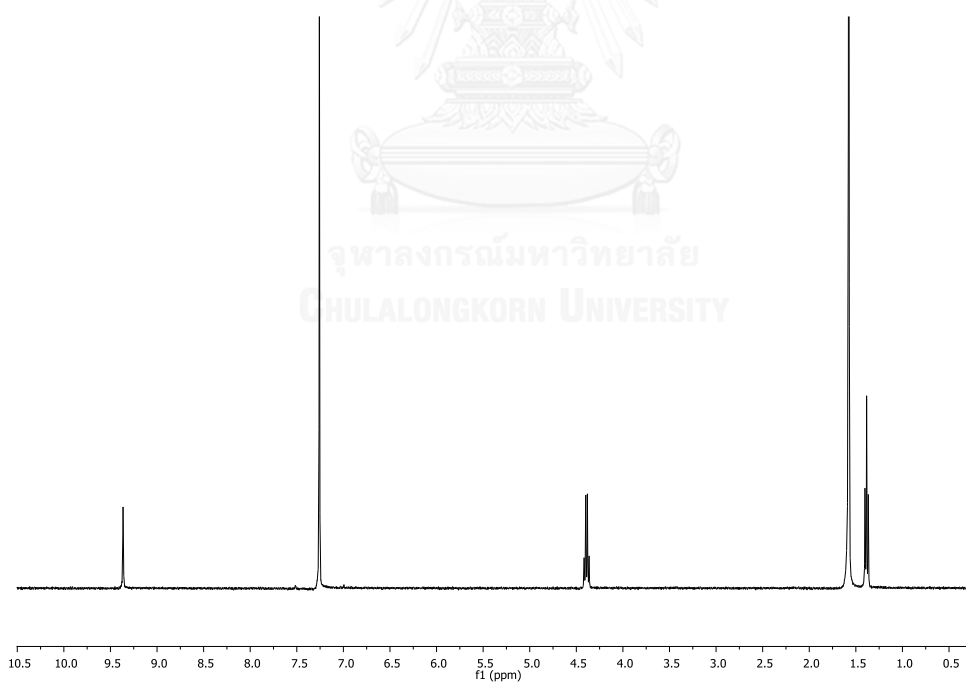


Figure A.6  $^1\text{H}$  NMR ( $\text{CDCl}_3$ ) spectrum of compound 14

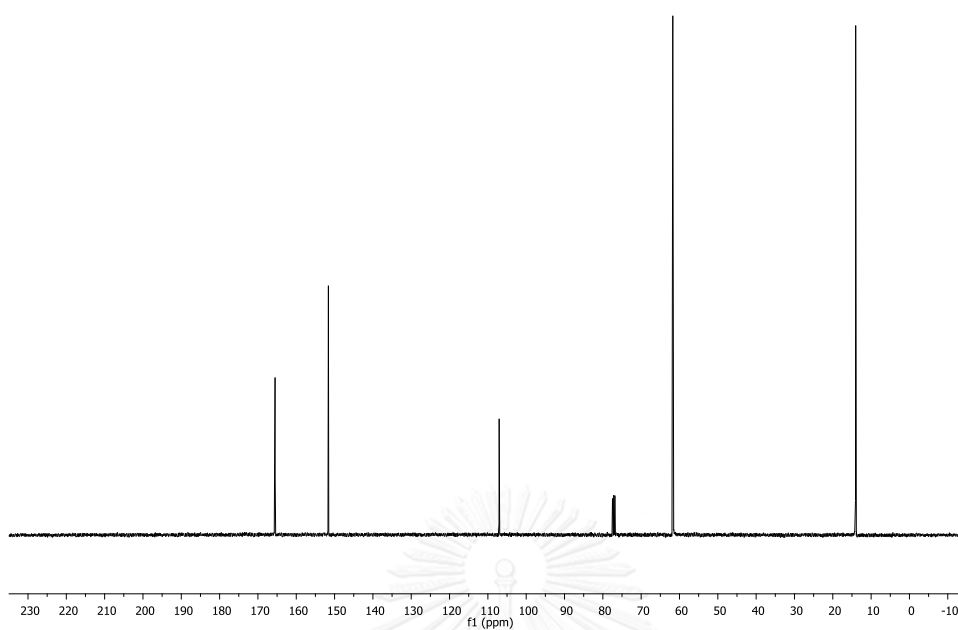


Figure A.7  $^{13}\text{C}$  NMR ( $\text{CDCl}_3$ ) spectrum of compound 14

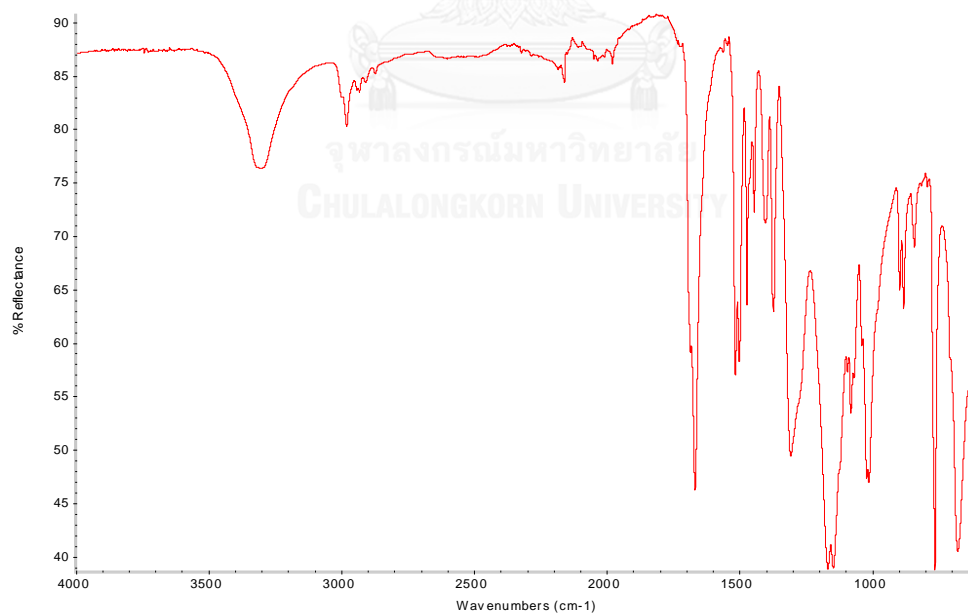


Figure A.8 IR spectrum of compound 14

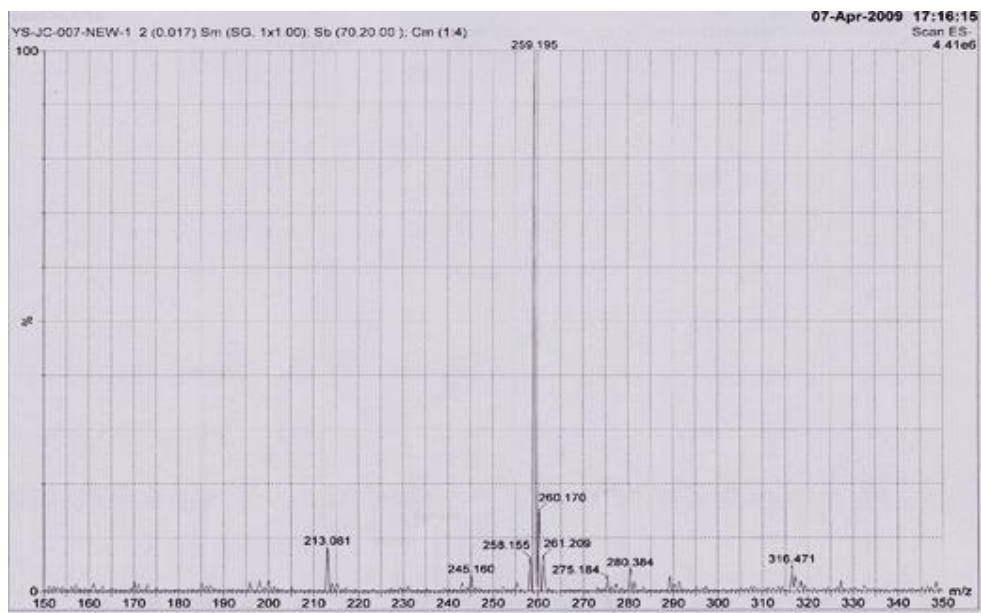


Figure A.9 Mass spectrum of compound 14

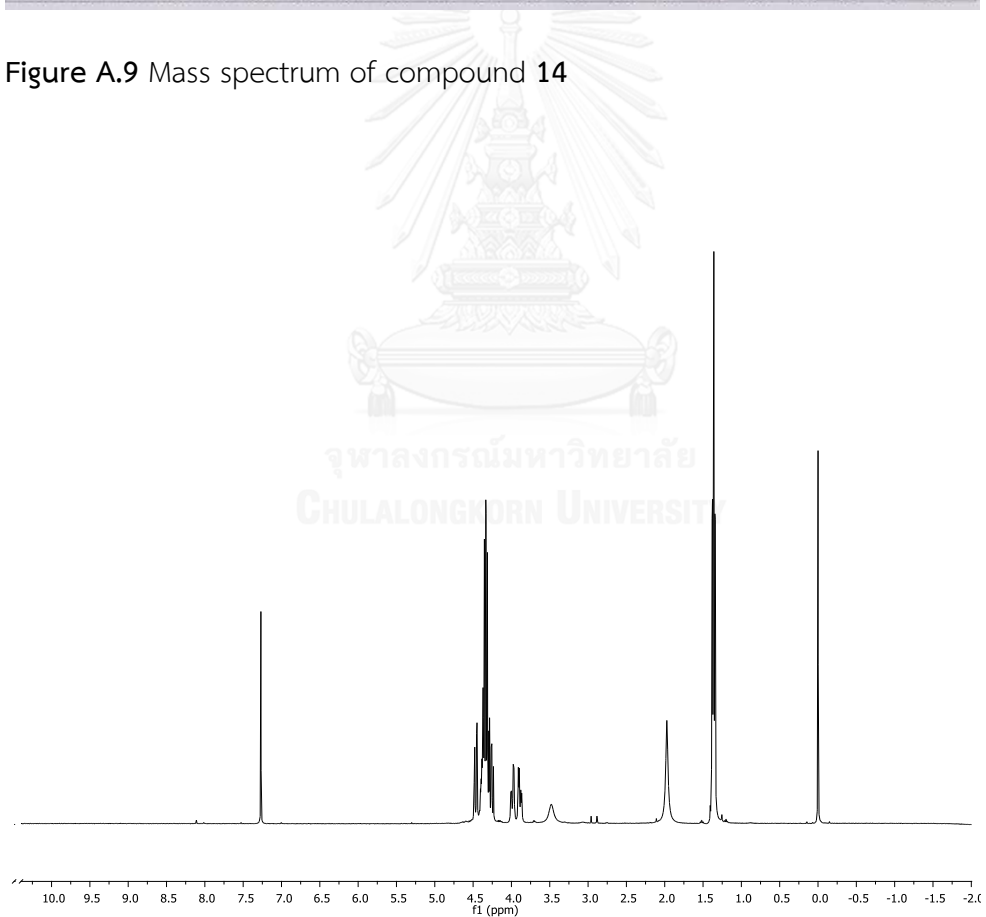


Figure A.10  $^1\text{H}$  NMR ( $\text{CDCl}_3$ ) spectrum of compound 15

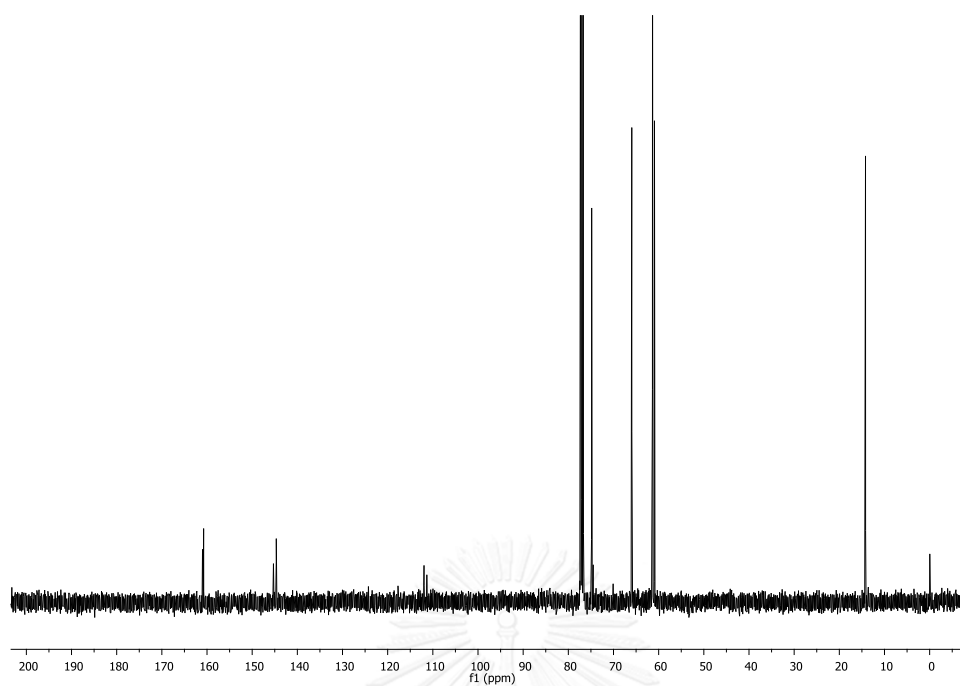


Figure A.11  $^{13}\text{C}$  NMR ( $\text{CDCl}_3$ ) spectrum of compound 15

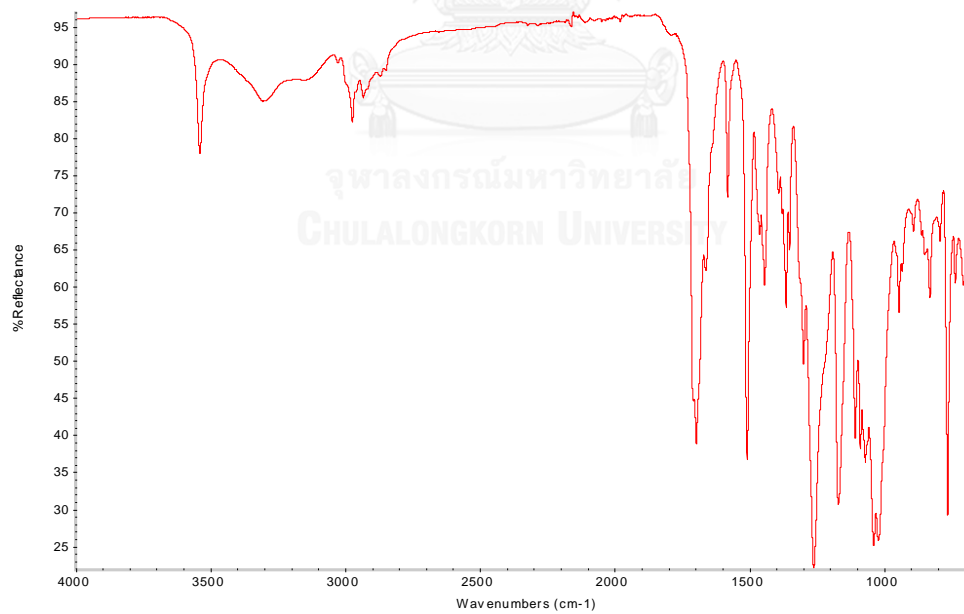


Figure A.12 IR spectrum of compound 15

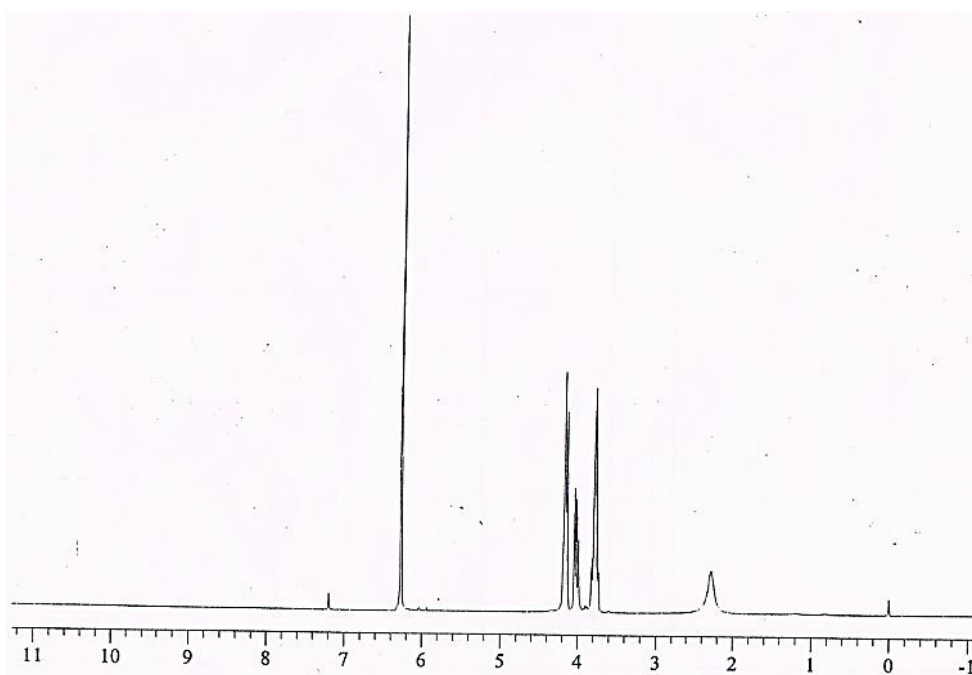


Figure A.13  $^1\text{H}$  NMR ( $\text{CDCl}_3$ ) spectrum of compound 16

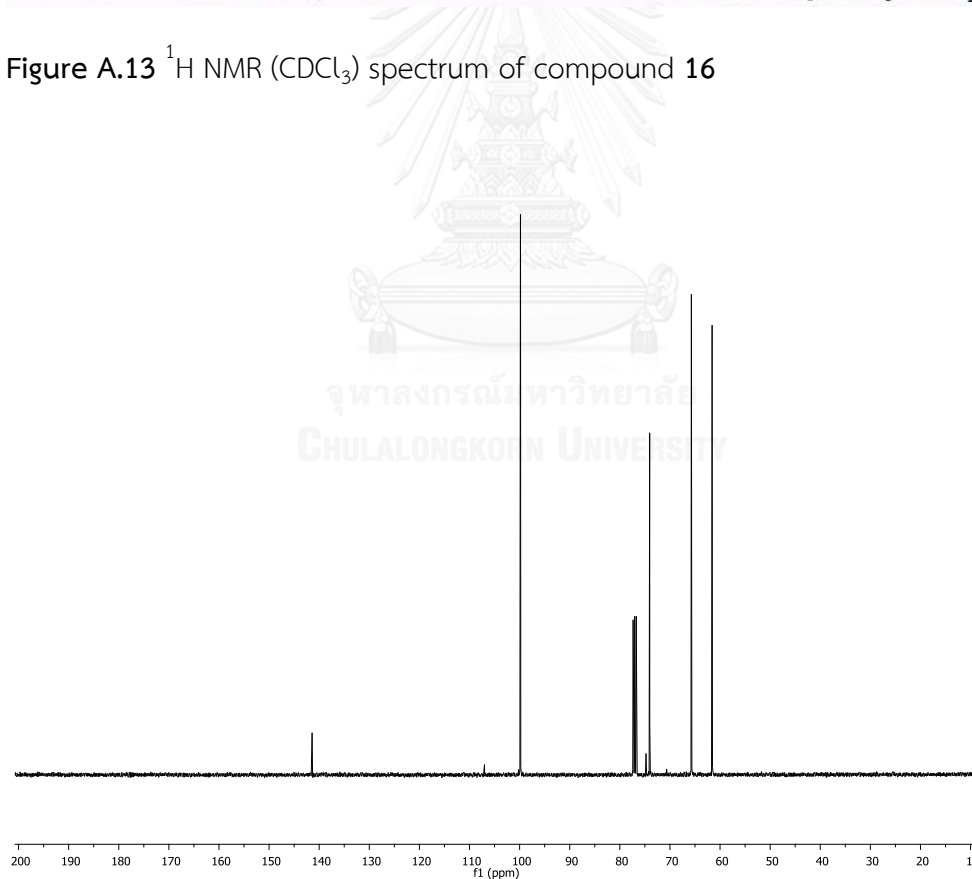


Figure A.14  $^{13}\text{C}$  NMR ( $\text{CDCl}_3$ ) spectrum of compound 16

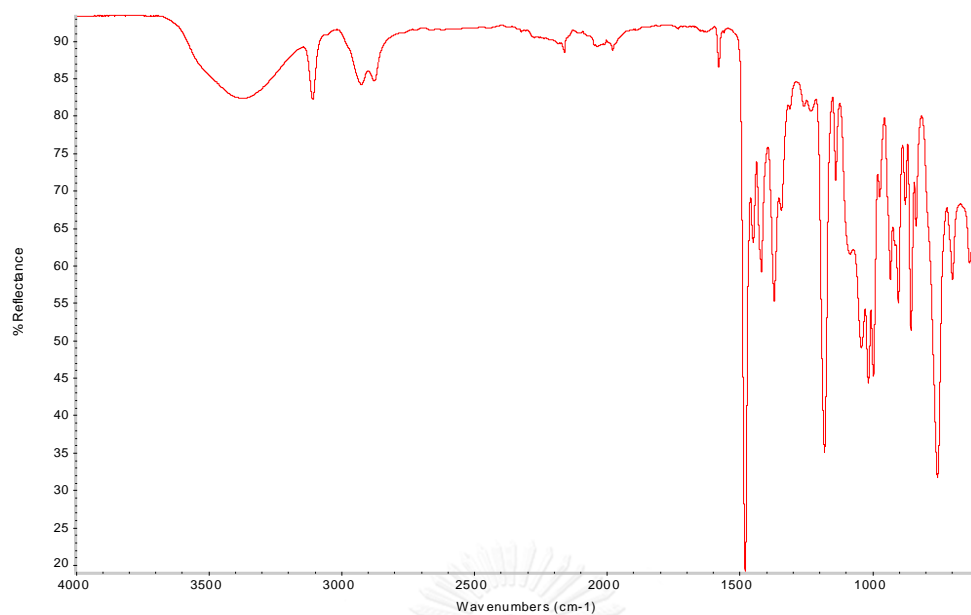


Figure A.15 IR spectrum of compound 16

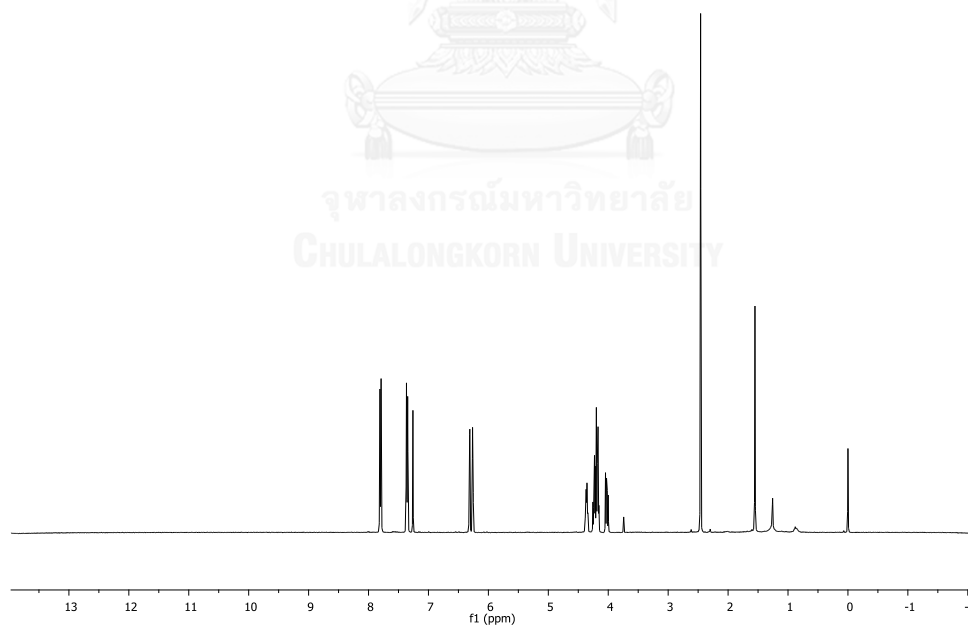


Figure A.16 <sup>1</sup>H NMR (CDCl<sub>3</sub>) spectrum of compound 17

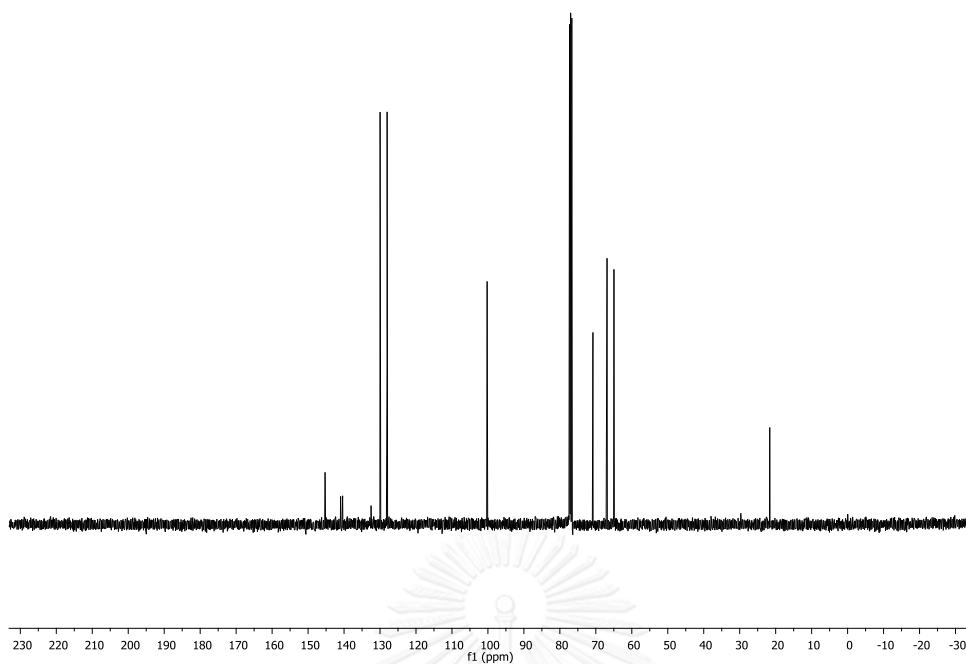


Figure A.17  $^{13}\text{C}$  NMR ( $\text{CDCl}_3$ ) spectrum of compound 17

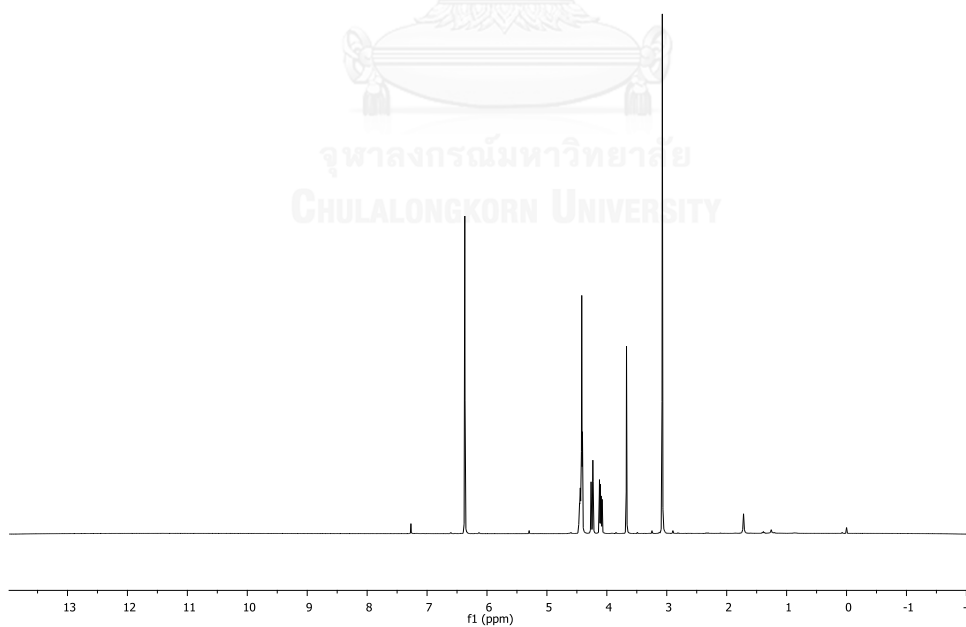


Figure A.18  $^1\text{H}$  NMR ( $\text{CDCl}_3$ ) spectrum of compound 18

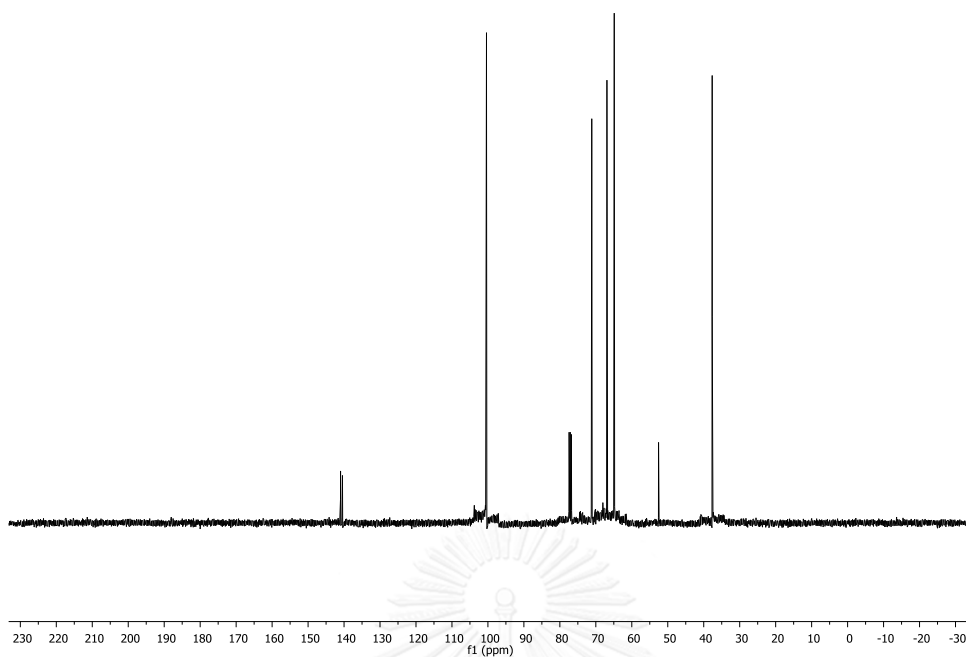


Figure A.19  $^{13}\text{C}$  NMR ( $\text{CDCl}_3$ ) spectrum of compound 18

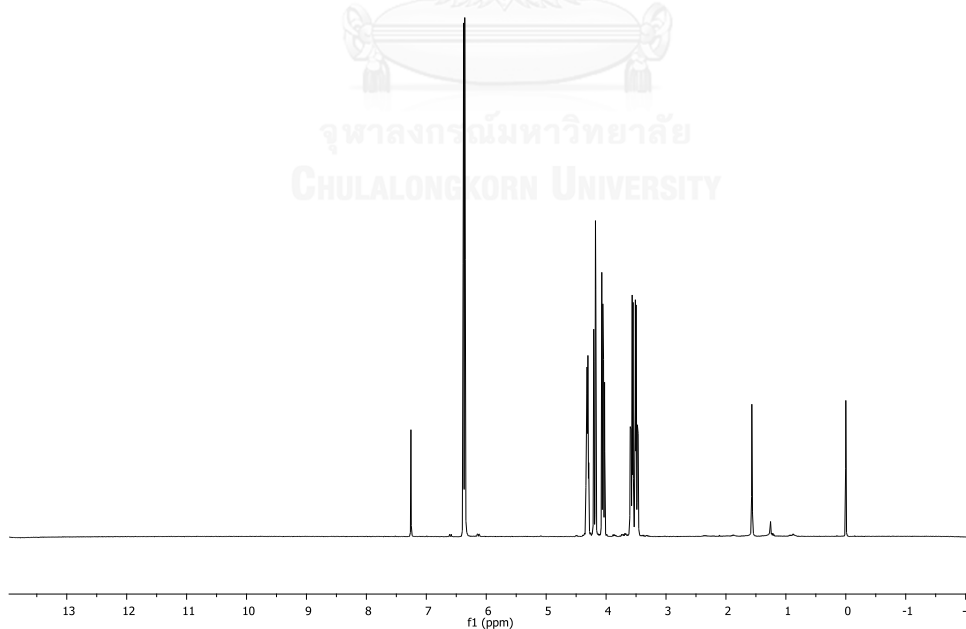


Figure A.20  $^1\text{H}$  NMR ( $\text{CDCl}_3$ ) spectrum of compound 19



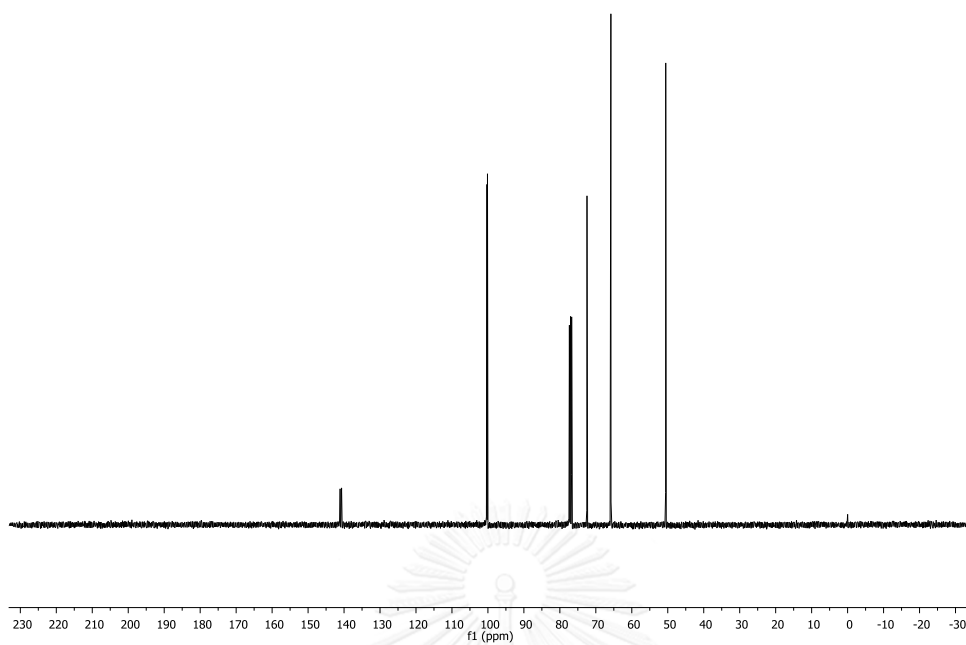


Figure A.21  $^{13}\text{C}$  NMR ( $\text{CDCl}_3$ ) spectrum of compound 19

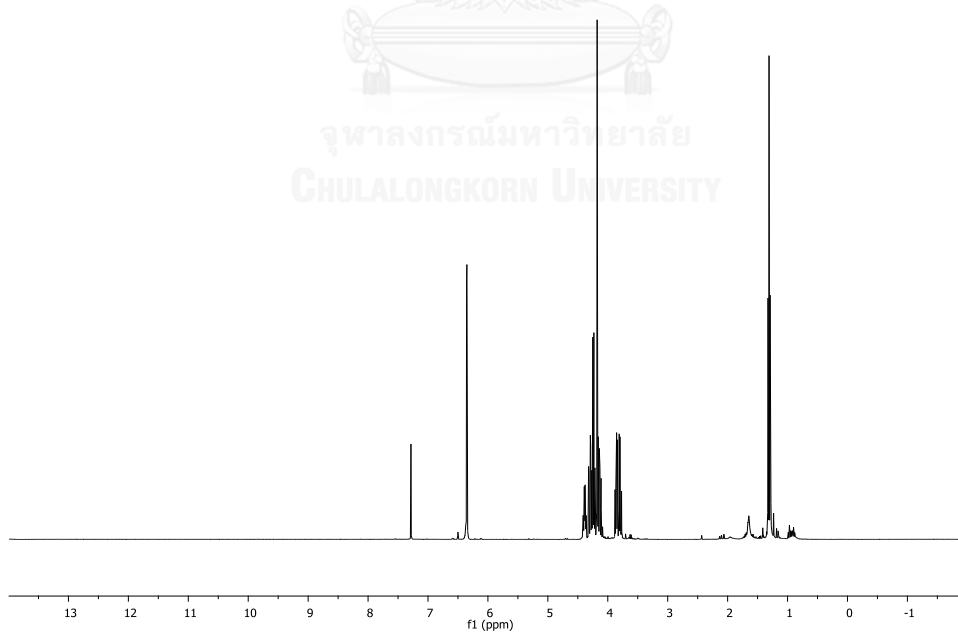


Figure A.22  $^1\text{H}$  NMR ( $\text{CDCl}_3$ ) spectrum of compound 20

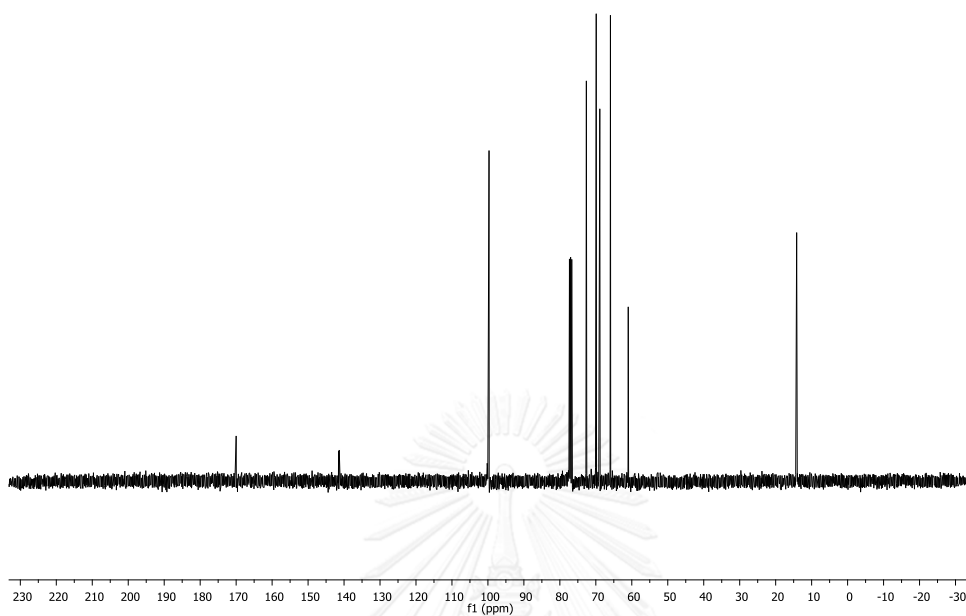


Figure A.23  $^{13}\text{C}$  NMR ( $\text{CDCl}_3$ ) spectrum of compound 20

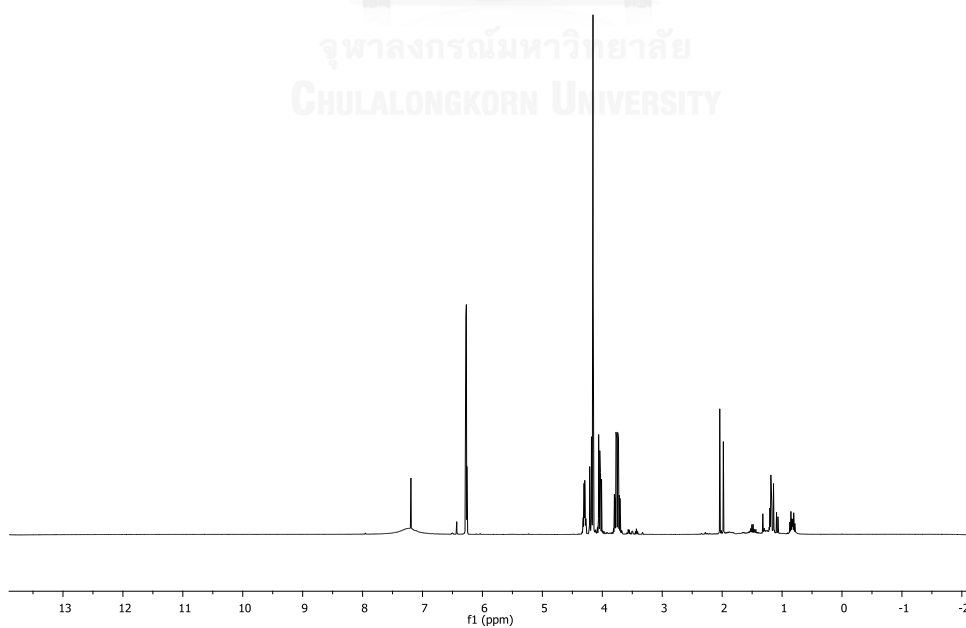


Figure A.24  $^1\text{H}$  NMR ( $\text{CDCl}_3$ ) spectrum of compound 21

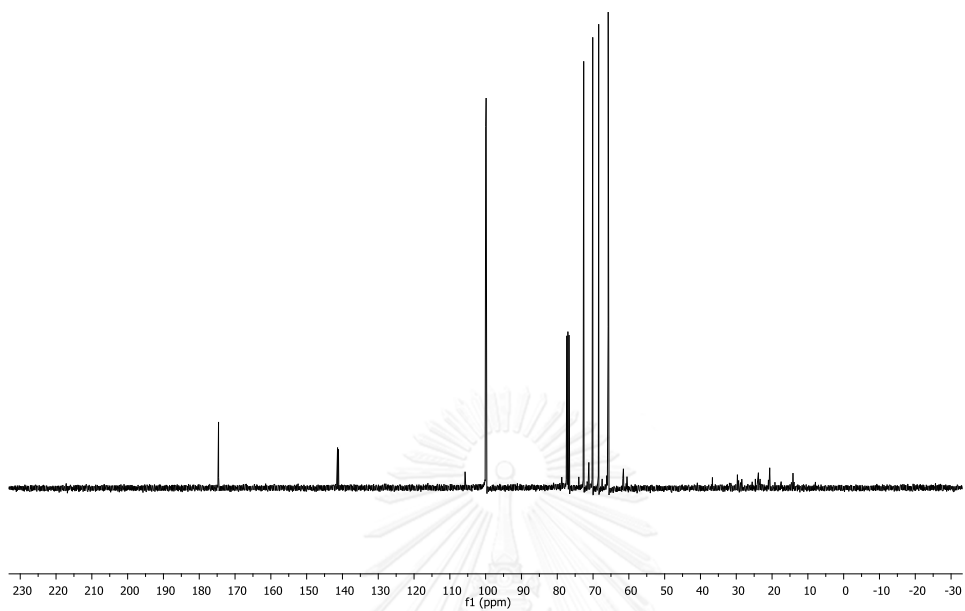


Figure A.25  $^{13}\text{C}$  NMR ( $\text{CDCl}_3$ ) spectrum of compound 21

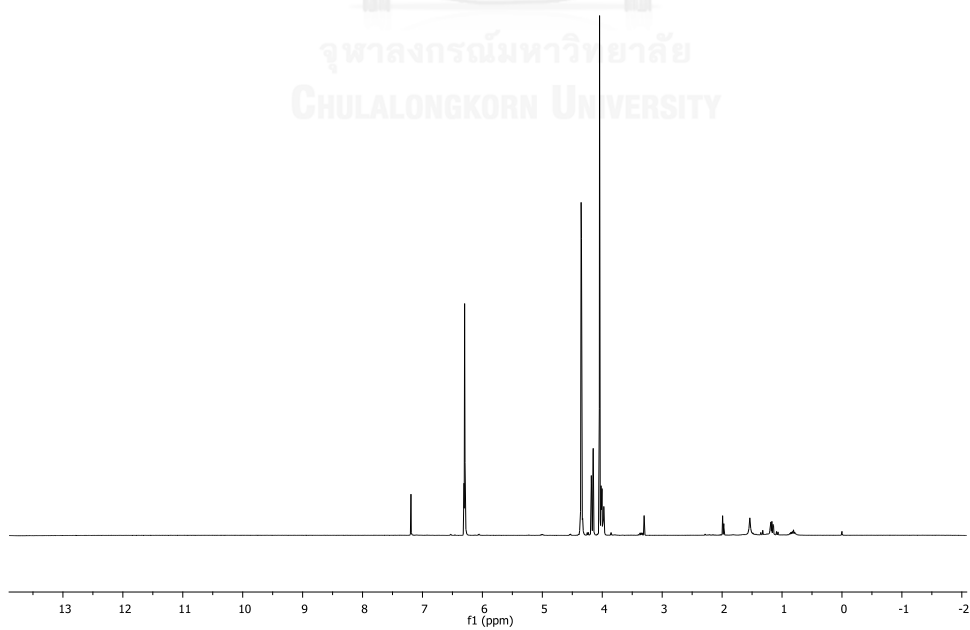


Figure A.26  $^1\text{H}$  NMR ( $\text{CDCl}_3$ ) spectrum of compound 22

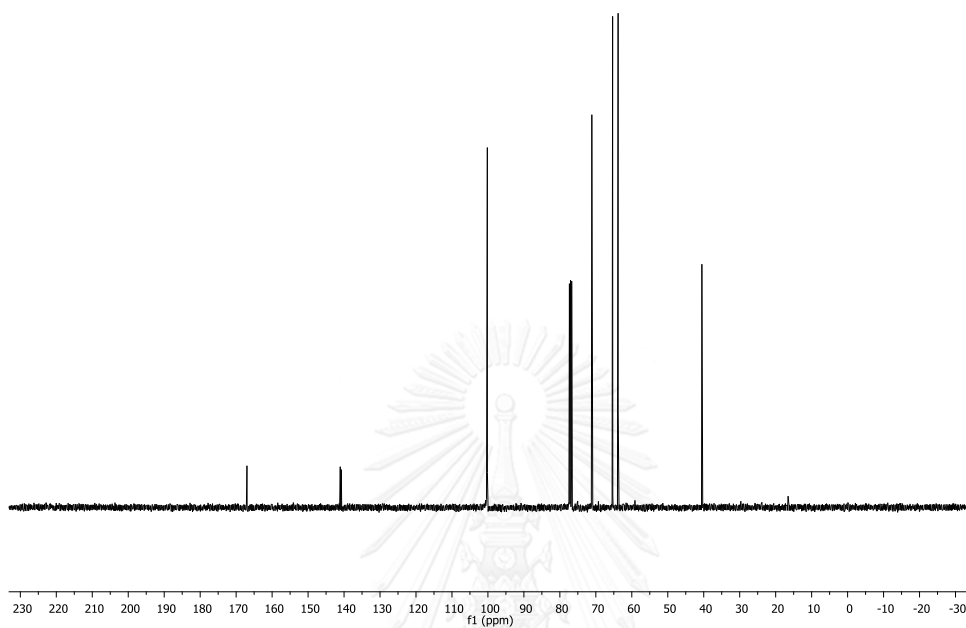


Figure A.27  $^{13}\text{C}$  NMR ( $\text{CDCl}_3$ ) spectrum of compound 22

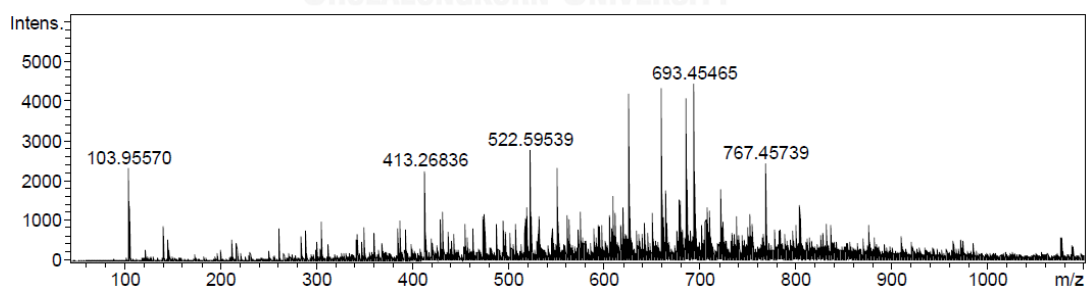


Figure A.28 High resolution mass spectrum of compound 23

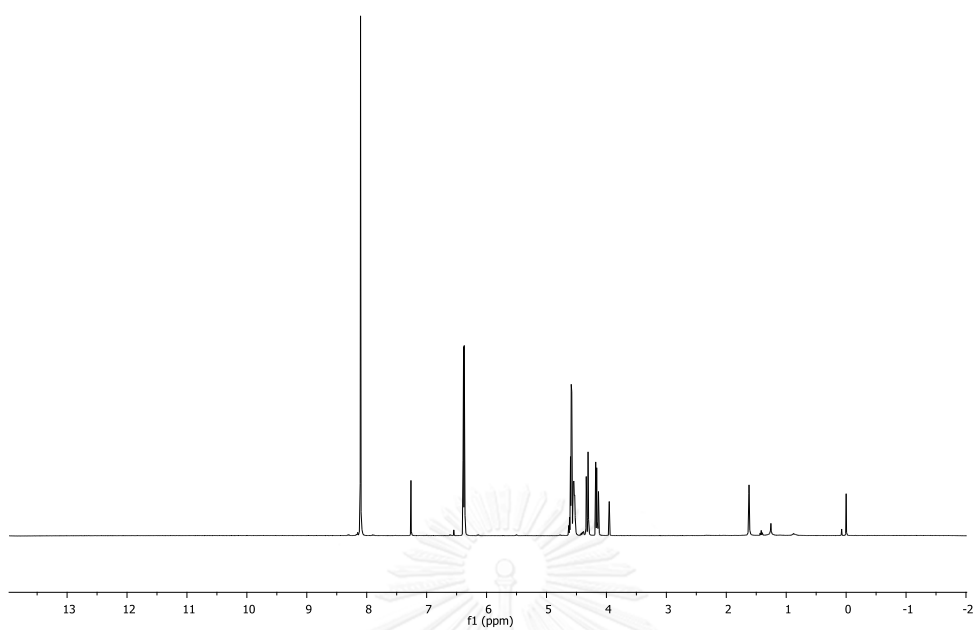


Figure A.29  $^1\text{H}$  NMR ( $\text{CDCl}_3$ ) spectrum of compound **23**

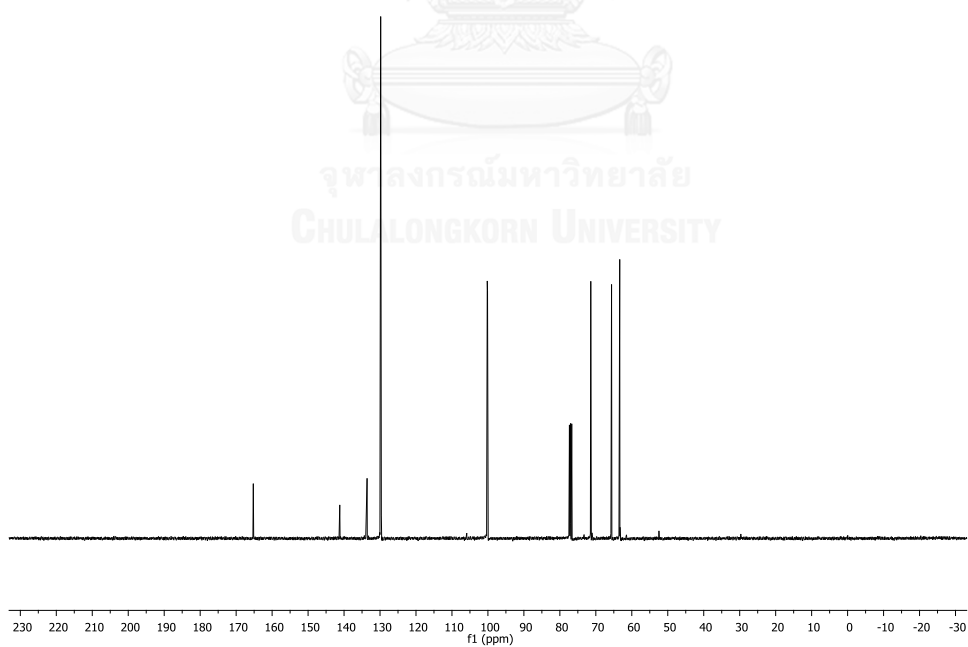


Figure A.30  $^{13}\text{C}$  NMR ( $\text{CDCl}_3$ ) spectrum of compound **23**

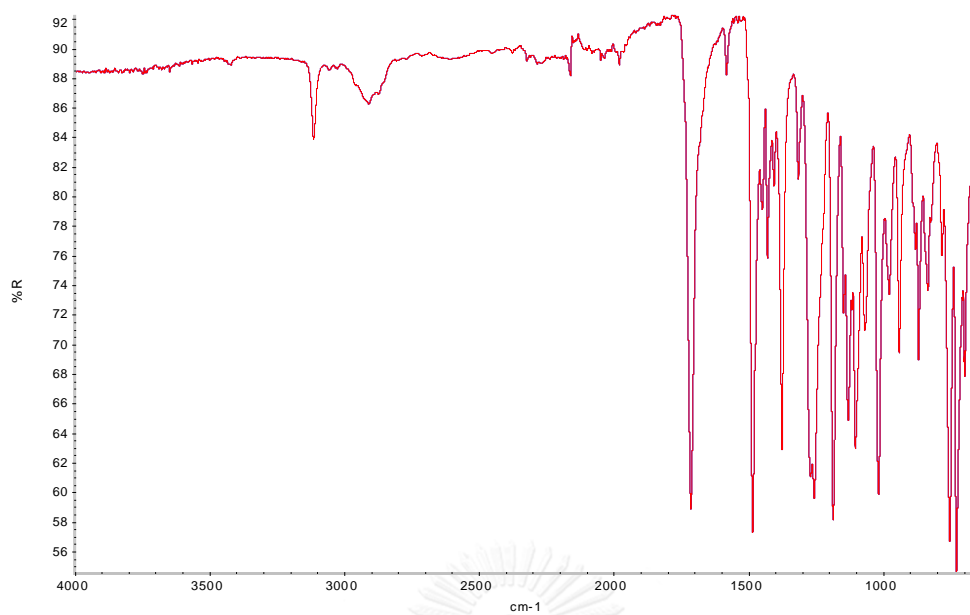


Figure A.31 IR spectrum of compound 23

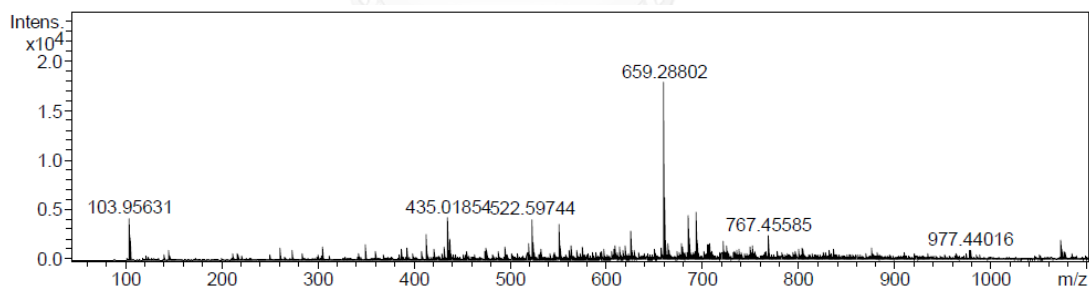


Figure A.32 High resolution mass spectrum of compound 24

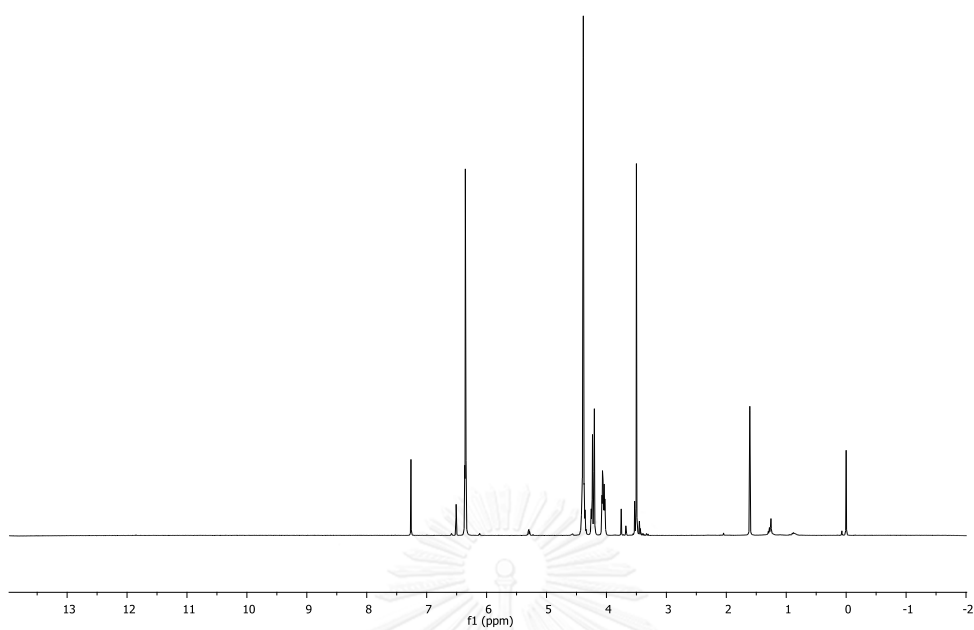


Figure A.33  $^1\text{H}$  NMR ( $\text{CDCl}_3$ ) spectrum of compound 24

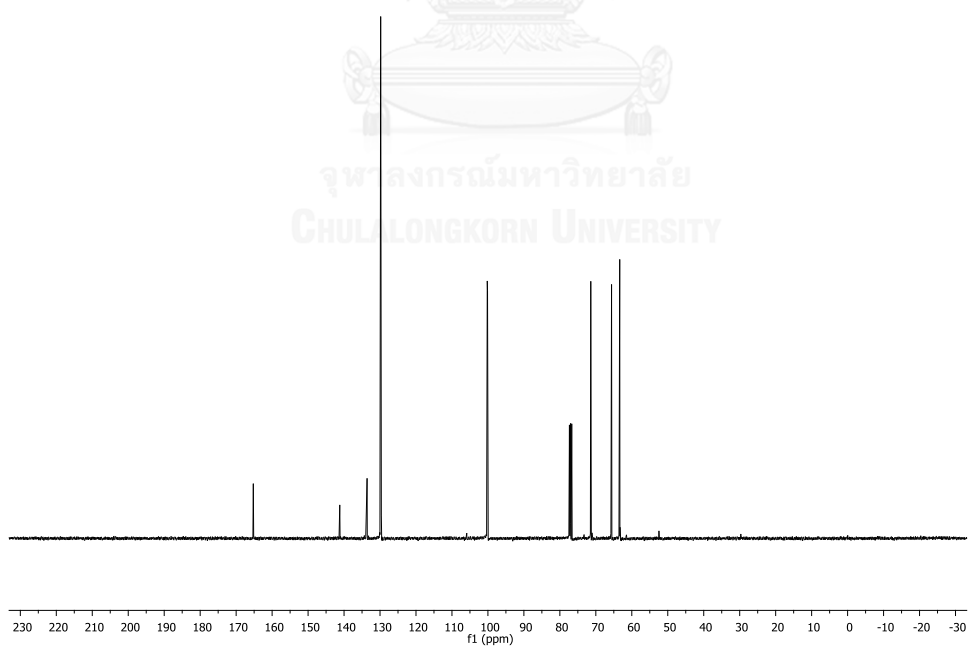


Figure A.34  $^{13}\text{C}$  NMR ( $\text{CDCl}_3$ ) spectrum of compound 24

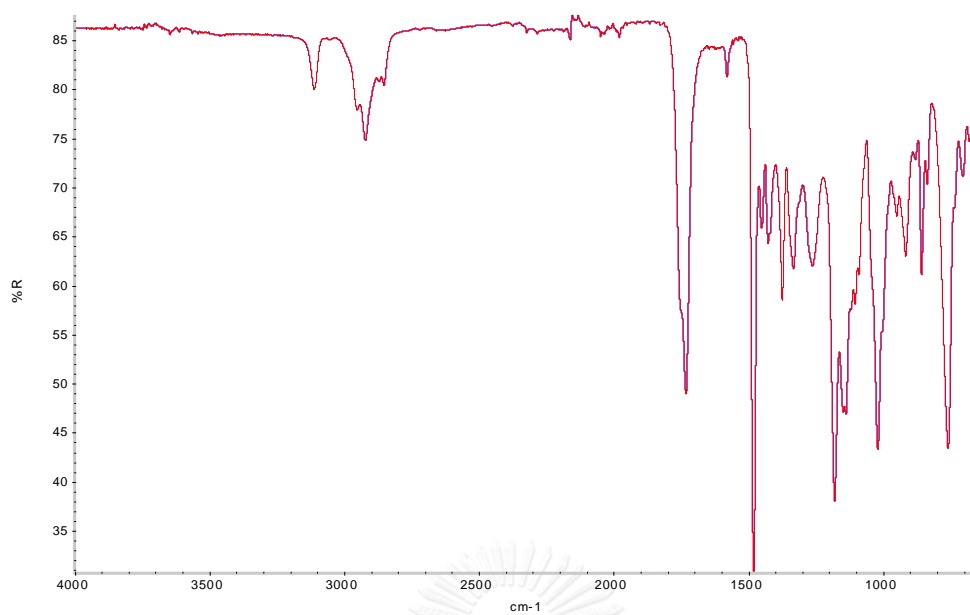


Figure A.35 IR spectrum of compound 24

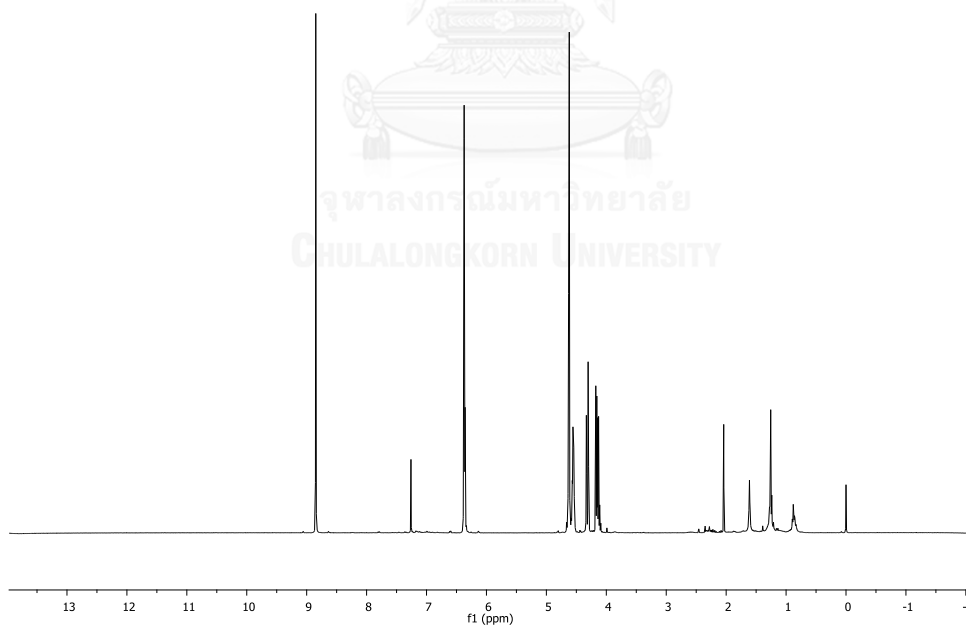


Figure A.36 <sup>1</sup>H NMR (CDCl<sub>3</sub>) spectrum of compound 25



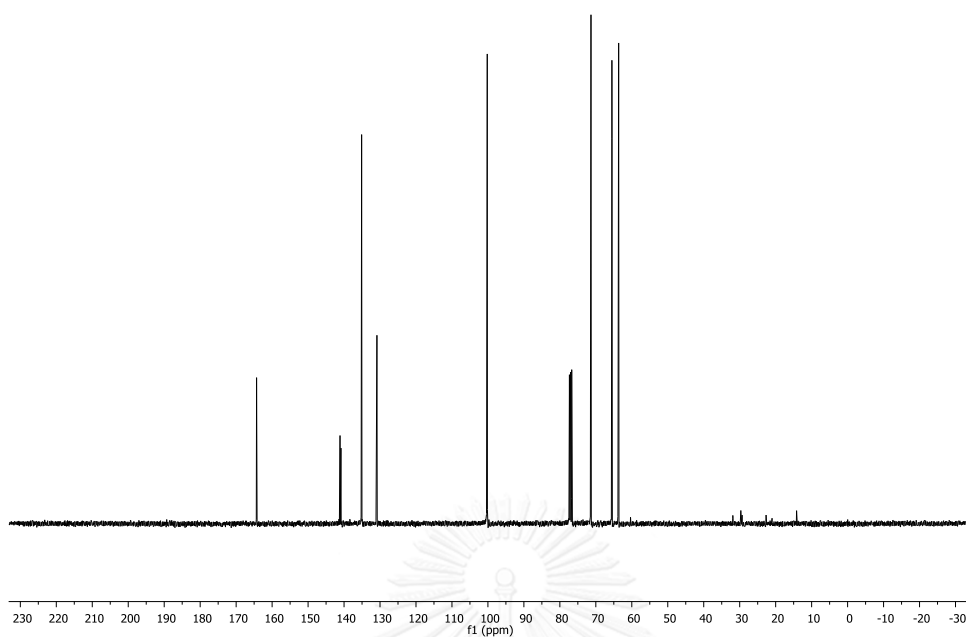


Figure A.37  $^{13}\text{C}$  NMR ( $\text{CDCl}_3$ ) spectrum of compound 25

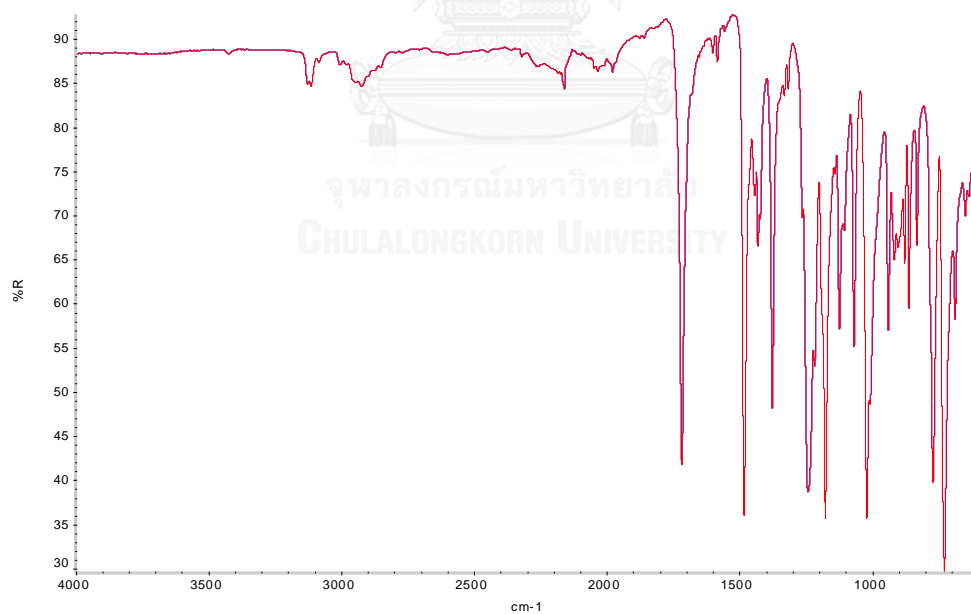


Figure A.38 IR spectrum of compound 25

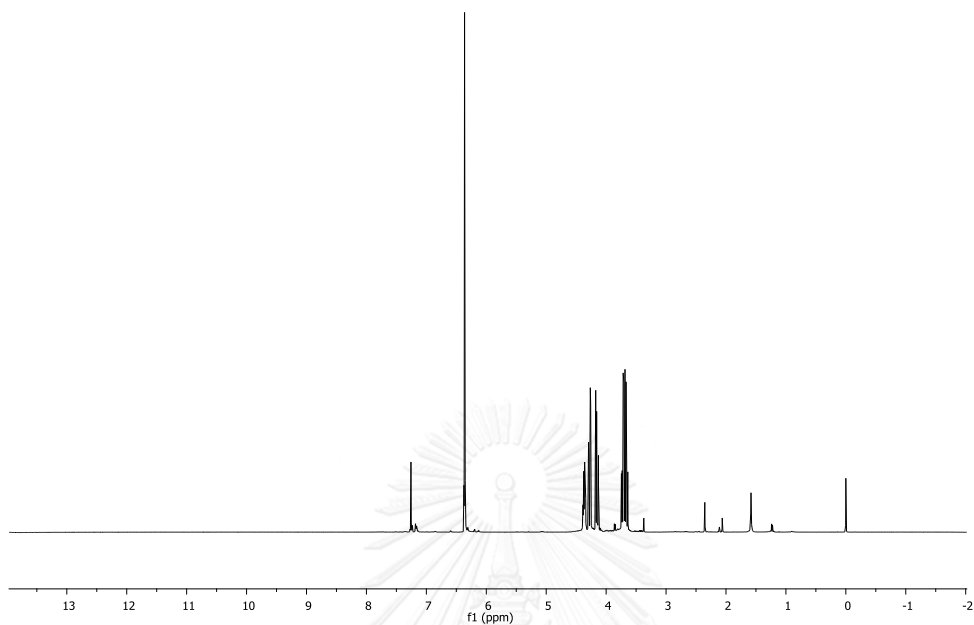


Figure A.39  $^1\text{H}$  NMR ( $\text{CDCl}_3$ ) spectrum of compound **26**

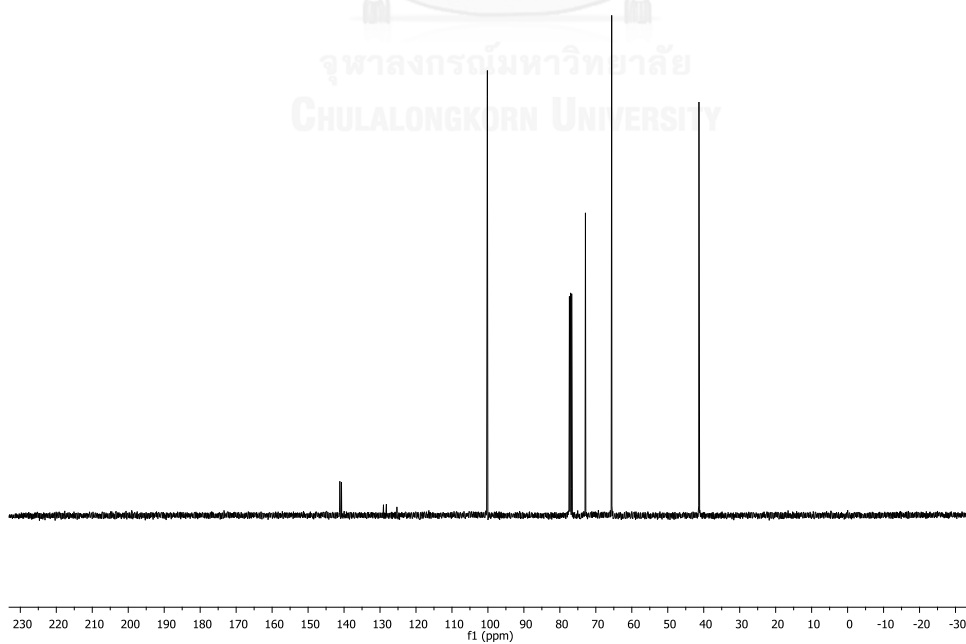


Figure A.40  $^{13}\text{C}$  NMR ( $\text{CDCl}_3$ ) spectrum of compound **26**

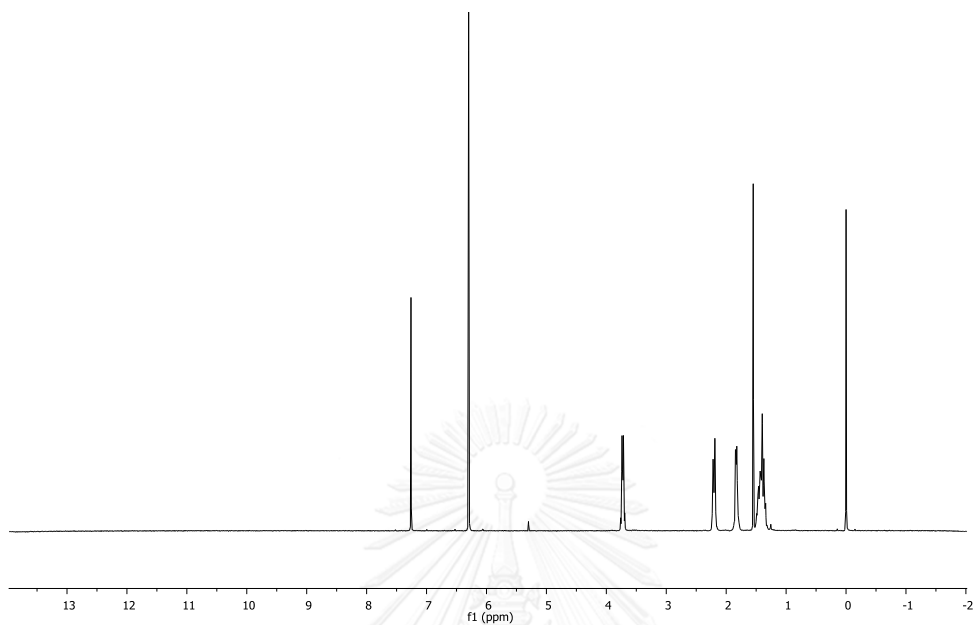


Figure A.41  $^1\text{H}$  NMR ( $\text{CDCl}_3$ ) spectrum of compound 27

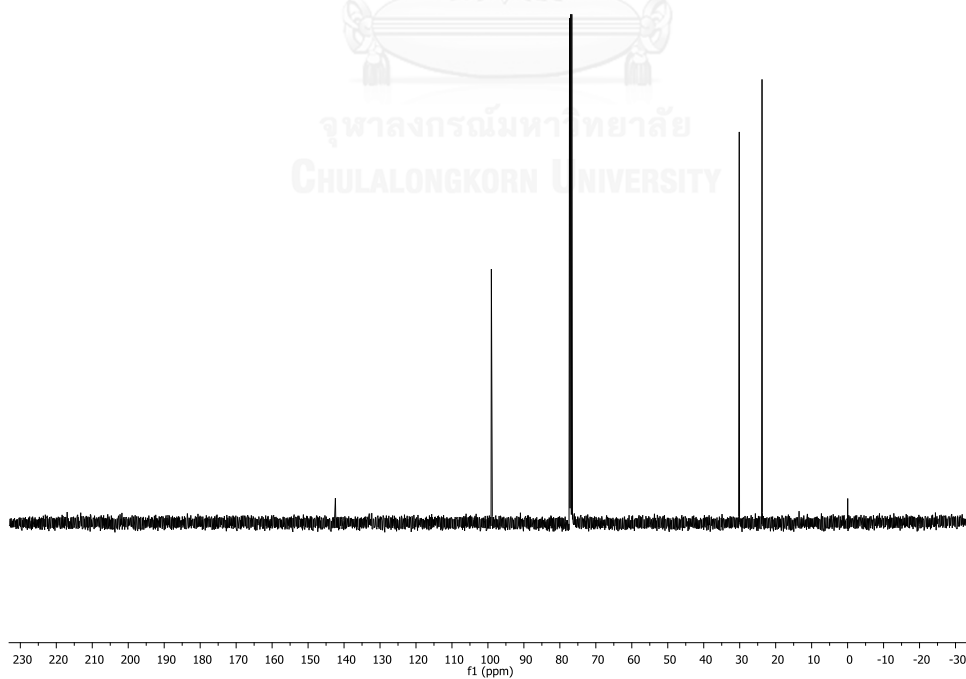


Figure A.42  $^{13}\text{C}$  NMR ( $\text{CDCl}_3$ ) spectrum of compound 27

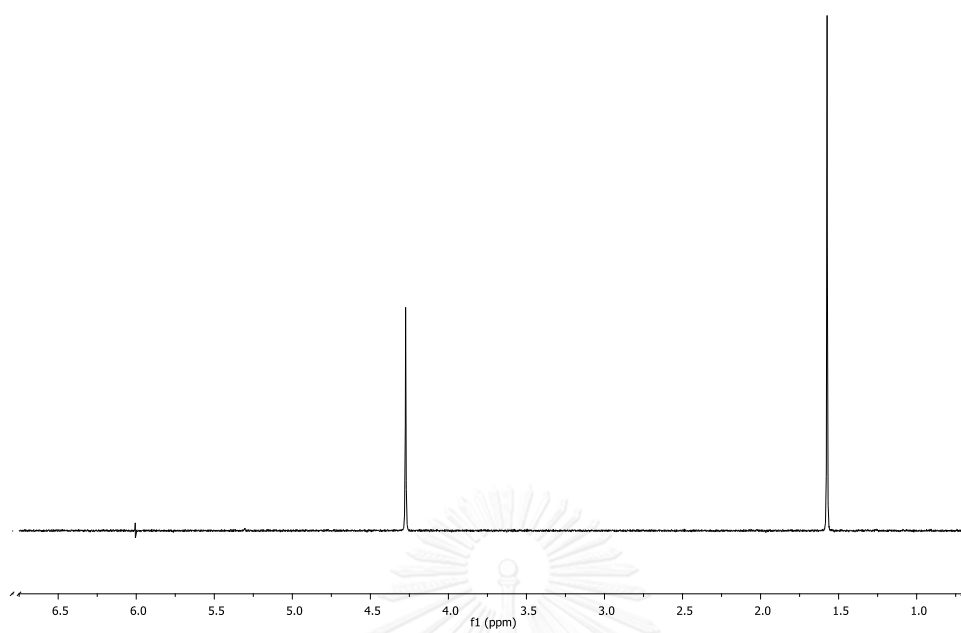


Figure A.43  $^1\text{H}$  NMR ( $\text{CDCl}_3$ ) spectrum of compound 28

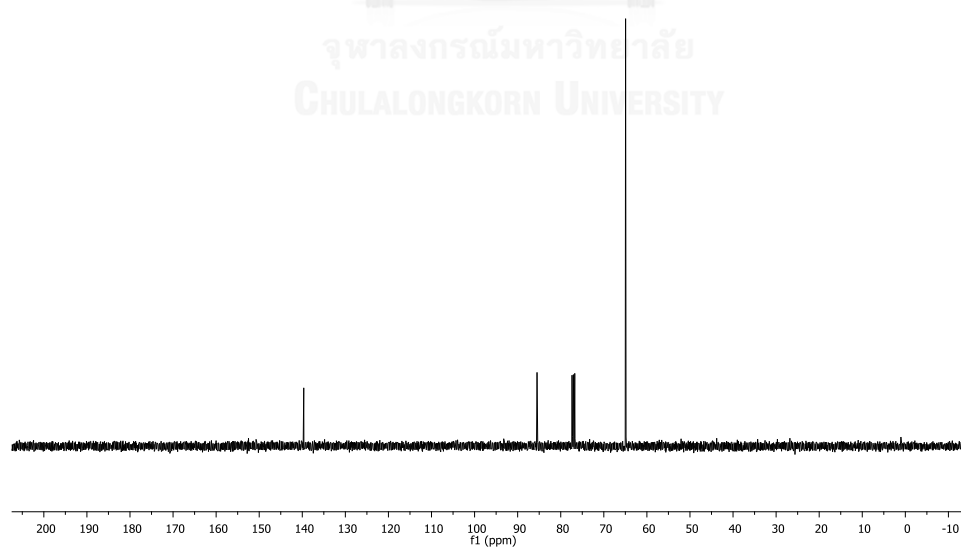


Figure A.44  $^{13}\text{C}$  NMR ( $\text{CDCl}_3$ ) spectrum of compound 28

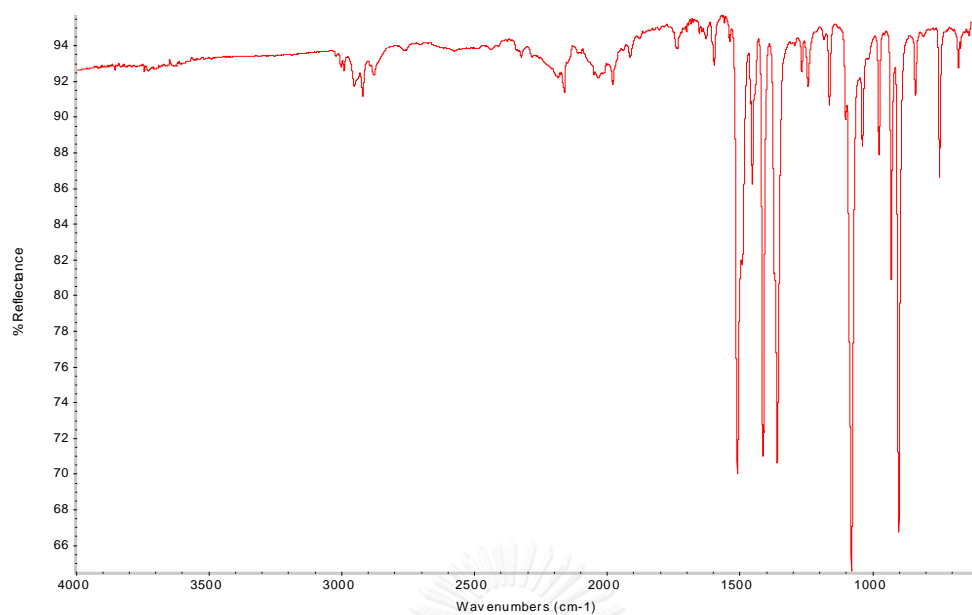


Figure A.45 IR spectrum of compound 28

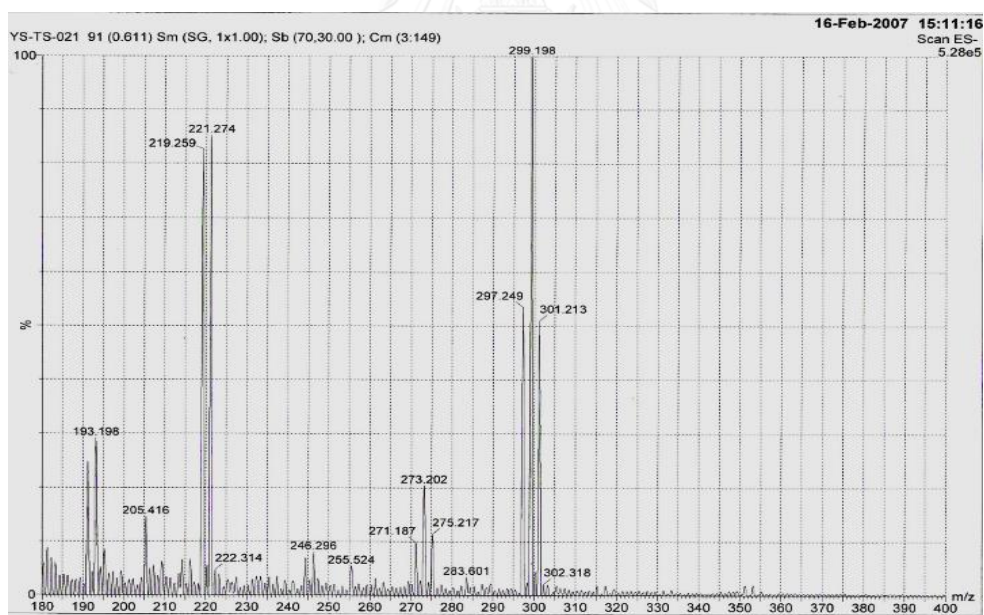


Figure A.46 Mass spectrum of compound 28

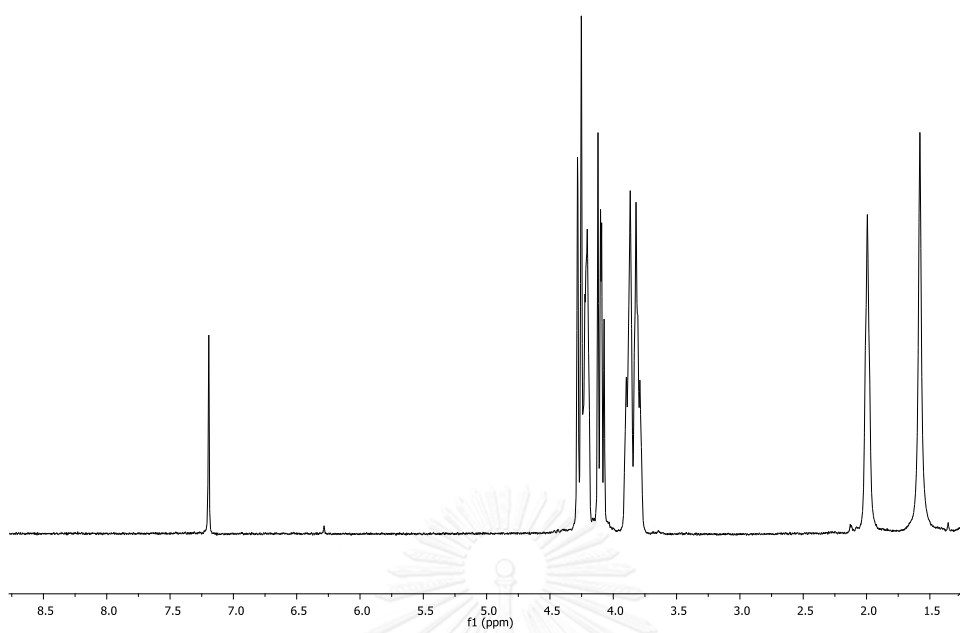


Figure A.47  $^1\text{H}$  NMR ( $\text{CDCl}_3$ ) spectrum of compound 29

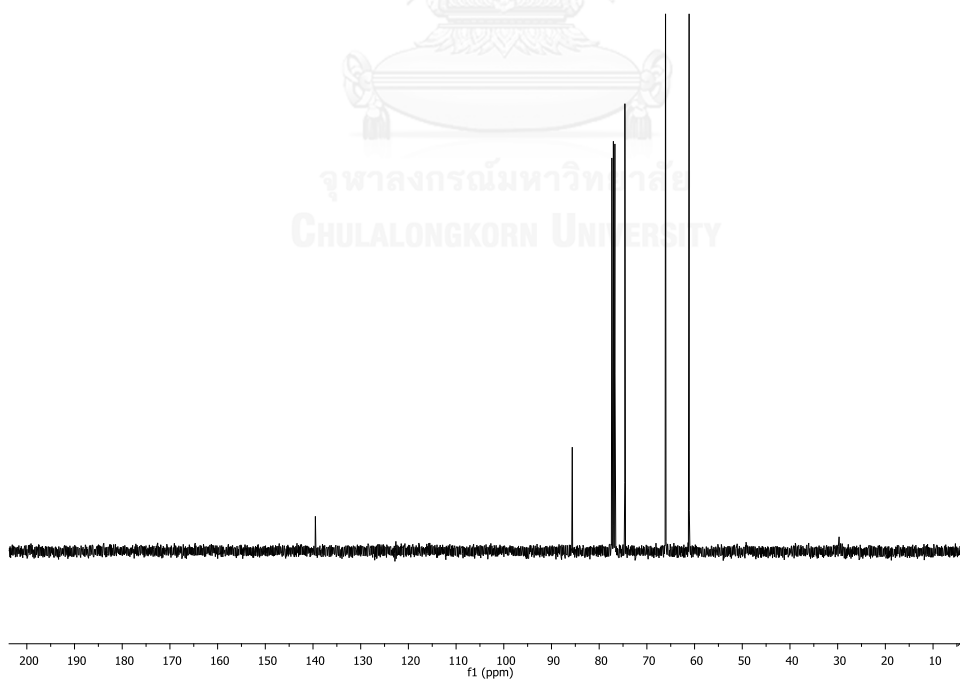


Figure A.48  $^{13}\text{C}$  NMR ( $\text{CDCl}_3$ ) spectrum of compound 29

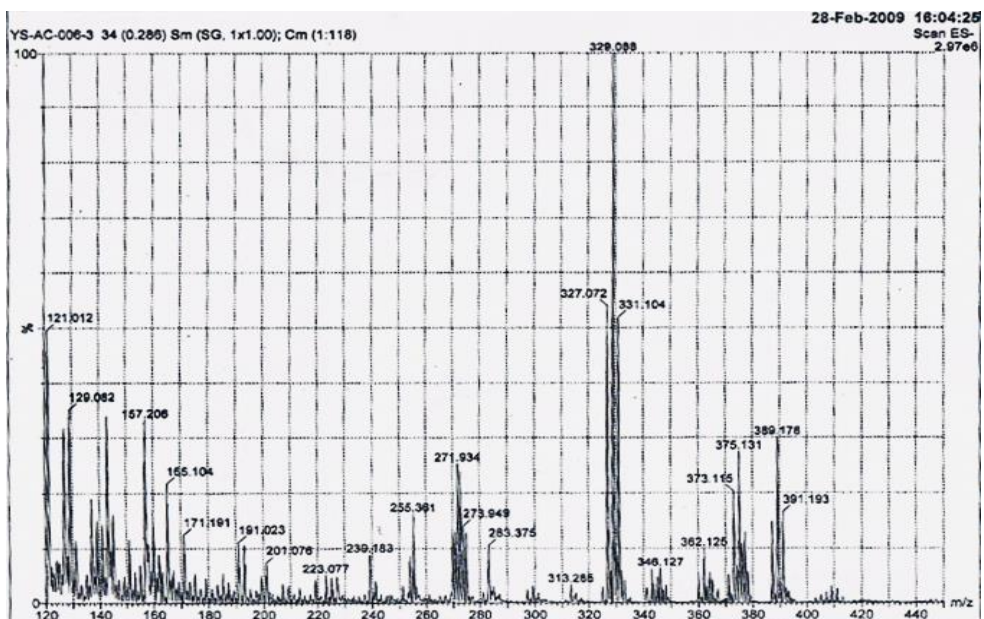


Figure A.49 Mass spectrum of compound 29

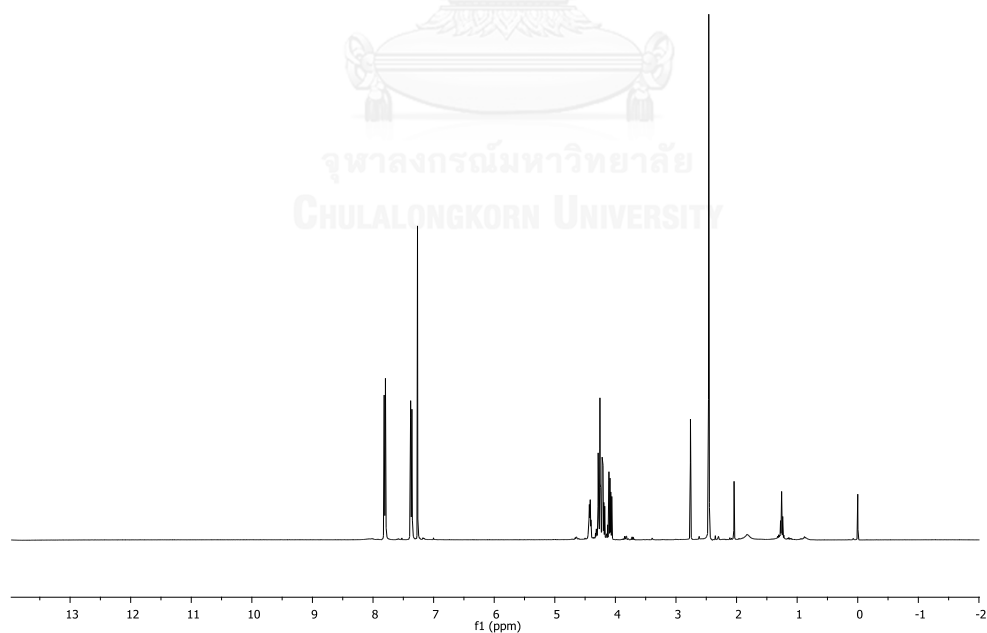


Figure A.50  $^1\text{H}$  NMR ( $\text{CDCl}_3$ ) spectrum of compound 30

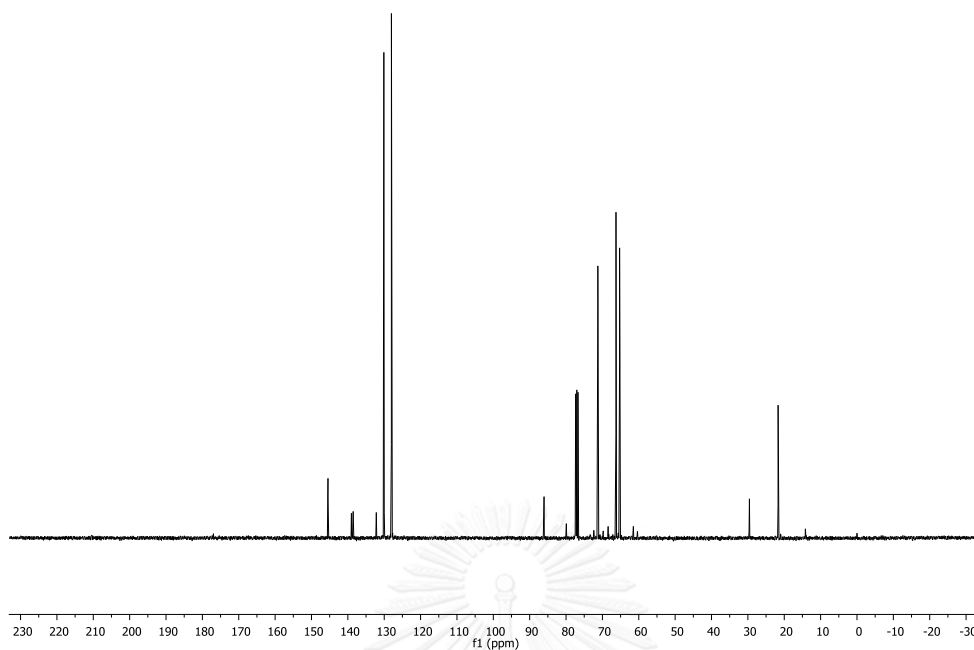


Figure A.51  $^{13}\text{C}$  NMR ( $\text{CDCl}_3$ ) spectrum of compound **30**

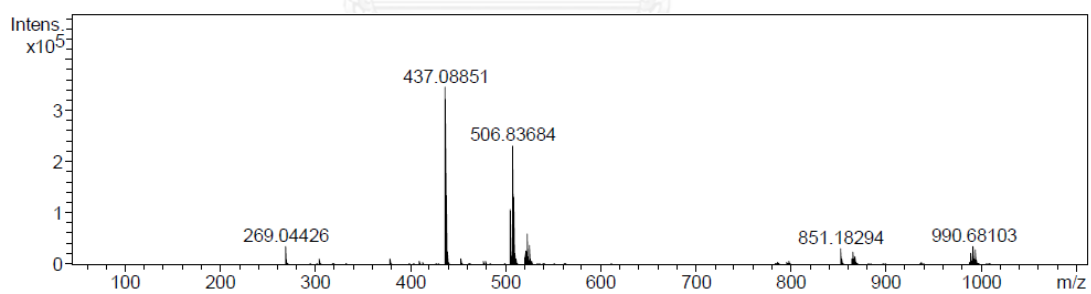


Figure A.52 High resolution mass spectrum of compound **30**



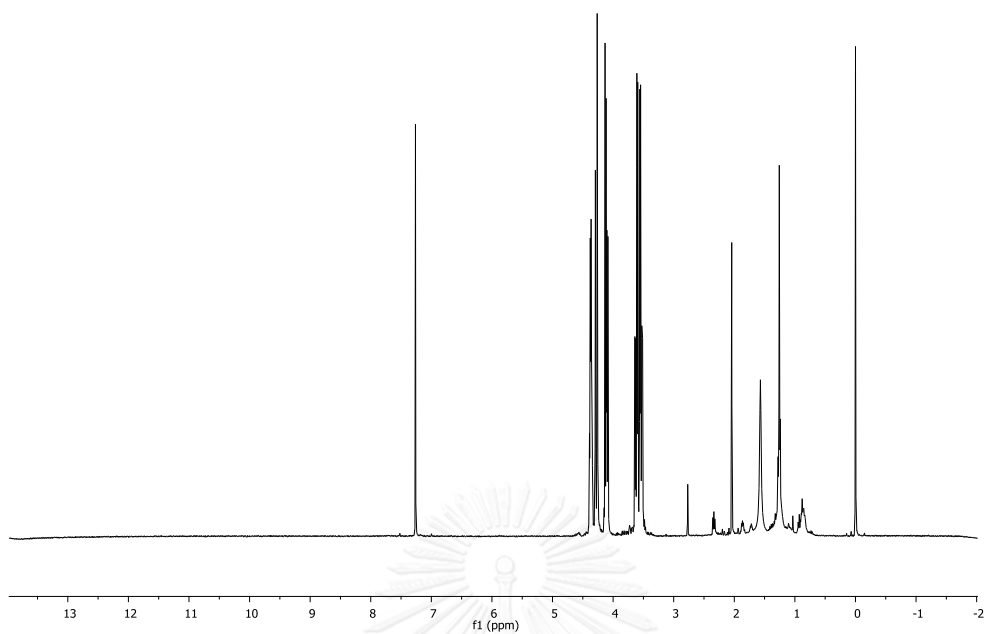


Figure A.53  $^1\text{H}$  NMR ( $\text{CDCl}_3$ ) spectrum of compound **31**

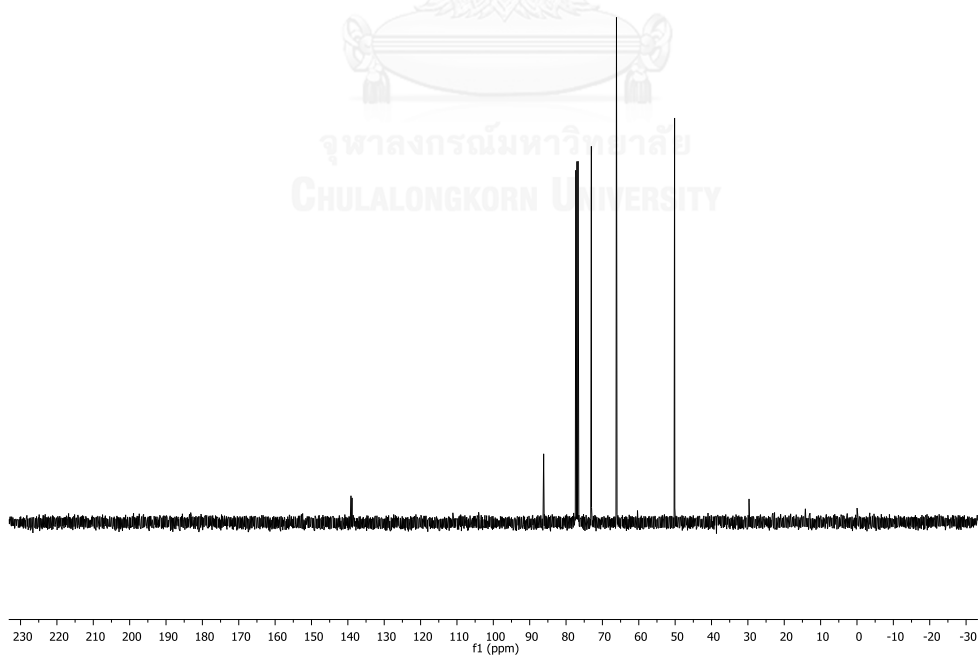


Figure A.54  $^{13}\text{C}$  NMR ( $\text{CDCl}_3$ ) spectrum of compound **31**

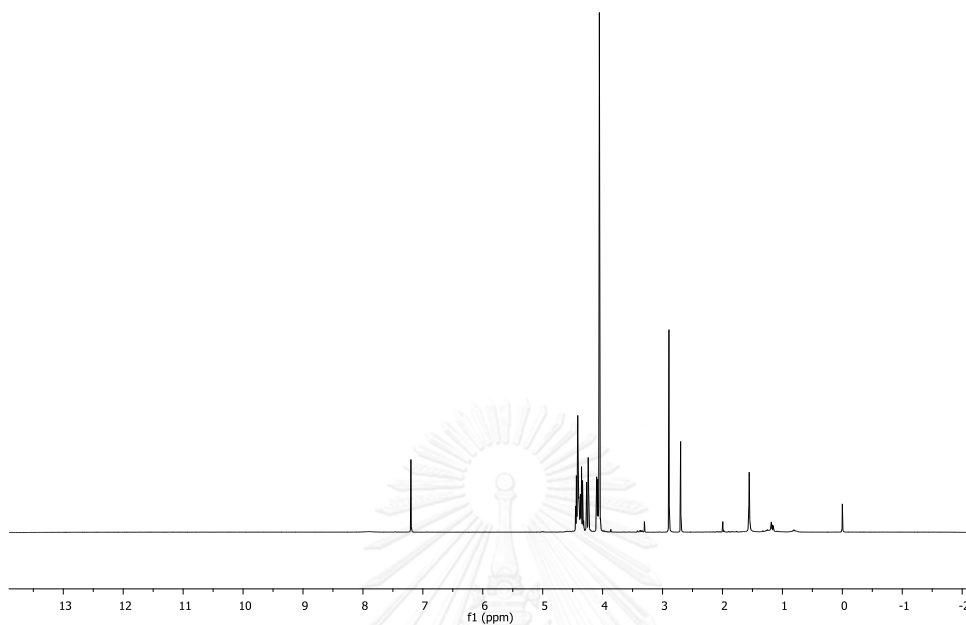


Figure A.55  $^1\text{H}$  NMR ( $\text{CDCl}_3$ ) spectrum of compound **32**

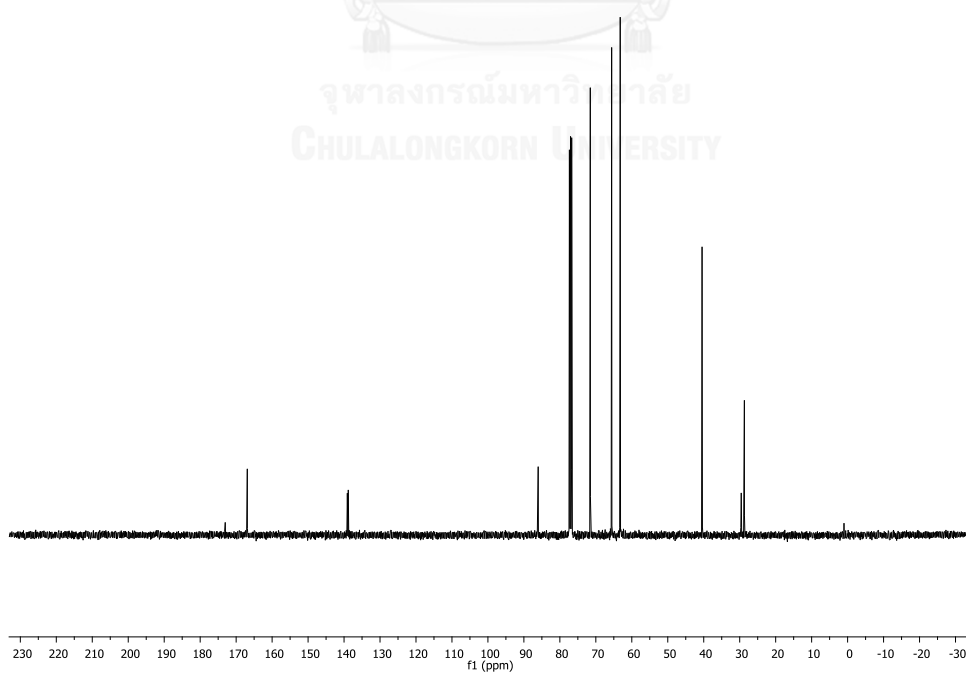


Figure A.56  $^{13}\text{C}$  NMR ( $\text{CDCl}_3$ ) spectrum of compound **32**

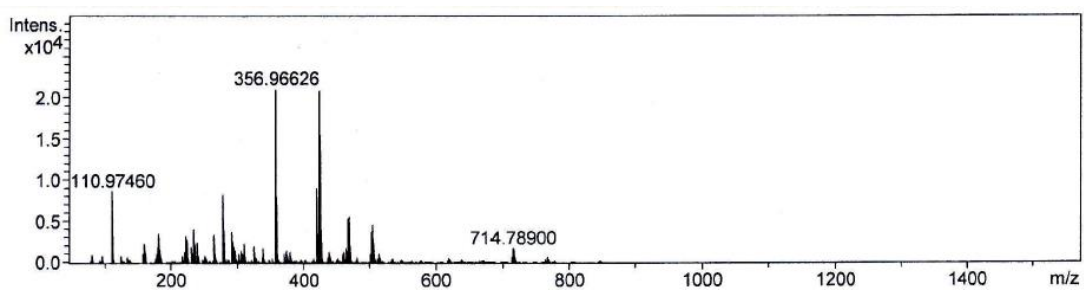


Figure A.57 High resolution mass spectrum of compound 32

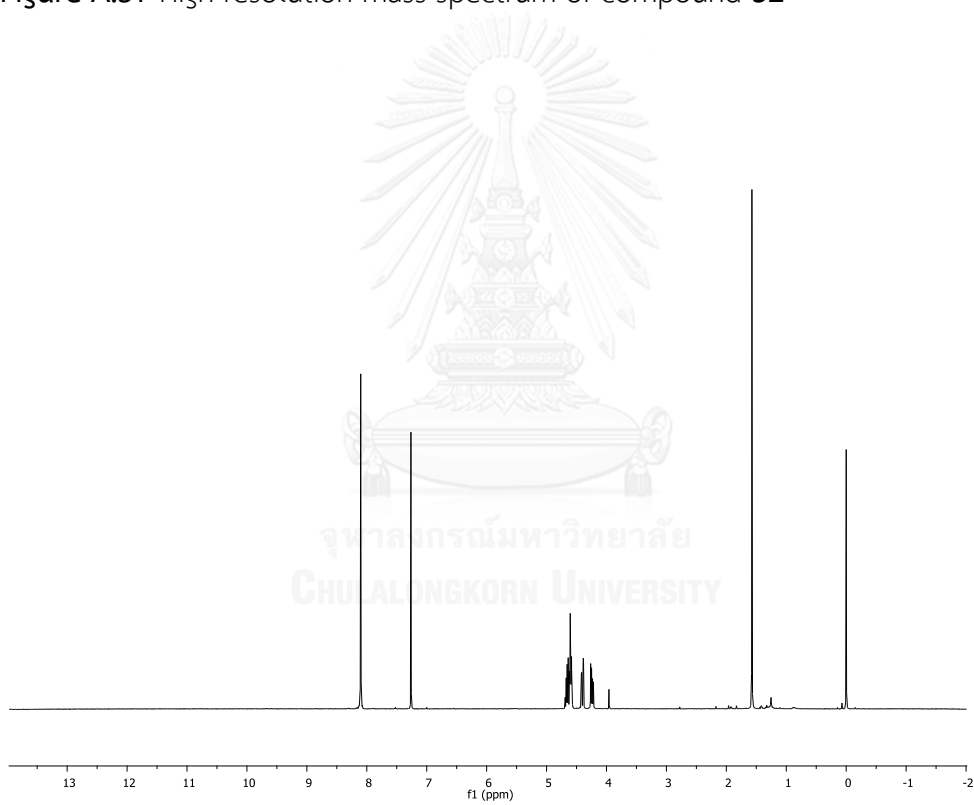


Figure A.58  $^1\text{H}$  NMR ( $\text{CDCl}_3$ ) spectrum of compound 33

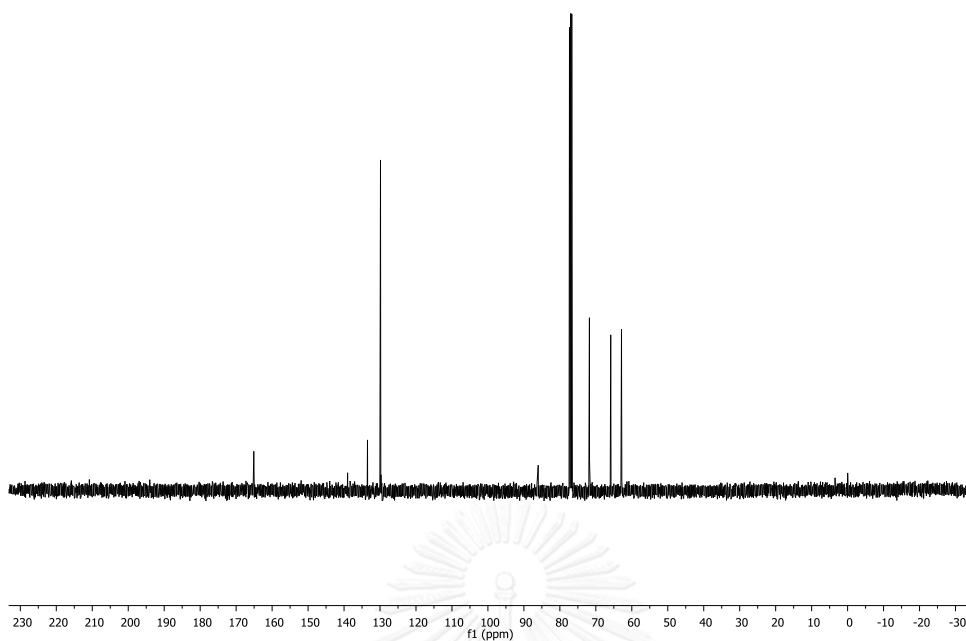


Figure A.59  $^{13}\text{C}$  NMR ( $\text{CDCl}_3$ ) spectrum of compound 33

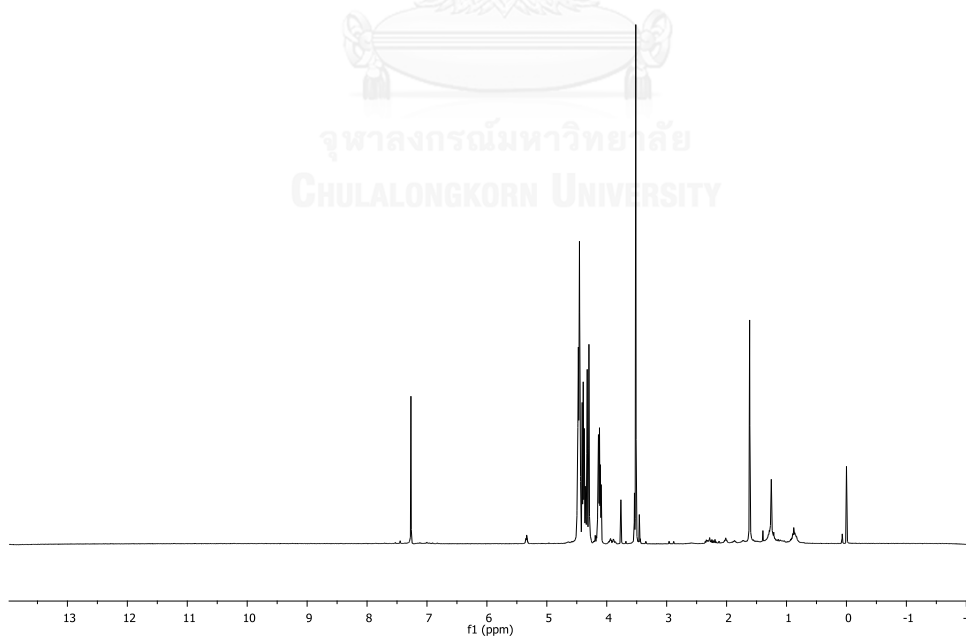


Figure A.60  $^1\text{H}$  NMR ( $\text{CDCl}_3$ ) spectrum of compound 34

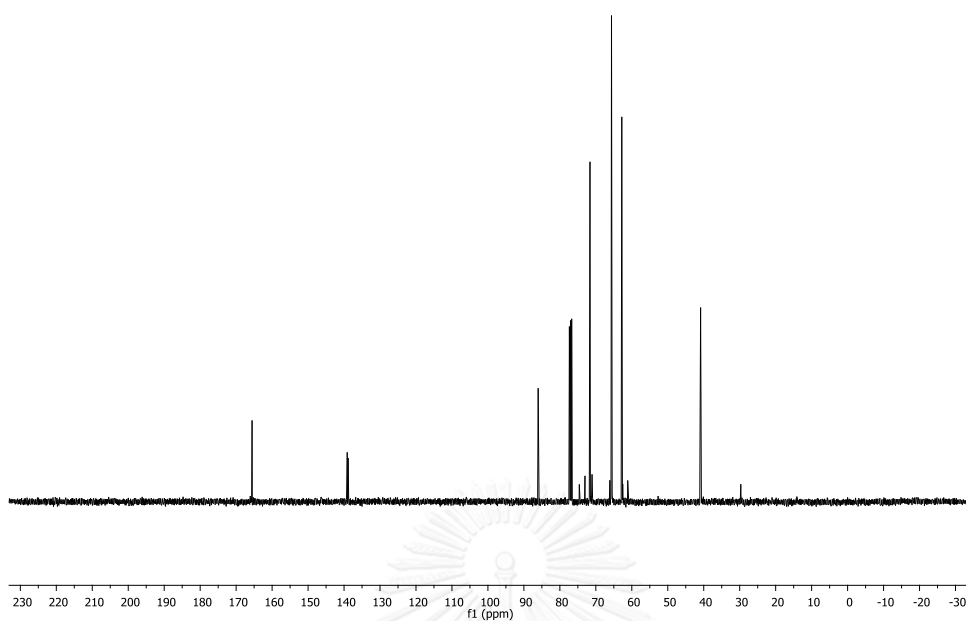


Figure A.61  $^{13}\text{C}$  NMR ( $\text{CDCl}_3$ ) spectrum of compound 34

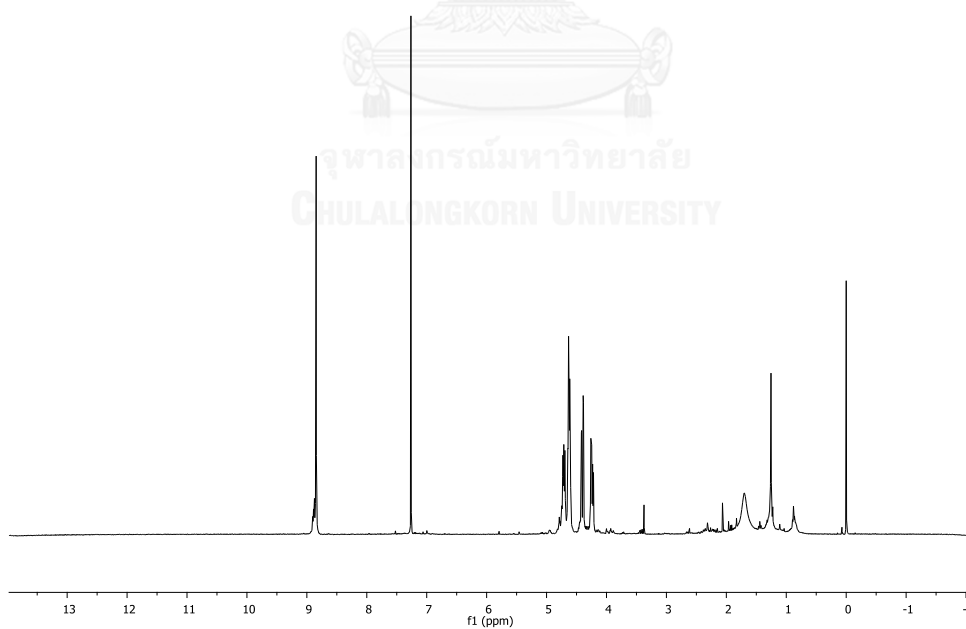


Figure A.62  $^1\text{H}$  NMR ( $\text{CDCl}_3$ ) spectrum of compound 35

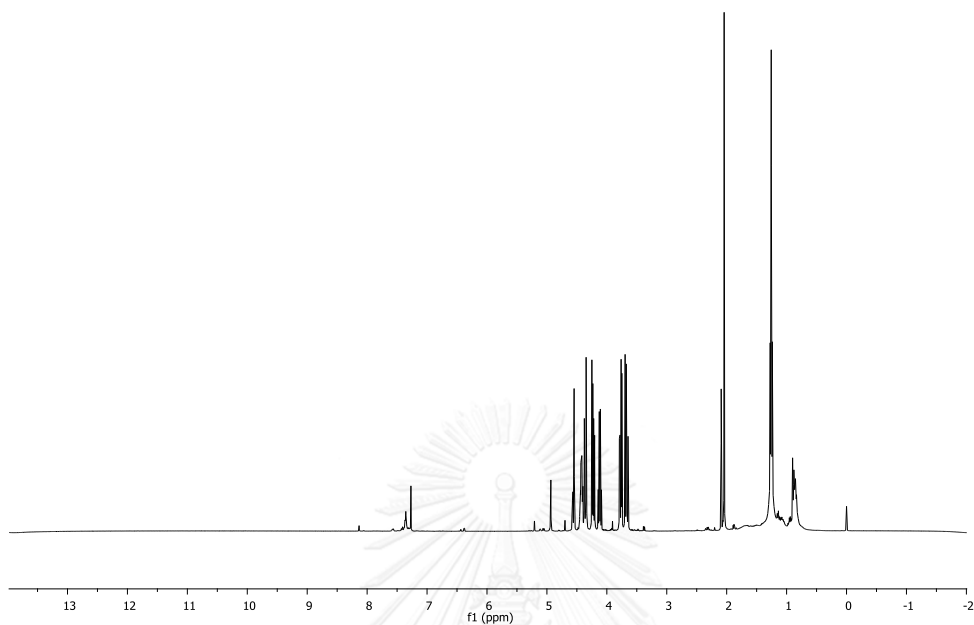


Figure A.63  $^1\text{H}$  NMR ( $\text{CDCl}_3$ ) spectrum of compound 36

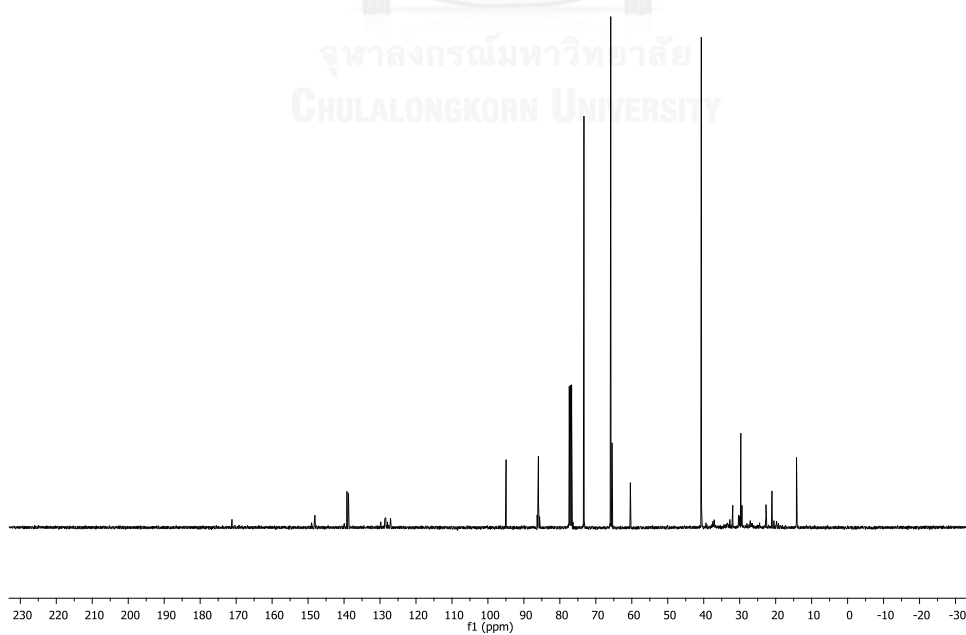


Figure A.64  $^{13}\text{C}$  NMR ( $\text{CDCl}_3$ ) spectrum of compound 36

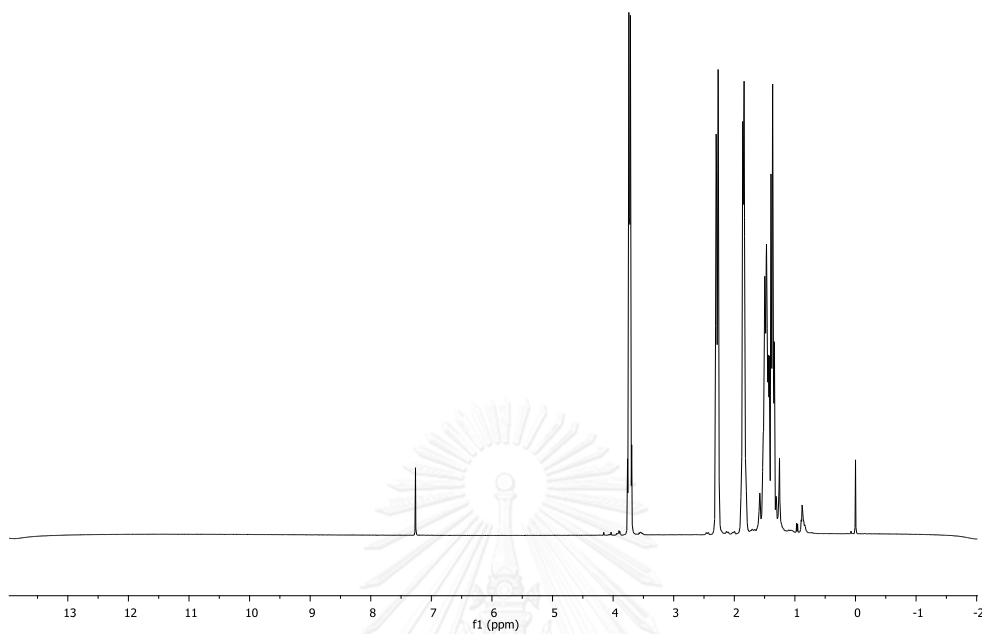


Figure A.65  $^1\text{H}$  NMR ( $\text{CDCl}_3$ ) spectrum of compound 37

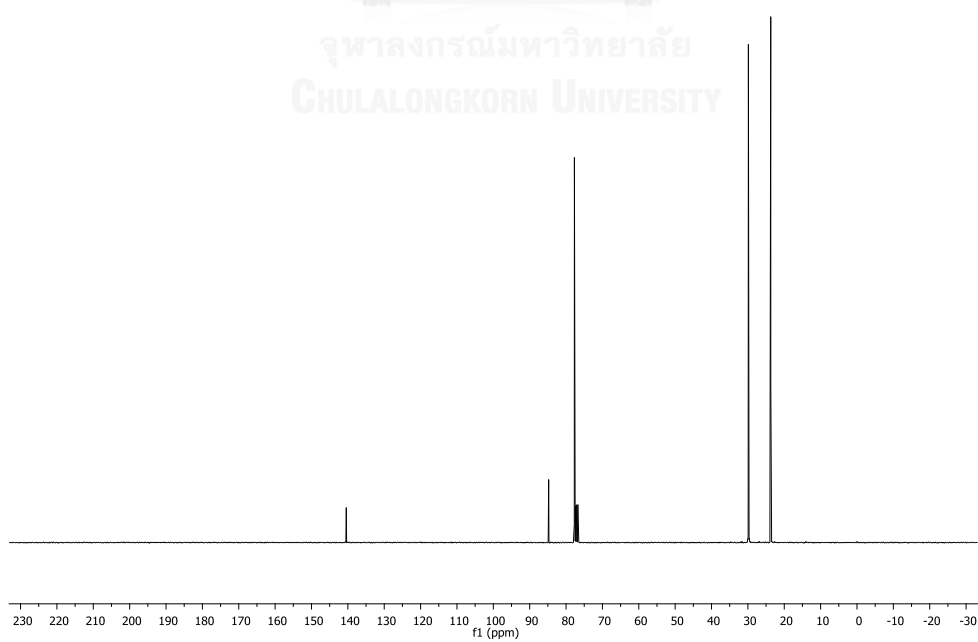


Figure A.66  $^{13}\text{C}$  NMR ( $\text{CDCl}_3$ ) spectrum of compound 37

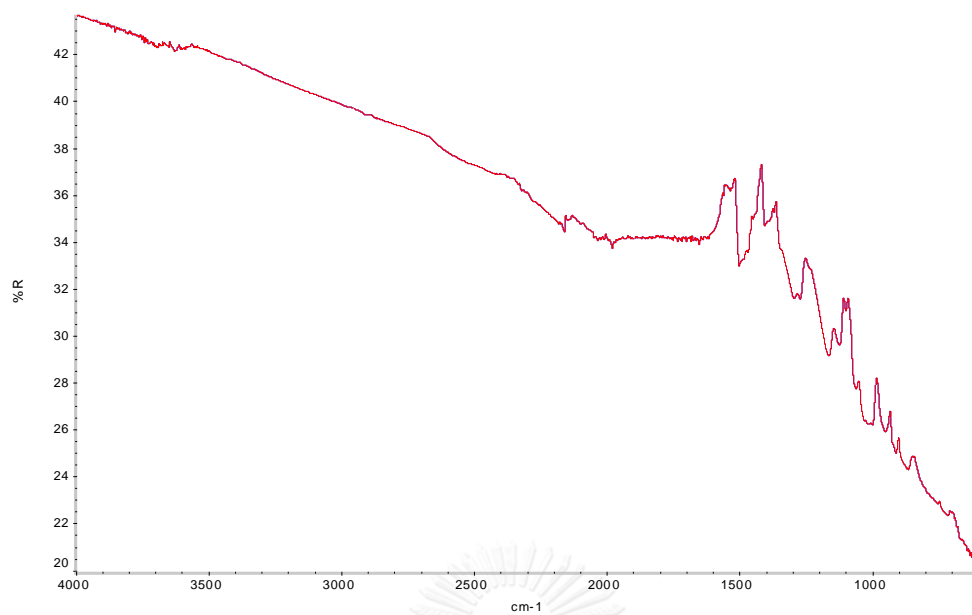


Figure A.67 IR spectrum of SSP-PEDOT 38

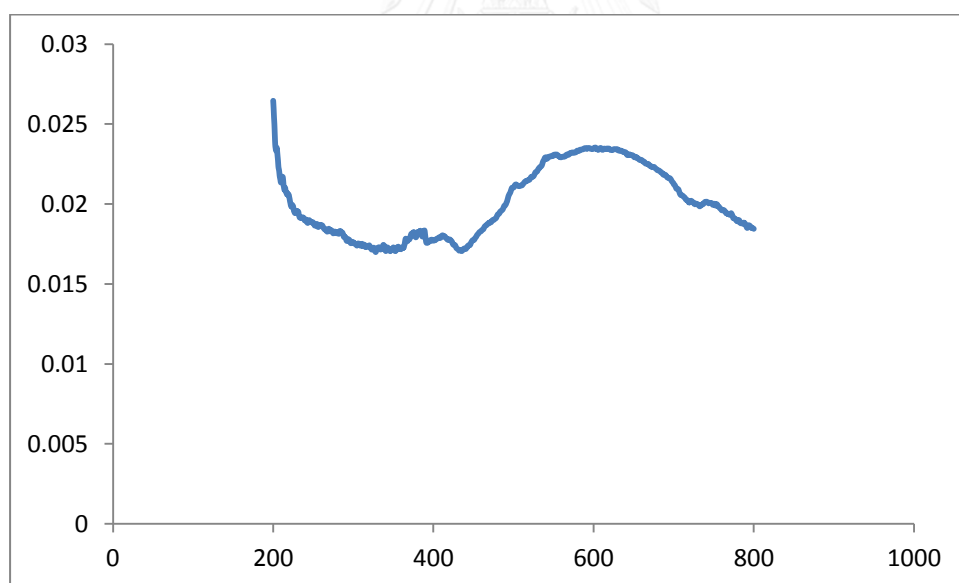


Figure A.68 UV-vis spectrum of SSP-PEDOT 38



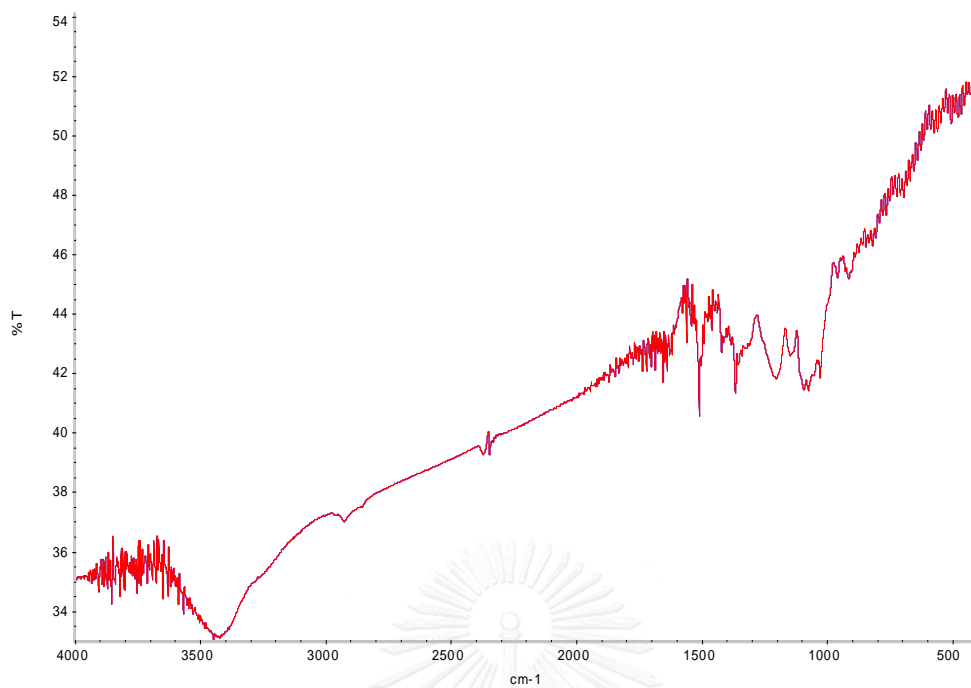


Figure A.69 IR spectrum of polymer 39

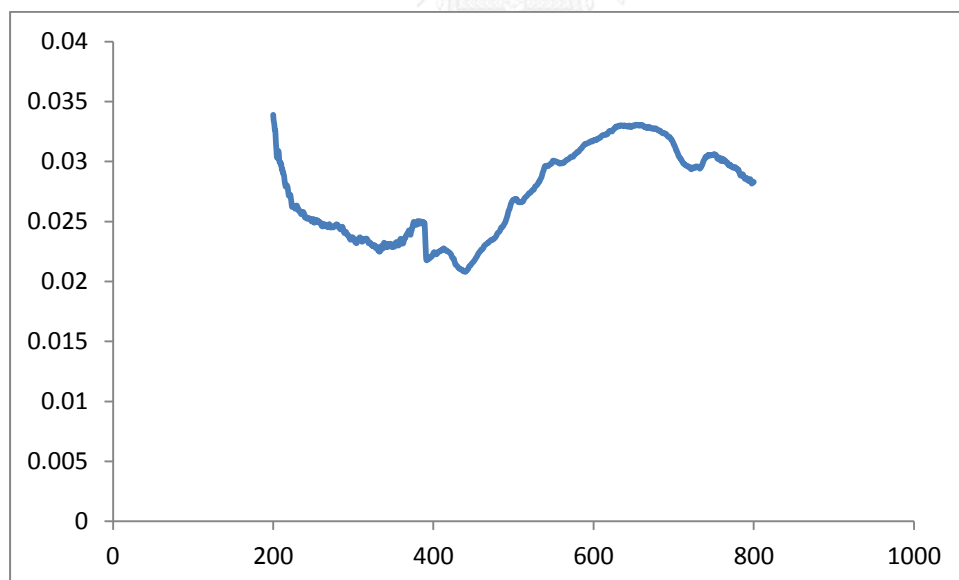


Figure A.70 UV-vis spectrum of polymer 39

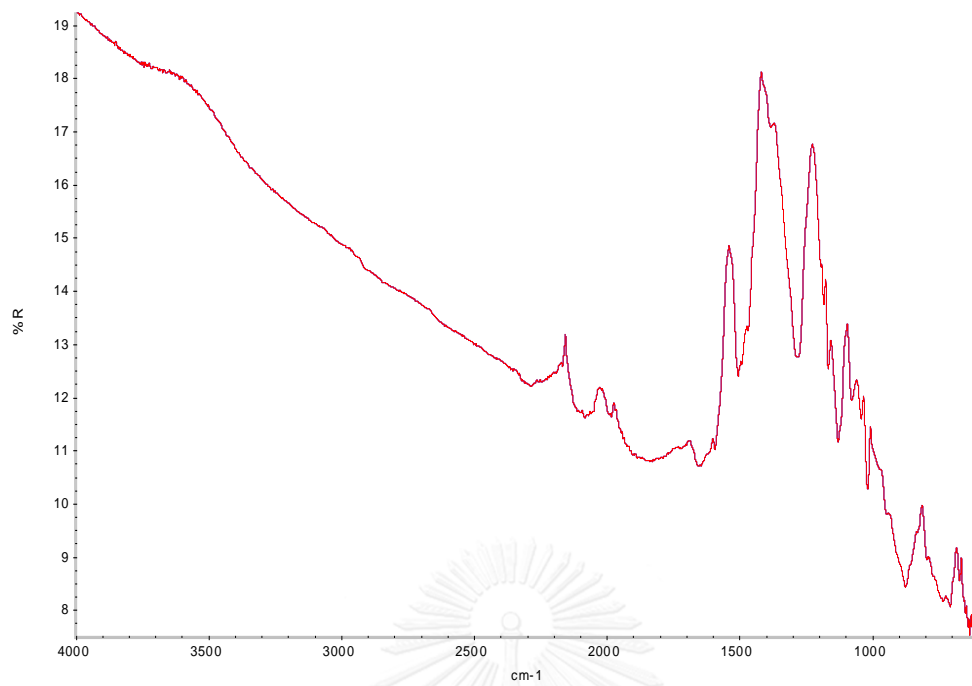


Figure A.71 IR spectrum of polymer 40

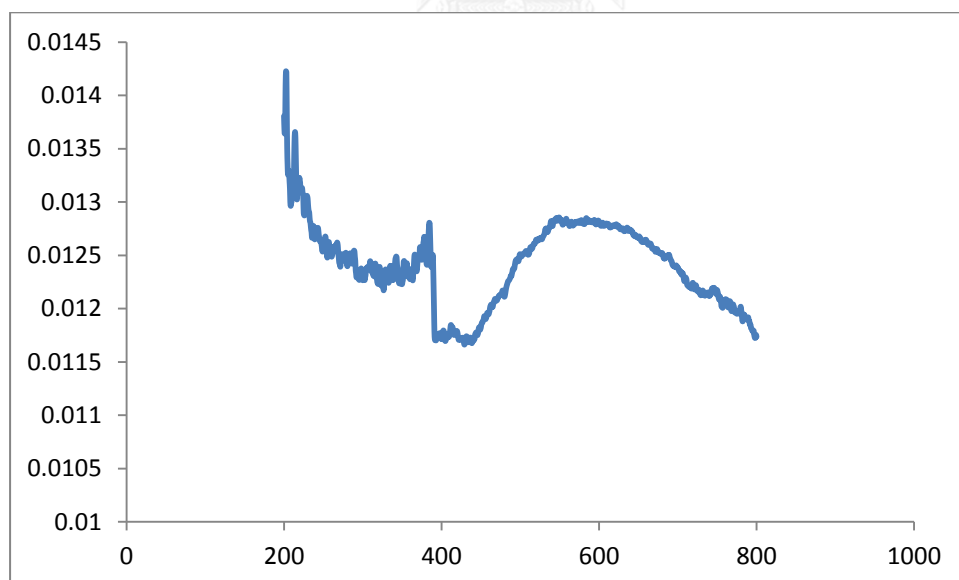


Figure A.72 UV-vis spectrum of polymer 40

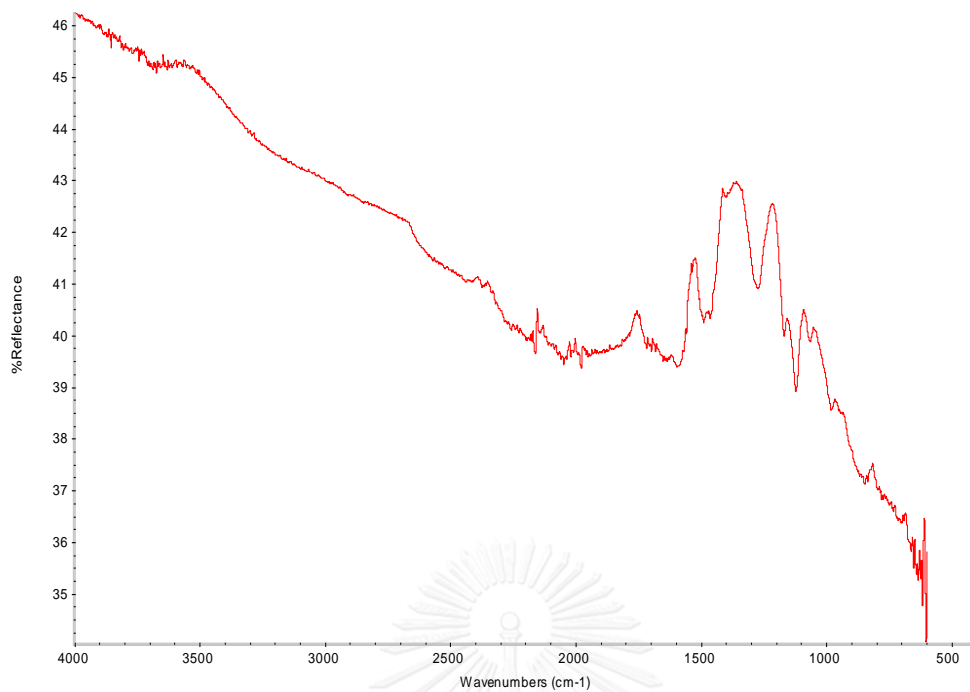


Figure A.73 IR spectrum of polymer 41

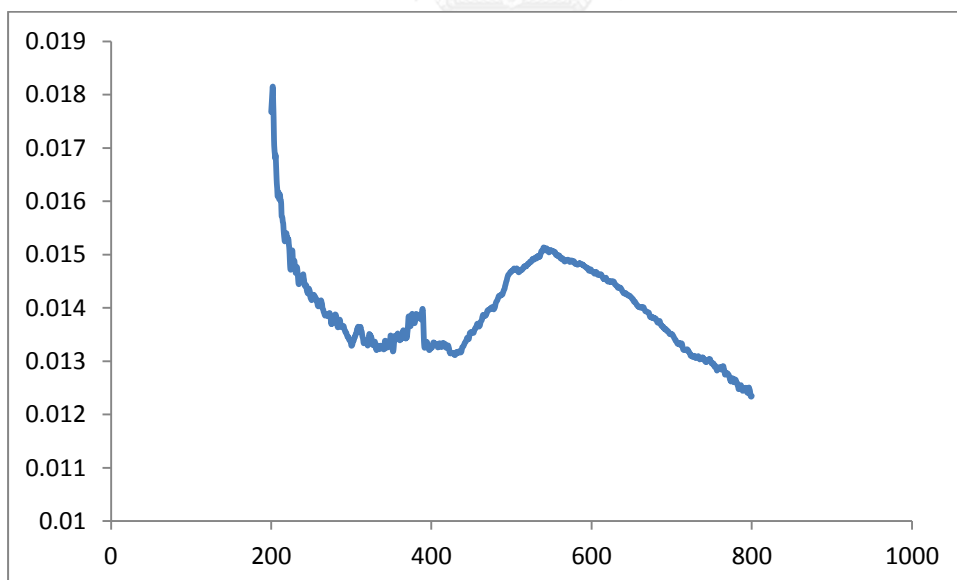


Figure A.74 UV-vis spectrum of polymer 41

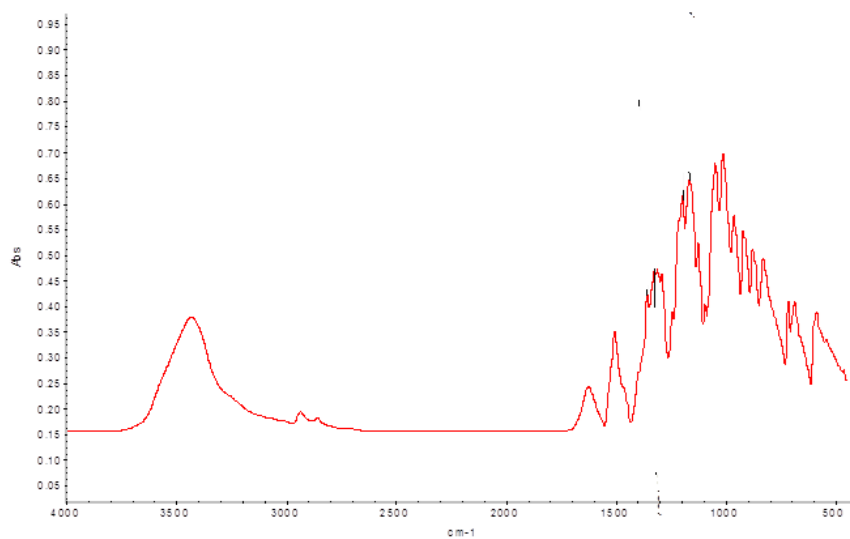


Figure A.75 IR spectrum of polymer 42

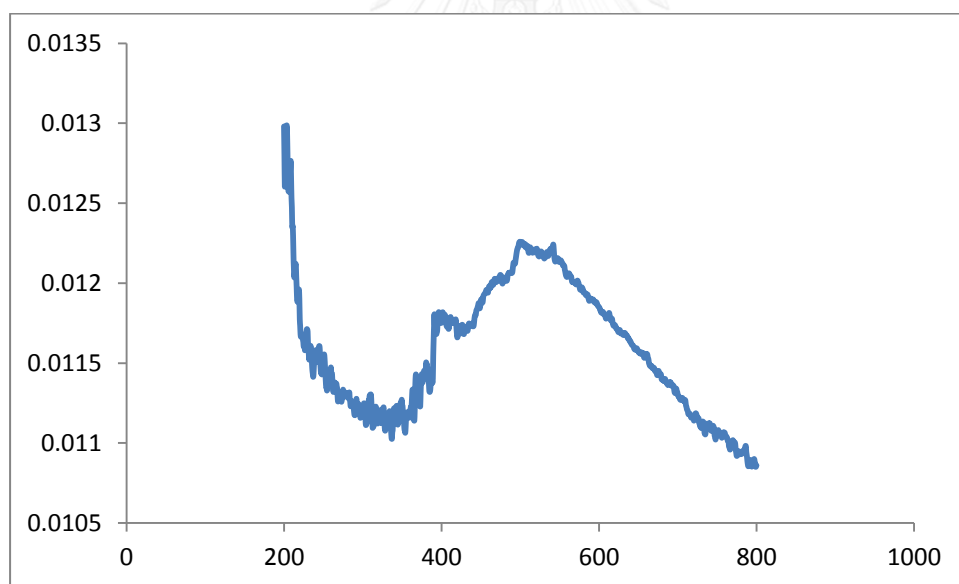


Figure A.76 UV-vis spectrum of polymer 42

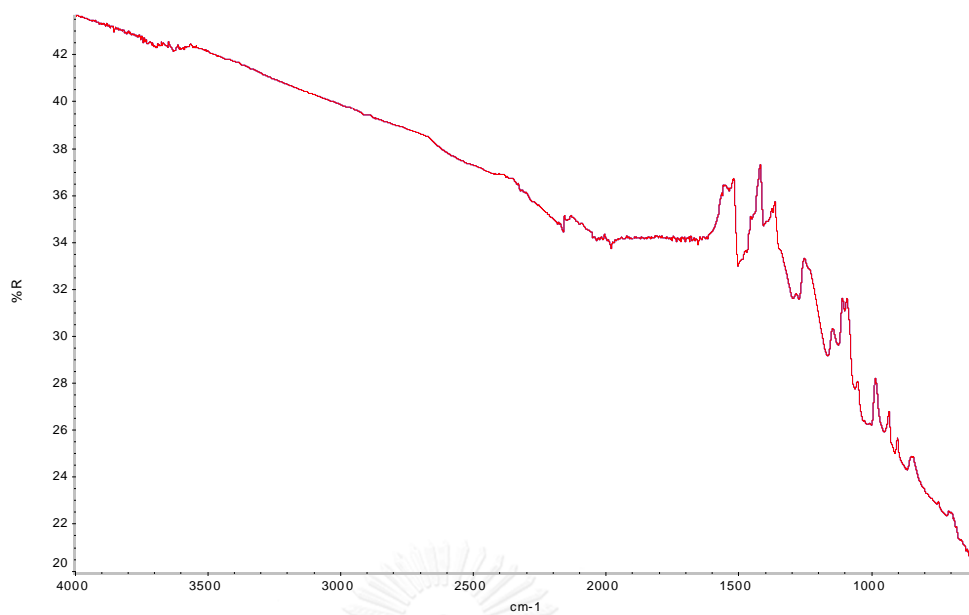


Figure A.77 IR spectrum of polymer 38c

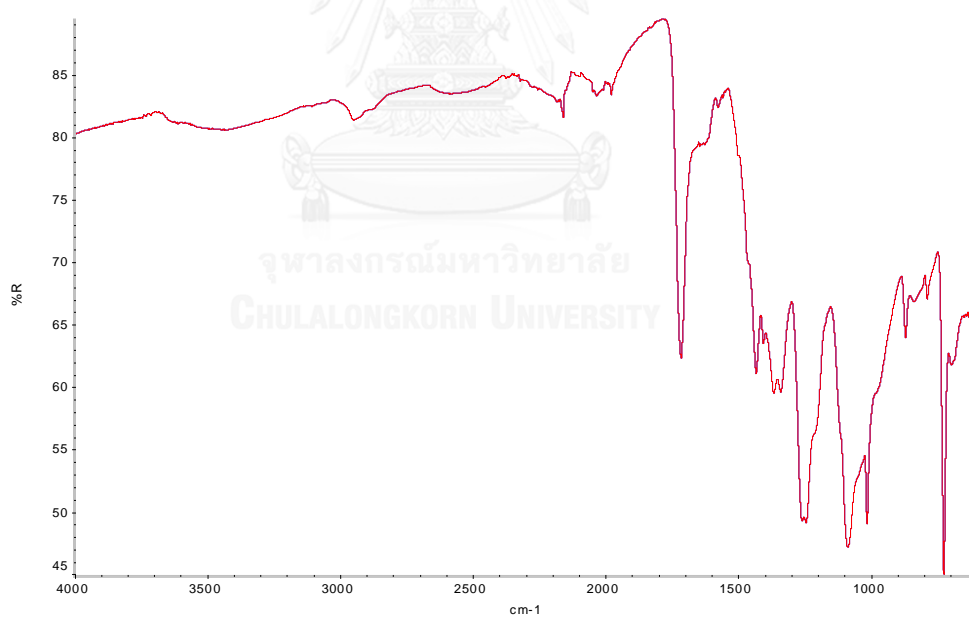


Figure A.78 IR spectrum of polymer 44

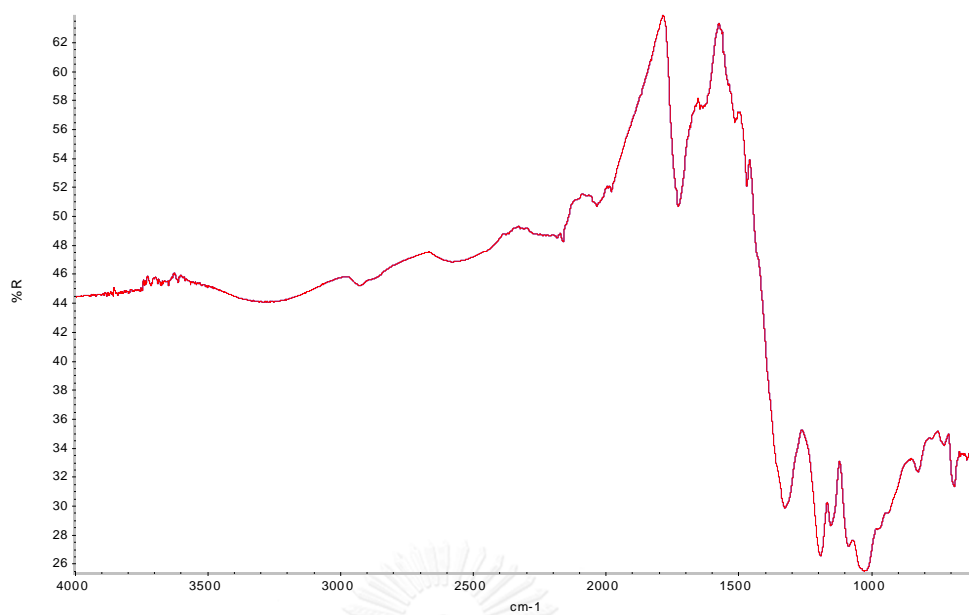


Figure A.79 IR spectrum of polymer 45

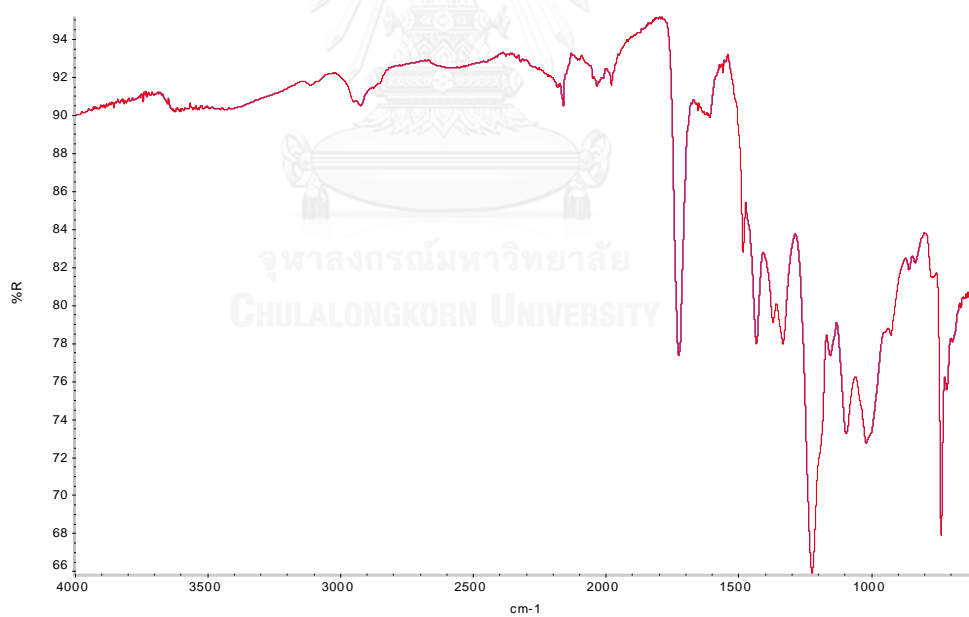


Figure A.80 IR spectrum of polymer 46

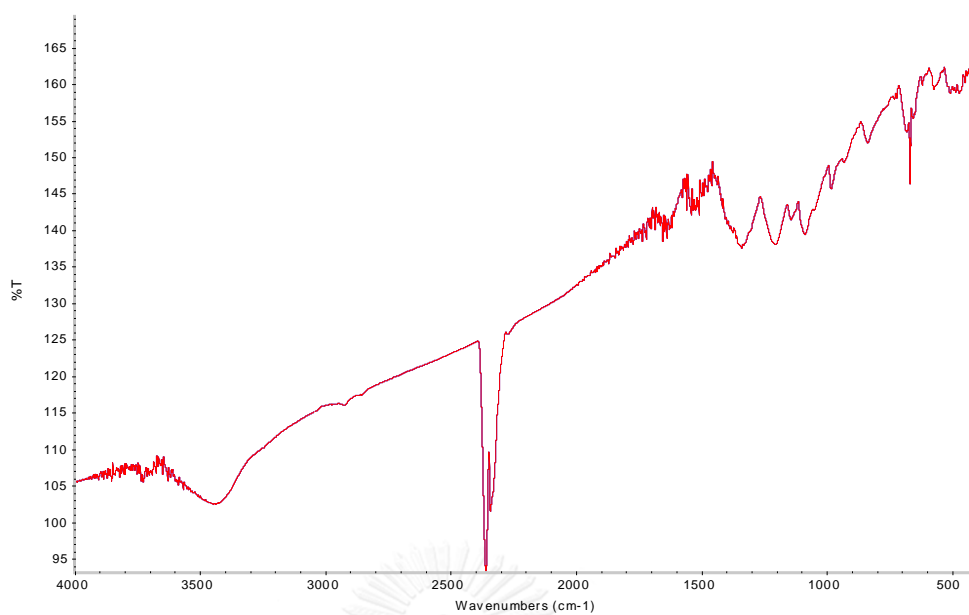
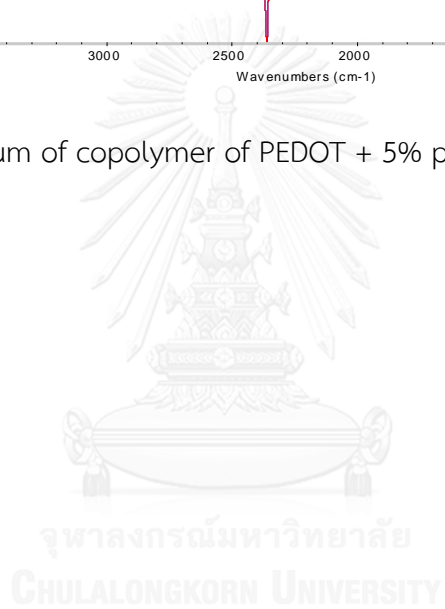


Figure A.81 IR spectrum of copolymer of PEDOT + 5% polymer 44





จุฬาลงกรณ์มหาวิทยาลัย  
APPENDIX B  
CHULALONGKORN UNIVERSITY



### The Four-point Probe Method for Electrical Conductivity Measurement

Four tiny electrodes are arranged in straight line separated at exactly equal distance ( $d$ ) and touched the surface of the sample to be measured. Then the electrodes are further connected with an electrical circuit equipped with an Amp meter (A) and a Voltmeter (V). **(Figure B.1)** Contacts between the 4 electrodes and the sample surface must be equal. During the measurement, the current ( $I$ ) is applied through electrode contact 1 to 4, and the potential difference ( $\Delta V$ ) across electrode contacts 2 and 3 is measured. The resistivity and conductivity of the sample can be calculated from the equations **B-1** and **B-2**, respectively. The conductivity is determined by the equation below:

$$\text{Resistivity } (\Omega\cdot\text{cm}); \quad \rho = (\pi t / \ln 2)(V/I) = 4.53(Rt) \quad (\text{B-1})$$

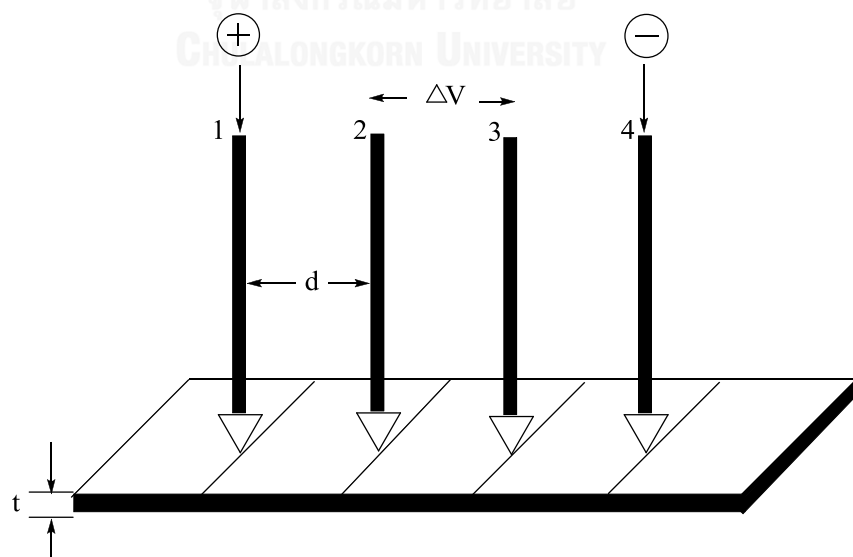
$$\text{Conductivity } (\text{S}/\text{cm}) \quad \sigma = 1/\rho \quad (\text{B-2})$$

Where  $I$  is current (A)

$V$  is voltage (volt)

$R$  is resistant ( $\Omega$ )

$t$  is film thickness (cm)



**Figure B.1** Conductivity measurement by four-point probe method

I-V Graph

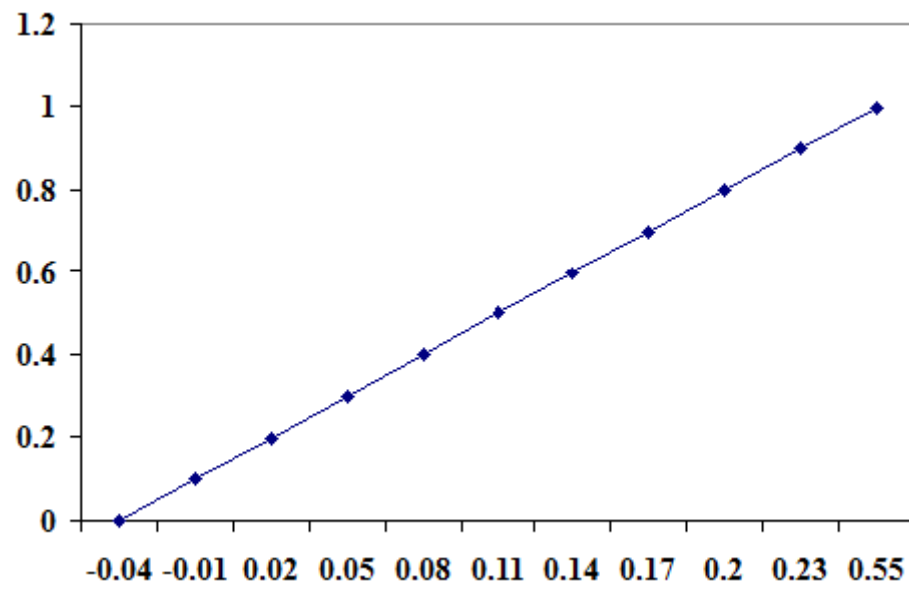


Figure B.2 Example of an I-V curve obtained from four point probe technique



**Table B.1** Electrical conductivity measurements of the synthesized polymers

Samples	$t_{av}$ (cm)	Resistivity ( $\Omega$ .cm);	Conductivity (S/cm)	SD	%SD
PEDOT (Chemically polymerized)	0.0301	0.276	3.62	0.215	6.3
		0.313	3.19		
		average	3.41		
PEDOT (SSP)	0.0475	0.200	5.00	0.418	7.5
		0.171	5.86		
		0.169	5.91		
		average	5.59		
Polymer <b>39</b> (SSP)	0.0240	$2.25 \times 10^{-2}$	44.5	0.850	1.9
		$2.35 \times 10^{-2}$	42.5		
		$2.27 \times 10^{-2}$	44.0		
		average	43.7		
Polymer <b>40</b> (SSP)	0.0265	$6.68 \times 10^{-2}$	15.0	4.13	28.9
		0.112	8.95		
		$5.27 \times 10^{-2}$	19.0		
		average	14.3		
Polymer <b>41</b> (SSP)	0.0285	0.969	1.03	0.0411	3.8
		0.923	1.07		
		0.887	1.13		
		average	1.08		
Polymer <b>42</b> (SSP at 80°C)	0.0678	5.60	0.179	0.0548	22.1
		3.20	0.313		
		3.96	0.253		
		average	0.248		
Polymer <b>42</b> (SSP at 120°C)	0.0410	$6.20 \times 10^{-3}$	161	30.0	23.0
		$7.73 \times 10^{-3}$	129		
		$9.89 \times 10^{-3}$	101		
		average	130		
Polymer <b>44</b> (Chemically polymerized)	0.0235	$3.22 \times 10^4$	$3.11 \times 10^{-5}$	$5.47 \times 10^{-6}$	14.4
		$2.62 \times 10^4$	$3.82 \times 10^{-5}$		
		$2.25 \times 10^4$	$4.45 \times 10^{-5}$		
		average	$3.79 \times 10^{-5}$		

$t_{av}$  = thickness average

Table B.1 (continued)

Samples	$t_{av}$ (cm)	Resistivity ( $\Omega$ .cm);	Conductivity (S/cm)	SD	%SD
Polymer <b>45</b> (Chemically polymerized)	0.0115	29.9	$3.34 \times 10^{-2}$	$2.87 \times 10^{-4}$	0.9
		30.2	$3.31 \times 10^{-2}$		
		30.5	$3.27 \times 10^{-2}$		
		average	$3.31 \times 10^{-2}$		
Copolymer PEDOT+5% polymer <b>44</b> (Chemically polymerized)	0.0148	0.179	5.58	0.308	5.1
		0.164	6.08		
		0.158	6.32		
		average	5.99		

$t_{av}$  = thickness average



## VITA

Mr. Narut Gulprasertrat was born on March 6, 1985 in Bangkok, Thailand. He received a Bachelor's degree of Science from Department of Chemistry, Faculty of Science, Chulalongkorn University, Thailand in 2007. He was admitted to a Doctor of Philosophy Degree Program in Chemistry, Faculty of Science, Chulalongkorn University and completed the program in 2014. His address is 19 yak 6-1 Sukhumvit road, kwang Bangjak, Prakanong, Bangkok 10260.

